INVERSE PROBLEMS RELATED TO TRANSIENT CONVECTION IN THE THERMAL ENTRANCE REGION BETWEEN PARALLEL PLATES

Thesis for the Degree of Ph. D.

MICHIGAN STATE UNIVERSITY
RAYMOND S. COLLADAY

1969

This is to certify that the

thesis entitled

INVERSE PROBLEMS RELATED TO TRANSIENT CONVECTION
IN THE THERMAL ENTRANCE REGION
BETWEEN PARALLEL PLATES

presented by

RAYMOND S. COLLADAY

has been accepted towards fulfillment
of the requirements for

Doctoral degree in Mech. Engr.

James V. Beck
Major professor

Date September 10, 1969

O-169

ABSTRACT

INVERSE PROBLEMS RELATED TO TRANSIENT CONVECTION
IN THE THERMAL ENTRANCE REGION BETWEEN PARALLEL PLATES

By

Raymond S. Colladay

Transient heat transfer in the thermal entrance region between parallel plates with a fully developed laminar velocity profile is studied for low Peclet number flows. Axial heat conduction is included and its effect on the temperature profiles upstream of the heated region as well as in the entrance region itself is noted. The energy equation is solved numerically using an alternating direction implicit finite difference method. Two boundary condition cases are presented, (1) a uniform wall heat flux and (2) a uniform wall temperature. The plate boundary upstream of the heated region is insulated in both cases. Steady state and transient results are presented for a range of Peclet numbers between 1 and 50. These results have not been previously obtained.

Using this solution as a basic building block in superposition, a number of inverse problems are formulated and presented in terms of integral equations. Particular emphasis is given to the inverse problem of estimating the mean velocity from temperature measurements at the wall and the solution of the energy equation. The optimum wall heat flux profile and optimum axial location of wall thermocouples which give the best estimate of this velocity parameter are studied. An example of the nonlinear estimation procedure used in calculating the mean velocity is also presented. This work is the first to formulate these inverse problems related to convection.

INVERSE PROBLEMS RELATED TO TRANSIENT CONVECTION IN THE THERMAL ENTRANCE REGION BETWEEN PARALLEL PLATES

By

Raymond S. Colladay

A THESIS

Submitted to
Michigan State University
in partial fulfillment of the requirements
for the degree of

DOCTOR OF PHILOSOPHY

Department of Mechanical Engineering

1969

661330
4-3-70

ACKNOWLEDGEMENT

The author wishes to express his sincere appreciation to his major professor, Dr. James V. Beck, for his valued guidance and encouragement during the period of research and graduate study. He also wishes to thank Dr. Charles R. St. Clair for his helpful advice throughout the years at Michigan State University.

Thankful acknowledgement is extended to the other members of the Guidance Committee: Dr. John F. Foss, Dr. Merle C. Potter, Dr. David H. Yen, and Dr. George E. Mase.

The author is grateful for financial support received from a NASA Traineeship and supplementing funds from the University.

To his wife Judy, the author dedicates this dissertation for her understanding and cooperation during graduate study and research.

TABLE OF CONTENTS

LIST OF FIGURES

LIST OF TABLES

NOMENCLATURE

T = Temperature

u,v = Velocity components

x,y = Physical coordinates

t = Time

a = Half-plate separation distance

μ = Absolute viscosity

C_p = Specific heat

k = Thermal conductivity

p = Density

α = Thermal diffusivity = k/pC_p

$\bar{u}$ = Mean velocity

Re = Reynolds number = $p\bar{u}a/\mu$

Pr = Prandtl number = $\mu C_p/k$

Pe = Peclet number = RePr = $\bar{u}a/\alpha$

h_{cx} = Local heat transfer coefficient

Nu = Local Nusselt number = $h_{cx}a/k$

X^+ = Dimensionless physical coordinate = $x/a\mathrm{Pe}$

y^+ = Dimensionless physical coordinate = y/a

t^+ = Dimensionless time = $t\alpha/a^2$

u^+ = Dimensionless velocity = $u/\bar{u}$

q'' = Wall heat flux

T_o = Uniform upstream temperature and initial temperature

T_s = Wall temperature

$T^+ = T - T_o / \frac{q''a}{k}$ = Dimensionless temperature for uniform heat flux boundary condition

$T^+ = T - T_o / T_s - T_o$ = Dimensionless temperature for uniform wall temperature boundary condition

T_b = Bulk temperature

τ = Duration of experiment

x_θ = Location of wall thermocouples

x_L = Heating length

T_{max} = Maximum temperature constraint

ΔT_{max} = Maximum temperature rise constraint = $T_{max} - T_o$

Φ = Objective function - basic criterion to be extremized

Pe $\partial T/\partial Pe$ = Sensitivity Coefficient with respect to the Peclet number.

I. DESCRIPTION OF THE PROBLEM

1.1 Introduction

The problem of extracting information from a set of measured data obtained under optimum experimental conditions has recently gained wide interest. In the area of convection, where it may be difficult to measure the velocity with a probe, parameters associated with the velocity profile can be estimated from thermal measurements at the boundary - an application which has considerable appeal. An optimum experiment insures that the parameters are determined more accurately than by any other similar experiment with the same errors in the temperature measurements.

The solution of the partial differential equation describing a process is often labeled as an inverse type problem when conditions are overspecified at a given boundary. The energy equation, with both the heat flux and temperature at the boundary known and the velocity an unknown coefficient to be determined falls into this category.

In this work, the basic objective is to investigate inverse problems related to the thermal entrance region between parallel plates under transient conditions. Consequently, an accurate transient solution to the thermal entrance region problem is needed, particularly in the liquid metal-small Peclet number range.

Many extensions to the original Graetz problem (1) of steady laminar heat transfer to a constant property fluid in the thermal entrance region of a constant wall temperature tube with a parabolic velocity profile have appeared in the literature. The corresponding flat plate geometry has been considered by various investigators (2, 3, 4); their work was followed by the treatment of such additional effects as transient conditions (5, 6), uniform heat flux boundary condition (7-9), hydrodynamically undeveloped flow (7-15), nonuniform properties (16, 17), wall surface resistance (18, 19), flow in an annulus (20), viscous dissipation (11, 21), power velocity profiles (22, 23), and nonuniform boundary conditions (24).

In all of these studies, the one fundamental assumption made is that the fluid conduction in the axial direction is negligible. In many cases this assumption is justified. However, when the Pe number is small (say less than 100), <u>or</u> when results in the entrance region in the immediate vicinity of, and including $x = 0$ (location where heating begins) are of interest, these solutions are not applicable. Another case where axial conduction should not be neglected is wherever the boundary conditions at the plate vary substantially over small regions.

In many modern heat exchanger devices involving large heat fluxes such as nuclear reactors, the use of liquid metals has become more popular. Due to the good thermal conductivity of these metals, solutions that include axial conduction are required.

In reviewing the literature, it is apparent that very few publications treat this problem. References (25-31) include the axial conduction term in the energy equation, but apply a uniform temperature boundary condition at $x = 0$. This forces the solution at this location to be the same as for the case of negligible axial conduction. However, it is at the start of the heating section, more than anywhere else in the entrance region, that the effect of axial conduction is most significant.

Some authors (32-36) have considered the "complete" problem; allowing axial conduction upstream of the $x = 0$ location by assuming a uniform temperature profile far upstream of the heated region. A uniform velocity profile is assumed in (32-34). Only Agrawal (35) and Hennecke (36) treat this case for a parabolic velocity profile; both under steady state conditions. The former assumes a flat plate geometry and the latter treats a tube geometry. Using analytical methods, Agrawal treats a constant temperature boundary condition at the wall; that is, the regions $x > 0$ and $x < 0$ at the wall are maintained at constant temperatures T_s and T_o respectively. In addition to this boundary condition, Hennecke treats the wall condition of constant heat flux for $x \geq 0$ and insulated upstream.

An analytical solution of the energy equation assuming a fully developed parabolic velocity profile leads to a differential equation whose eigenfunctions are not orthogonal. Representing the eigenfunctions by infinite Fourier sine series, this difficulty is reflected in the fact that to date only the first five eigenvalues have been reported, (35). These few values are not sufficient for accurate evaluation of the temperature distribution in the neighborhood of $x = 0$ since at this location, the convergence of the series is very slow. Hence, Agrawal's solution in this region is not reliable.

The methods of both (35) and (36) require numerically matching the temperature solutions from the upstream and downstream regions at the interface $x = 0$. In transient calculations this could require a substantial amount of computer time.

To the author's knowledge, no results for the complete problem of transient laminar flow between parallel plates have appeared in the open literature.

Once the wall temperatures are available from the solution of the entrance region problem, an optimum experiment can be designed to estimate the velocity (or some parameter of the velocity profile) from temperature measurements at the wall. The experiment is optimized with respect to the heat flux profile and location of thermocouples at the wall for a given duration of the experiment and maximum temperature rise. Optimum conditions permit the estimation of the parameters more accurately than any other similar experiment with the same constraints.

Nonlinear estimation - the procedure for calculating unknown parameters in a differential equation describing a physical process - has its first known reference by Gauss (47). The method, as applied to optimum experimental conditions, has been developed from a statistical approach by Box and coworkers (48-50) and recently extended to applications involving partial differential equations by Beck (51-53).

1.2 Problem Description

In this dissertation, the thermal entrance region between parallel plates is studied. The energy equation, with axial conduction and transient effects included, is solved numerically using an alternating direction implicit (ADI) method. Assuming a hydrodynamic development section upstream of the heated region, the velocity profile is parabolic. Two sets of boundary conditions at the wall are treated, (1) a uniform heat flux is applied to both plates in the region $x \geq 0$ (where x is the spatial coordinate in the axial direction) at time $t = 0$, and insulated in the region $x < 0$; and (2) the plates are maintained at the same uniform temperature in the region $x \geq 0$ beginning at $t = 0$ and insulated upstream. Axial conduction is allowed upstream by assuming a uniform temperature profile at $x = -\infty$.

The ADI numerical method does not require matching the solutions to the upstream and downstream regions at $x = 0$. Both the regions are treated together as a single domain.

Since the thermal conductivity and the velocity are assumed independent of temperature, the energy equation is linear in x and t, making superposition of solutions possible. A number of inverse problems are formulated using Duhamel's superposition integral with the uniform heat flux boundary condition solution as a basic building block.

Particular emphasis is given to the inverse problem of estimating the mean velocity from temperature measurements at the wall. A basic criterion is developed which gives a measure of the effectiveness of an experiment for determining the mean velocity. This criterion is then maximized with respect to the heat flux profile (a function of x and t) and wall thermocouple location to establish an optimum experiment.

The effect of errors in the temperature measurements is investigated. Also, an example using the nonlinear estimation procedure under optimum conditions is presented.

II. MATHEMATICAL DESCRIPTION

2.1 Energy Equation

Transient convection for fully developed laminar flow of an incompressible viscous fluid with constant properties is considered in the region between parallel plates. Two cases are investigated, Case I: a constant wall heat flux for $x \geq 0$ (see Figure 2.1) and insulated upstream, $x < 0$; and Case II: a constant surface temperature for $x \geq 0$ and insulated upstream.

For negligible viscous dissipation and flow work and constant thermal conductivity, the equation expressing energy conservation is,

$$\rho C_p \left(\frac{\partial T}{\partial t} + u \frac{\partial T}{\partial X} + v \frac{\partial T}{\partial y}\right) = k\left(\frac{\partial^2 T}{\partial x^2} + \frac{\partial^2 T}{\partial y^2}\right) \tag{2.1}$$

For fully developed flow, u and v are given by,

$$u = \frac{3}{2} \bar{u}\left[1 - \left(\frac{y}{a}\right)^2\right] \tag{2.2}$$

$$v = 0 \tag{2.3}$$

where the mean velocity, $\bar{u} = \frac{1}{a} \int_0^a u dy$ (2.4)

Equation (2.1) is linear in temperature, T since k, ρ, C_p, and $\bar{u}$ are assumed to be independent of T.

Since the thermal entrance region is of particular interest, the axial conduction term $\partial^2 T/\partial x^2$ must be retained.

Solutions to Equations (2.1), (2.2), and (2.3) are obtained for the two sets of boundary conditions on $T(x,y,t)$ given below.

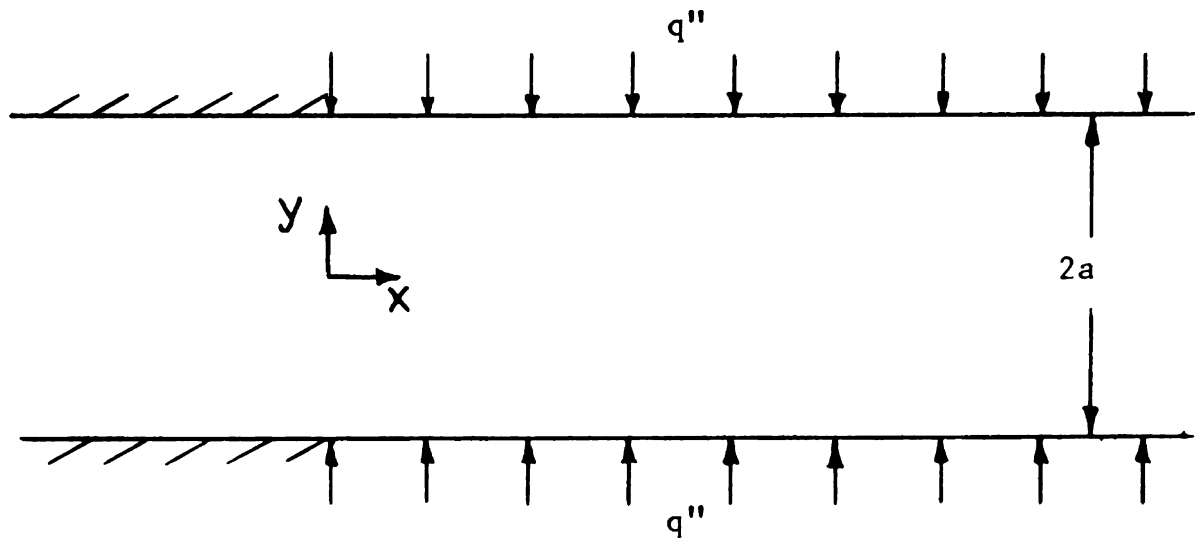

UNIFORM HEAT FLUX - CASE I

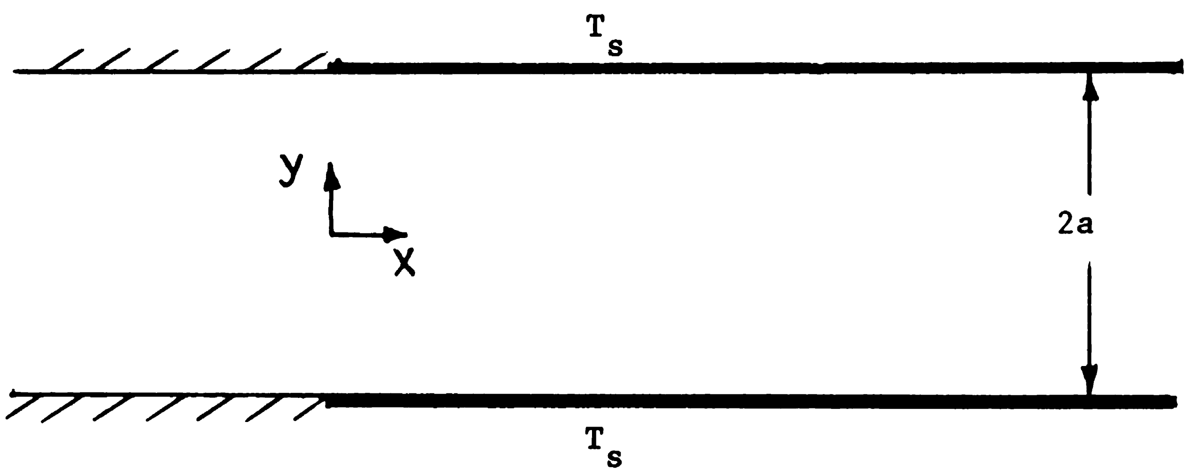

UNIFORM WALL TEMPERATURE - CASE II

FIGURE 2.1: PLATE GEOMETRY

CASE I: UNIFORM HEAT FLUX

$$T(x,y,0) = T_o \tag{2.5a}$$

$$T(-\infty,y,t) = T_o \tag{2.5b}$$

$$\frac{\partial^2 T(\infty,y,t)}{\partial x^2} = 0 \tag{2.5c}$$

$$\frac{\partial T(x,0,t)}{\partial y} = 0 \tag{2.5d}$$

$$k\frac{\partial T(x,a,t)}{\partial y} = \begin{matrix} 0 & \text{for} & x < 0 \\ q'' & \text{for} & x \geq 0 \end{matrix} \tag{2.5e}$$

CASE II: UNIFORM WALL TEMPERATURE

$$T(x,y,0) = T_o \tag{2.6a}$$

$$T(-\infty,y,t) = T_o \tag{2.6b}$$

$$\frac{\partial T(\infty,y,t)}{\partial x} = 0 \tag{2.6c}$$

$$\frac{\partial T(x,0,t)}{\partial y} = 0 \tag{2.6d}$$

$$T(x,a,t) = T_s \quad \text{for} \quad x \geq 0 \tag{2.6e}$$

$$\frac{\partial T(x,a,t)}{\partial y} = 0 \quad \text{for} \quad x < 0 \tag{2.6f}$$

It is convenient to express the energy equation and its boundary conditions in dimensionless form. Let the variables be non-dimensionalized as follows, using the half plate separation distance, a, as the characteristic length.[1]

[1] Note that some references for the characteristic length use the hydraulic diameter, defined D_H = 4x(Flow Area/Perimeter). For the parallel plate case, $D_H = 4a$. When comparison is made with results based on D_H, a factor of 4 will be introduced.

$$X^+ = \frac{x/a}{Pe} \tag{2.7a}$$

$$y^+ = \frac{y}{a} \tag{2.7b}$$

$$t^+ = \frac{t\alpha}{a^2} \tag{2.7c}$$

$$u^+ = \frac{u}{\bar{u}} \tag{2.7d}$$

$$T^+ = \frac{T-T_o}{q''a/k} \quad \text{for Case I} \tag{2.7e}$$

$$T^+ = \frac{T-T_o}{T_s-T_o} \quad \text{for Case II} \tag{2.7f}$$

Equation (2.1) becomes,

$$\frac{\partial T^+}{\partial t^+} + u^+ \frac{\partial T^+}{\partial X^+} = \frac{1}{Pe^2} \frac{\partial^2 T^+}{\partial X^{+2}} + \frac{\partial^2 T^+}{\partial y^{+2}} \tag{2.8}$$

with boundary conditions:

CASE I

$$T^+(X^+, y^+, 0) = 0 \tag{2.9a}$$

$$T^+(-\infty, y^+, t^+) = 0 \tag{2.9b}$$

$$\frac{\partial^2 T^+(\infty, y^+, t^+)}{\partial X^{+2}} = 0 \tag{2.9c}$$

$$\frac{\partial T^+(X^+, 0, t^+)}{\partial y^+} = 0 \tag{2.9d}$$

$$\frac{\partial T^+(X^+, 1, t^+)}{\partial y^+} = \begin{array}{ll} 0 & \text{for } X^+ < 0 \\ 1 & \text{for } X^+ \geq 0 \end{array} \tag{2.9e}$$

CASE II

$$T^+(X^+,y^+,0) = 0 \qquad (2.10a)$$

$$T^+(-\infty,y^+,t^+) = 0 \qquad (2.10b)$$

$$\frac{\partial T^+(\infty,y^+,t^+)}{\partial X^+} = 0 \qquad (2.10c)$$

$$\frac{\partial T^+(X^+,0,t^+)}{\partial y^+} = 0 \qquad (2.10d)$$

$$T^+(X^+,1,t^+) = 1 \quad \text{for} \quad X^+ > 0 \qquad (2.10e)$$

$$\frac{\partial T^+(X^+,1,t^+)}{\partial y^+} = 0 \quad \text{for} \quad X^+ < 0 \qquad (2.10f)$$

2.2 Other Useful Relations

The local Nusselt number, Nu, used in expressing the local heat transfer coefficient, h_x, in dimensionless form is of particular interest, especially in the entrance region near $X^+ = 0$.

The defining equation for h_x is,

$$q'' = h_x(T_s - T_b) \qquad (2.11)$$

where T_b is the bulk temperature as defined by Equation (2.16). Also, the heat flux is given by,

$$q'' = k\left(\frac{\partial T}{\partial y}\right)_{y=a} \qquad (2.12)$$

The Nu number is then formed as follows,

$$Nu = \frac{h_x a}{k} = \frac{\frac{q''a}{k}}{T_s - T_b} = \frac{a\left(\frac{\partial T}{\partial y}\right)_{y=a}}{(T_s - T_b)} \qquad (2.13)$$

Expressing Equation (2.13) in terms of the appropriate dimensionless variables of Equation (2.7), we have:

for Case I:

$$Nu = \frac{1}{\frac{T_s - T_o}{\frac{q''a}{k}} - \frac{T_b - T_o}{\frac{q''a}{k}}} = \frac{1}{T_s^+ - T_b^+}$$

or based on $D_H = 4a$,

$$Nu = \frac{4}{T_s^+ - T_b^+} \tag{2.14}$$

for Case II:

$$Nu = \frac{\frac{\partial}{\partial(\frac{y}{a})} \left(\frac{T - T_o}{T_s - T_o}\right)_{\frac{y}{a}=1}}{\left(\frac{T_s - T_o}{T_s - T_o}\right) - \left(\frac{T_b - T_o}{T_s - T_o}\right)} = \frac{\left(\frac{\partial T^+}{\partial y^+}\right)_{y^+=1}}{1 - T_b^+}$$

and based on D_H

$$Nu = \frac{4 \left.\frac{\partial T^+}{\partial y^+}\right|_{y^+=1}}{1 - T_b^+} \tag{2.15}$$

The bulk temperature, as used in the above equations, is defined as

$$T_b(x,t) = \frac{1}{A_c \bar{u}} \int_{A_c} u \; T \; dA_c$$

where A_c is the cross sectional area normal to the direction of flow. For the given geometry,

$$T_b = \frac{1}{a\bar{u}} \int_o^a u \; T \; dy \tag{2.16}$$

For the particular boundary conditions of this problem, T_b in dimensionless form becomes, using Equation (2.7),

Case I:

$$T_b^+ = \frac{T_b - T_o}{\frac{q''a}{k}} = \frac{1}{a\bar{u}} \int_o^a u \frac{T}{\frac{q''a}{k}} dy - \frac{1}{a\bar{u}} \int_o^a u \frac{T_o}{\frac{q''a}{k}} dy$$

Since $\frac{1}{a\bar{u}} \int_o^a u dy = 1$ and $\frac{q''a}{k}$ = constant. Therefore,

$$T_b^+ = \frac{1}{a\bar{u}} \int_o^a u \left(\frac{T - T_o}{\frac{q''a}{k}} \right) dy$$

or

$$T_b^+ = \int_o^1 u^+ T^+ dy^+ \tag{2.17}$$

Case II:

$$T_b^+ = \frac{T - T_o}{T_s - T_o} = \frac{1}{a\bar{u}} \int_o^a u \frac{T}{T_s - T_o} dy - \frac{1}{a\bar{u}} \int_o^a u \frac{T_o}{T_s - T_o} dy$$

and again,

$$T_b^+ = \int_o^1 u^+ T^+ dy^+ \tag{2.17}$$

The Nusselt number as defined in Equation (2.13) is a function of x and t. One can consider an average $\overline{Nu}$ over an axial length L, or time τ, or both.

$$\overline{Nu}(t) = \frac{1}{L} \int_o^L Nu \, dx \tag{2.18}$$

$$\overline{Nu}(x) = \frac{1}{\tau} \int_o^\tau Nu \, dt \tag{2.19}$$

$$\overline{Nu} = \frac{1}{\tau L} \int_o^L \int_o^\tau Nu \, dt \, dx \tag{2.20}$$

For both cases, the Nusselt number is zero for $x < 0$. In the region $x \geq 0$, a numerical method of solution is used and is described in the next chapter.

III. NUMERICAL METHOD

3.1 Finite Difference Expressions

Expanding a function $f(x,y,t)$ about a point x in a Taylor Series gives for $(x + \Delta x, y, t)$,

$$f(x+\Delta x,y,t) = f(x,y,t) + \Delta x \frac{\partial f(x,y,t)}{\partial x} + \frac{(\Delta x)^2}{2!}\frac{\partial^2 f(x,y,t)}{\partial x^2} + \frac{(\Delta x)^3}{3!}\frac{\partial^3 f(x,y,t)}{\partial x^3} + \frac{(\Delta x)^4}{4!}\frac{\partial^4 f(x,y,t)}{\partial x^4} + \ldots \quad (3.1)$$

and for $(x-\Delta x,y,t)$,

$$f(x-\Delta x,y,t) = f(x,y,t) - \Delta x \frac{\partial f(x,y,t)}{\partial x} + \frac{(\Delta x)^2}{2!}\frac{\partial^2 f(x,y,t)}{\partial x^2} - \frac{(\Delta x)^3}{3!}\frac{\partial^3 f(x,y,t)}{\partial x^3} + \frac{(\Delta x)^4}{4!}\frac{\partial^4 f(x,y,t)}{\partial x^4} + \ldots \quad (3.2)$$

Subtracting we have,

$$\frac{\partial f(x,y,t)}{\partial x} = \frac{f(x+\Delta x,y,t) - f(x-\Delta x,y,t)}{2\Delta x} - \frac{(\Delta x)^2}{6}\frac{\partial^3 f(x,y,t)}{\Delta x^3} + \ldots \quad (3.3)$$

and adding,

$$\frac{\partial^2 f(x,y,t)}{\partial x^2} = \frac{f(x+\Delta x,y,t) - 2f(x,y,t) + f(x-\Delta x,y,t)}{(\Delta x)^2} - \frac{(\Delta x)^2}{12}\frac{\partial^4 f(x,y,t)}{\partial x^4} + \ldots \quad (3.4)$$

A rectangular grid with a mesh size Δx by Δy and Δt in time is imposed on the region of interest (see Figure 3.1). If the

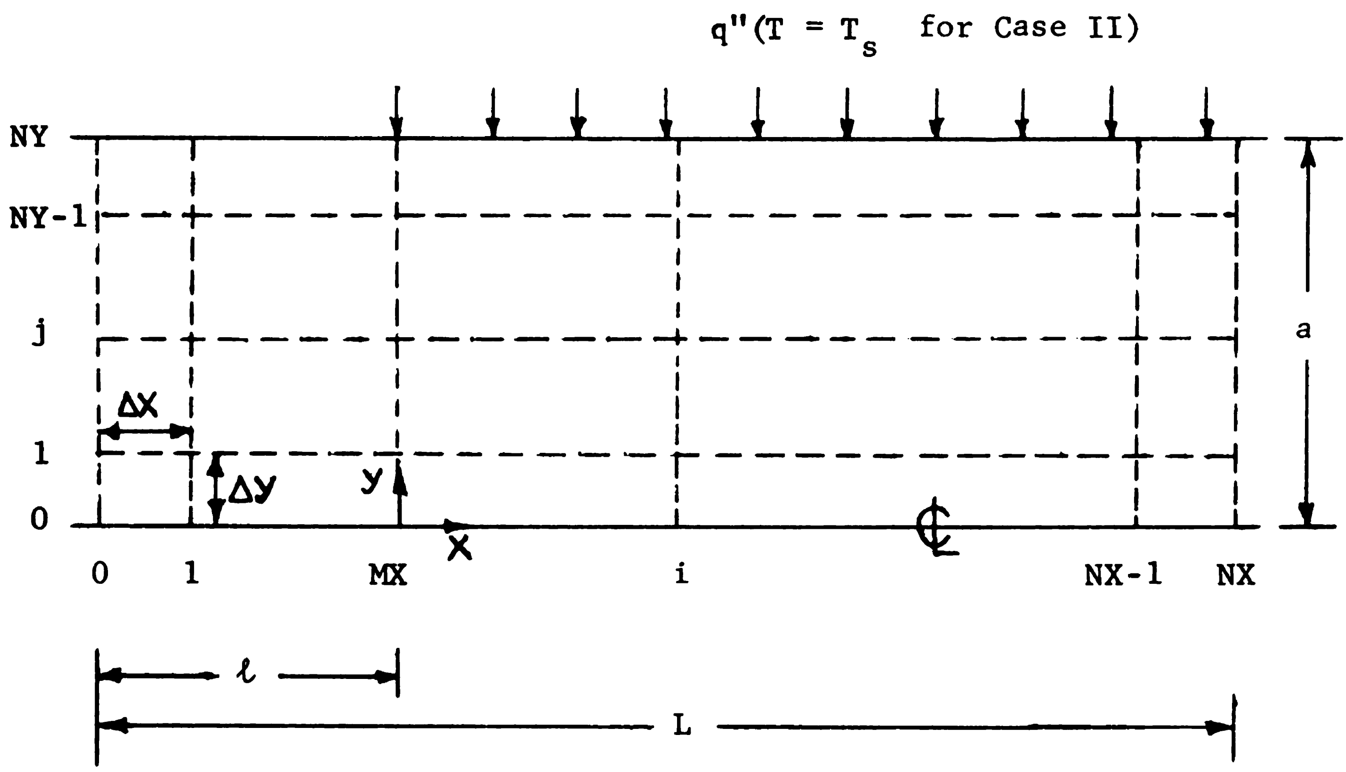

MX = Number of intervals into which the upstream length, ℓ is divided.

NX = Number of intervals into which the entire x-domain, L is divided.

NY = Number of intervals into which the half-plate separation distance a is divided.

x = 0 = MX(Δx) = Location where heating begins.

FIGURE 3.1: FINITE DIFFERENCE SPATIAL GRID FOR PARALLEL PLATE GEOMETRY

indices i,j, and n correspond to nodal points in x,y, and t respectively, then the temperature at a typical grid point in time and space is,

$$T(x_i,y_j,t_n) = T[i\Delta x, j\Delta y, n\Delta t]$$

Using space indices as subscripts and the time index as a superscript we have,

$$T^n_{i,j} = T(x_i,y_j,t_n)$$

Equations (3.3) and (3.4) then become in particular,

$$\frac{\partial T^n_{i,j}}{\partial x} \cong \frac{T^n_{i+1,j} - T^n_{i-1,j}}{2\Delta x} \boxed{- \frac{(\Delta x)^2}{6} \frac{\partial^3 T^n_{i,j}}{\partial x^3}} \tag{3.5}$$

$$\frac{\partial^2 T^n_{i,j}}{\partial x^2} \cong \frac{T^n_{i+1,j} - 2T^n_{i,j} + T^n_{i-1,j}}{(\Delta x)^2} \boxed{- \frac{(\Delta x)^2}{12} \frac{\partial^4 T^n_{i,j}}{\partial x^4}} \tag{3.6}$$

Similarly for the y derivative

$$\frac{\partial^2 T^n_{i,j}}{\partial y^2} \cong \frac{T^n_{i,j+1} - 2T^n_{i,j} + T^n_{i,j-1}}{(\Delta y)^2} \boxed{- \frac{(\Delta y)^2}{12} \frac{\partial^4 T^n_{i,j}}{\partial y^4}} \tag{3.7}$$

From Equation (3.1) the time derivative can be expressed as,

$$\frac{\partial T^n_{i,j}}{\partial t} \cong \frac{T^{n+1}_{i,j} - T^n_{i,j}}{\Delta t} \boxed{- \frac{(\Delta t)}{2} \frac{\partial^2 T^n_{i,j}}{\partial t^2}} \tag{3.8}$$

The boxed in terms in the above equations are retained only to give an order of the truncation error. See Appendix A.

Adopting the following notation for the first and second order central difference operators we have,

$$\delta_i(T^n_{i,j}) = T^n_{i+\frac{1}{2},j} - T^n_{i-\frac{1}{2},j} \simeq \tfrac{1}{2}(T^n_{i+1,j} - T^n_{i-1,j}) \tag{3.9a}$$

$$\delta^2_i(T^n_{i,j}) = T^n_{i+1,j} - 2T^n_{i,j} + T^n_{i-1,j} \tag{3.9b}$$

$$\delta^2_j(T^n_{i,j}) = T^n_{i,j+1} - 2T^n_{i,j} + T^n_{i,j-1} \tag{3.9c}$$

3.2 Alternating Direction Implicit Method

The numerical solution of finite difference approximations to parabolic equations can be accomplished in a number of ways depending on the time step at which the difference operators in Equation (3.9) are evaluated. A number of these approximations are described by Douglas (42).

The method used in this work is an alternating direction implicit (ADI) method similar to that of Douglas (42). This latter method is a modification of the method first proposed by Peaceman and Rachford (43), and later modified by Douglas and Rachford (44). To the author's knowledge, this numerical method has only been used in solving diffusion-type equations. Pearson and Serovy (41) used the method in solving the Navier-Stokes equations but did not include the first order derivatives in the alternating direction scheme.

Substituting Equation (3.9) into (2.8), (dropping the superscript "+" for simplicity) and alternately evaluating the x and y derivatives at the unknown or future time level, we have for the intermediate time step $n + \frac{1}{2}$,

$$\frac{T^{n+\frac{1}{2}}_{i,j} - T^n_{i,j}}{\Delta t/2} + \frac{1}{\Delta x} u_j \, \delta_i(T^n) = \frac{1}{(\Delta x)^2 Pe^2} \delta^2_i(T^n) + \frac{1}{(\Delta y)^2} \delta^2_j(T^{n+\frac{1}{2}}) \tag{3.10}$$

and for the (n+1) time step,

$$\frac{T_{i,j}^{n+1} - T_{i,j}^{n+\frac{1}{2}}}{\Delta t/2} + \frac{1}{\Delta x} u_j \delta_i (T^{n+1}) = \frac{1}{(\Delta x)^2 Pe^2} \delta_i^2 (T^{n+1})$$

$$+ \frac{1}{(\Delta y)^2} \delta_j^2 (T^{n+\frac{1}{2}}) \qquad (3.11)$$

Formulation in this way allows for the separation of unknowns into a y-direction calculation with NY unknowns and an x direction calculation with NX unknowns. Thus, the maximum number of simultaneous equations to solve is Max(NX,NY) rather than (NX) × (NY) for a fully implicit method.

Combining Equations (3.10) and (3.11) to eliminate the intermediate time step results in the following equation for the total time step,

$$\frac{T_{i,j}^{n+1} - T_{i,j}^{n}}{\Delta t} + \frac{1}{2(\Delta x)} u_j \delta_i (T^n + T^{n+1}) = \frac{1}{2(\Delta x)^2 Pe^2} \delta_i^2 (T^n + T^{n+1})$$

$$+ \frac{1}{2(\Delta y)^2} \delta_j^2 (T^n + T^{n+1}) + \frac{\Delta t}{4(\Delta x)^2 (\Delta y)^2 Pe^2} \delta_i^2 \delta_j^2 (T^n - T^{n+1})$$

$$- \frac{\Delta t}{4(\Delta y)^2 \Delta x} u_j \delta_j^2 \delta_i (T^n - T^{n+1}) \qquad (3.12)$$

The formulation as just described is that due to Peaceman and Rachford. If, however, the modified method of Douglas is used, the end result for a total time step is the same, but the particular x and y direction equations are much easier to solve. Rather than defining a half time step temperature $T^{n+\frac{1}{2}}$, let $T_{i,j}^{*}$ be an intermediate temperature defined by,

$$\frac{T^*_{i,j} - T^n_{i,j}}{\Delta t} + \frac{1}{\Delta x} u_j \delta_i(T^n) = \frac{1}{(\delta x)^2 Pe^2} \delta^2_i(T^n) + \frac{1}{2(\Delta y)^2} \delta^2_j(T^n + T^*) \quad (3.13)$$

and let $T^{n+1}_{i,j}$ be defined by,

$$\frac{T^{n+1}_{i,j} - T^n_{i,j}}{\Delta t} + \frac{1}{2(\Delta x)} u_j \delta_i(T^{n+1} + T^n) = \frac{1}{2(\Delta x)^2 Pe^2} \delta^2_i(T^{n+1} + T^n) + \frac{1}{2(\Delta y)^2} \delta^2_j(T^* + T^n) \quad (3.14)$$

Subtracting Equation (3.14) from (3.13) gives

$$T^*_{i,j} = T^{n+1}_{i,j} - \frac{\Delta t}{2(\Delta x)} u_j \delta_i(T^n - T^{n+1}) + \frac{\Delta t}{2(\Delta x)^2 Pe^2} \delta^2_i(T^n - T^{n+1}) \quad (3.15)$$

Substituting Equation (3.15) into (3.14) eliminating T^* results in exactly the same equation as (3.12) for the Peaceman-Rachford formulation, so the two methods are equivalent for the total time step.

The truncation error, which gives an indication of the error resulting from the replacement of the differential equation by its finite difference approximation, is dealt with in Appendix A. It is seen that the error associated with Equation (3.12) as given by Equation (A-8) is of order $O[(\Delta x)^2, (\Delta y)^2, (\Delta t)^2]$.

$$\text{ERROR} = \frac{(\Delta t)^2}{2} [T_{t^3} + u\, T_{txy^2} - \frac{1}{Pe^2} T_{tx^2y^2}]^n + \frac{(\Delta y)^2}{6} T^{n+\frac{1}{2}}_{y^4} + \frac{(\Delta x)^2}{6} [\frac{1}{Pe^2} T_{x^4} - u\, T_{x^3}]^{n+\frac{1}{2}}$$

A subscript notation has been used to denote derivatives, e.g. $T^n_{t^3} = \partial 3T^n/\partial t^3$.

Referring to Appendix B, one can see that a stability analysis predicts that the ADI method as formulated by Equation (3.12) is unconditionally stable for any size Δx, Δy, and Δt. However, for a mesh that is too coarse, the solution of the finite difference equation, though stable, differs significantly from the solution of the differential equation.

Define,

$$\alpha_x = \frac{2(\Delta x)^2}{\Delta t}$$

and

$$\alpha_y = \frac{2(\Delta y)^2}{\Delta t}$$

Then Equations (3.13) and (3.15) can be put in the form,

X-Direction:

$$(\alpha_x + \Delta x\, u_j \delta_i - \frac{1}{Pe^2}\, \delta_i^2) T_{i,j}^{n+1} =$$

$$\alpha_x T_{i,j}^{*} + (\Delta x\, u_j \delta_i - \frac{1}{Pe^2}\, \delta_i^2) T_{i,j}^{n} \qquad (3.16)$$

Y-Direction:

$$(\alpha_y - \delta_j^2) T_{i,j}^{*} =$$

$$(\alpha_y - 2\Delta x\, \frac{\alpha_y}{\alpha_x}\, u_j \delta_i + \frac{2}{Pe^2}\, \frac{\alpha_y}{\alpha_x}\, \delta_i^2 + \delta_j^2) T_{i,j}^{n} \qquad (3.17)$$

Written in matrix form, Equations (3.16) and (3.17) result in a tridiagonal system of the form,

$$\bar{B}_x + \bar{A}_{x_j} \bar{T}_j^{n+1} = \bar{Q}_{x_j} \qquad j = 0,1,\ldots,NY \qquad (3.16a)$$

$$\bar{B}_y + \bar{A}_y \bar{T}_i^{*} = \bar{Q}_{y_i} \qquad i = 1,2,\ldots,NX \qquad (3.17a)$$

$\bar{B}_x$ and $\bar{B}_y$ are boundary condition vectors for the x and y directions respectively,

$$\bar{B}_x = \begin{bmatrix} b_o \\ 0 \\ \vdots \\ 0 \\ b_{NX} \end{bmatrix} \qquad \bar{B}_y = \begin{bmatrix} b_o \\ 0 \\ \vdots \\ 0 \\ b_{NY} \end{bmatrix}$$

$\bar{Q}_x$ and $\bar{Q}_y$ are known vectors for the x and y direction equations respectively,

$$\bar{Q}_{x_j} = \begin{bmatrix} q_o \\ q_1 \\ \vdots \\ q_i \\ \vdots \\ q_{NX} \end{bmatrix} \text{ for each } j \qquad \bar{Q}_{y_i} = \begin{bmatrix} q_o \\ q_1 \\ \vdots \\ q_j \\ \vdots \\ q_{NY} \end{bmatrix} \text{ for each } i$$

where a typical element of $\bar{Q}_{x_j}$ is

$$q_i = \alpha_x T^*_{i,j} - R_j T^n_{i-1,j} + \frac{2}{Pe^2} T^n_{i,j} - S_j T^n_{i+1,j}$$

and a typical element of $\bar{Q}_{y_i}$ is

$$q_j = \Delta x \beta\, u_j (T^n_{i-1,j} - T^n_{i,j}) + E\, T^n_{i-1,j} + (\alpha_y - 2E) T^n_{i,j} + E\, T^n_{i+1,j}$$

where $$R_j = \frac{1}{Pe^2} + \frac{\Delta x}{2} u_j \qquad (3.18a)$$

$$S_j = \frac{1}{Pe^2} - \frac{\Delta x}{2} u_j \qquad (3.18b)$$

$$\beta = \frac{\alpha_y}{\alpha_x} \qquad (3.18c)$$

$$E = \frac{2}{Pe^2} \beta \qquad (3.18d)$$

$\bar{A}_{x_j}$ and $\bar{A}_y$ are tridiagonal coefficient matrices of order NX-1 and NY respectively,[1]

$$\bar{A}_{x_j} = \begin{bmatrix} A_x & -S_j & 0 & & \\ -R_j & A_x & -S_j & 0 & \\ & & & & \\ & & -R_j & A_x & -S_j \\ 0 & & 0 & -R_j & A_x \end{bmatrix} \quad \text{where } A_x = \alpha_x + \frac{2}{Pe^2}$$

$$\bar{A}_y = \begin{bmatrix} A_y & C & 0 & & 0 \\ -1 & A_y & -1 & & \\ & & & & \\ & & -1 & A_y & -1 \\ 0 & & 0 & d & A_y \end{bmatrix} \quad \text{where } A_y = \alpha_y + 2 \text{ and}$$

c and d depend on the boundary condition.

$\bar{T}^{n+1}$ and $\vec{T}^*$ are the unknown temperature vectors for the x and y directions respectively,

$$\bar{T}_j^{n+1} = \begin{bmatrix} T_{1,j}^{n+1} \\ T_{2,j}^{n+1} \\ \vdots \\ T_{i,j}^{n+1} \\ \vdots \\ T_{NX,j}^{n+1} \end{bmatrix} \qquad j = 0,1,\ldots,NY$$

---

(1) $\bar{A}_{x_j}$ is of order NX-1 since the boundary temperatures $T_{o,j}$ $j = 0,1,\ldots,NY$ are known for all times and therefore do not have to be calculated. Also, $\bar{A}_y$ will be of order NY-1 for $x \geq 0$ in Case II since $T_{i,NY}$ $i = MX,\ldots,NX$ is the specified surface temperature equal to 1 for all time.

$$\vec{T}^*_i = \begin{bmatrix} T^*_{i,o} \\ T^*_{i,1} \\ \vdots \\ T^{n+1}_{i,j} \\ \vdots \\ T^*_{i,NY} \end{bmatrix} \qquad i = 1,2,\ldots,NX$$

3.3 Method of Solution

Assume the temperatures over the first n time steps are known. To calculate the temperatures for the $(n+1)$ time step, Equation (3.17a) is solved for each $i = 1,\ldots,NX$ for the temperatures T^*, i.e. a tridiagonal system of NY equations and unknowns is solved $NX-1$ times. See Figure (3.2)

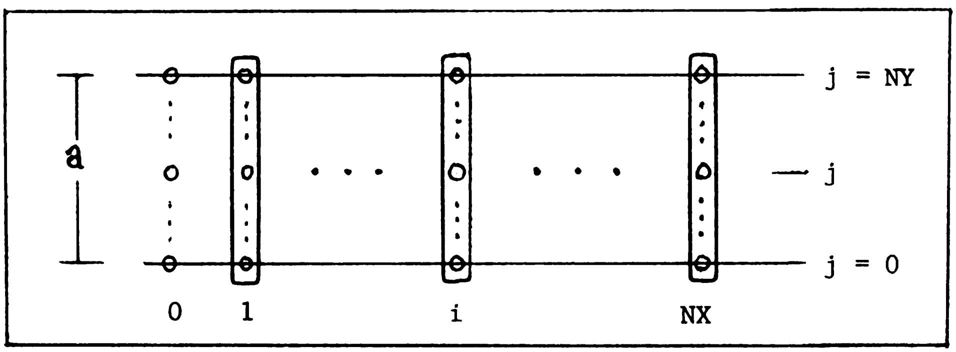

FIGURE 3.2: Y DIRECTION CALCULATION

Then with T^* known, Equation (3.16a) is solved for each $j = 0,1,\ldots,NY$ for the temperature T^{n+1}. This requires the solution of a tridiagonal system of $NX-1$ equations and unknowns NY times. See Figure (3.3).

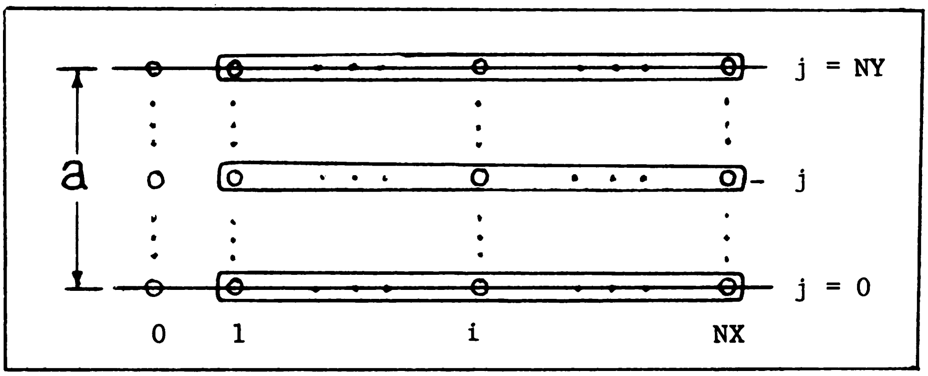

FIGURE 3.3: X DIRECTION CALCULATION

The tridiagonal matrices are easily upper triangularized to solve for T^{n+1} or T^* by Gauss elimination.

The solution time required to run the calculation to steady state with a typical mesh size of NX = 60 and NY = 10 on a CDC 3600 computer is from 30 seconds to 1 minute. Pe = 1 required NX = 108 with a run time of 1.5 minutes.

It should be mentioned that at $X^+ = 0$ where Δx must be very small for accurate calculation of the Nu number, the surface and bulk temperatures have been extrapolated to their respective T-intercept values as $(\Delta x)^2 \to 0$. Since the truncation error is of order $(\Delta x)^2$, $(\Delta y)^2$ and $(\Delta t)^2$ (see Appendix A), for a given $(\Delta y)^2$ and $(\Delta t)^2$ the temperature is linear in $(\Delta x)^2$ provided Δx is small enough. Two calculations for the same Δy and Δt and different Δx establishes the clope C_1 of the straight line,

$$T = C_1(\Delta x)^2 + C_2(\Delta y)^2 + C_3(\Delta t)^2 + T_o$$

C_2 and C_3 are nearly zero in the range of Δy and Δt used, so at $X^+ = 0$ we can express T_s and T_b as

$$T_s = C_{1s}(\Delta x)^2 + T_{so}$$

and

$$T_b = C_{1b}(\Delta x)^2 + T_{bo}$$

For the larger Pe numbers, T_{so} and T_{bo} are used in Equation (2.14). For smaller Pe and positions downstream from $X^+ = 0$, C_1 is negligible in the Δx range used.

3.4 Finite Difference Boundary Conditions

It is more instructive to formulate the boundary conditions from a conservation of energy principle on a finite element centered on a boundary node than from the Taylors series approach used for an interior node.

In this section, let the difference operators at a boundary be denoted by equating the subscript to the appropriate boundary index. For example, $\delta^2_{i=0}$, $\delta^2_{i=NX}$, $\delta^2_{j=0}$, $\delta^2_{j=NY}$ are the second order difference operators at the respective boundaries.

CASE I: Uniform Heat Flux

The upstream boundary condition on X^+ (Equation (2.9b)) is applied at $X^+ = -\ell$ where ℓ is large enough that the fluid temperature is not effected by the heated plates, (see Figure 3.1). This distance must be larger for the smaller Pe numbers.

At $X^+ = -\ell = -MX(\Delta x)$:

$$T^n_{o,j=0} \quad \begin{array}{l} j = 0,1,2,\ldots,NY \\ n = 0,1,\ldots \end{array}$$

At $y^+ = 0$

$$\delta_{j=\delta}(T^n) = 0$$

$$\delta^2_{j=o}(T^n) = 2(T^n_{i,1} - T^n_{i,o}) \qquad \begin{matrix} i = 1,2,\ldots,NX \\ n = 0,1,\ldots \end{matrix}$$

Consider the plate surface at $y^+ = 1$, $j = NY$.

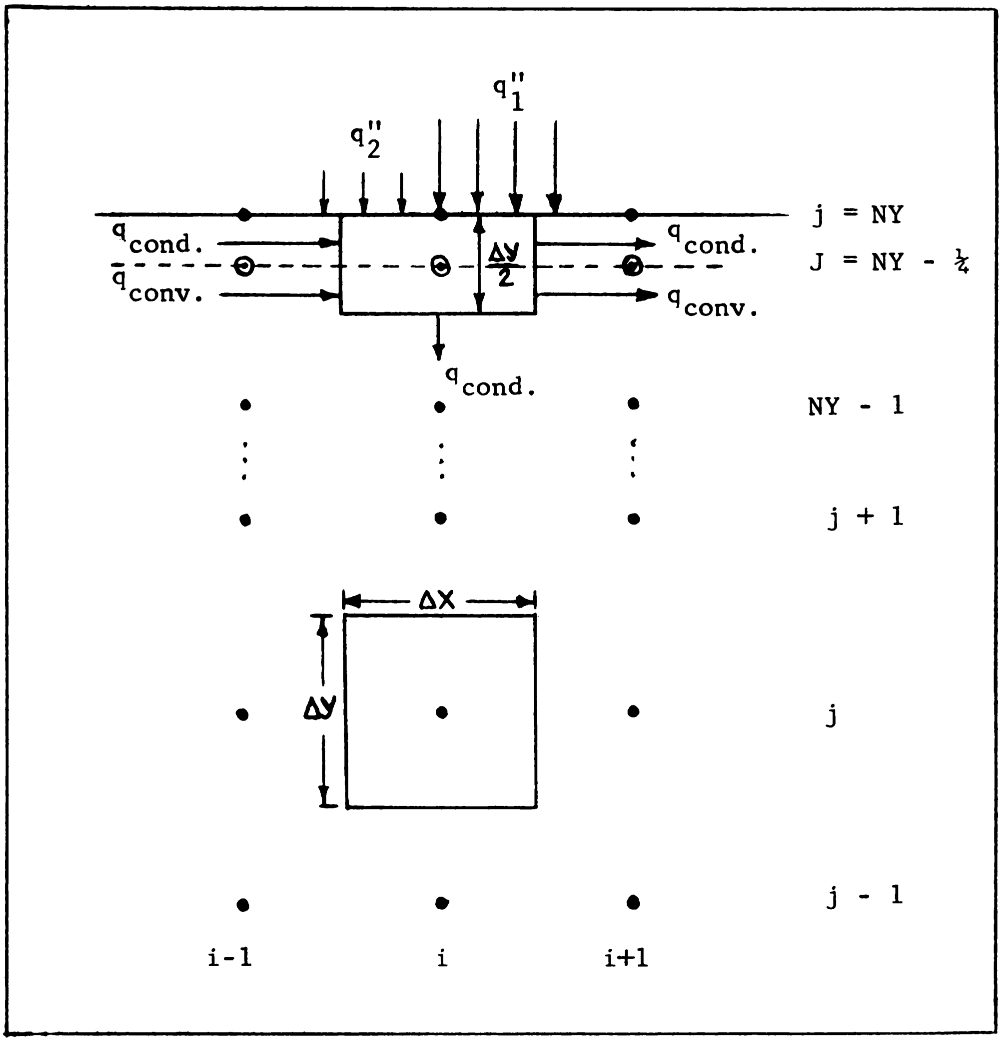

FIGURE 3.4: ENERGY BALANCE ON A DIFFERENTIAL ELEMENT

For an interior node, an energy balance applied to the element centered on the i,j node leads to the same finite difference equation derived before, Equation (3.12).

However, when considering a boundary node, the resulting "half" element or cell associated with this node should have fluxes centered on the half cell at a location $\Delta y/4$ from the plate surface (row of temperatures designated by θ connected by a dotted line in Figure 3.4).

The net rate of energy into the element is given as follows:

(1) Conduction: $\dot{q}_{cond}\Big|_{i-\frac{1}{2},J} - \dot{q}_{cond}\Big|_{i+\frac{1}{2},J} - \dot{q}_{cond}\Big|_{i,NY-\frac{1}{2}} =$

$$k\,\Delta z \left[\left(\frac{\Delta y}{2}\right)\frac{T_{i-1,J} - T_{i,J}}{\Delta x} - \left(\frac{\Delta y}{2}\right)\frac{T_{i,J} - T_{i+1,J}}{\Delta x} - \Delta x\,\frac{T_{i,NY} - T_{i,NY-1}}{\Delta y}\right]$$

where J designates the position $y_J = a - \frac{\Delta y}{4}$.

(2) Convection

$$\dot{q}_{conv.}\Big|_{i-\frac{1}{2},J} - \dot{q}\Big|_{i+\frac{1}{2},J} =$$

$$\rho u_J C_p \Delta z\,\frac{\Delta y}{2}\left[\frac{T_{i,J} + T_{i-1,J}}{2} - \frac{T_{i,J} + T_{i+1,J}}{2}\right]$$

Rate of energy accumulation within cell $= \rho C_p \Delta z \Delta x\,\frac{\Delta y}{2}\,\frac{\partial T}{\partial t}\Big|_{i,J}$

Completing the energy balance,

$$\rho C_p \frac{\partial T}{\partial t}\Big|_{i,J} + \rho C_p u_J \frac{T_{i+1,J} - T_{i-1,J}}{2\Delta x} =$$

$$k\left[\frac{T_{i+1,J} - 2T_{i,J} + T_{i-1,J}}{(\Delta x)^2} - 2\,\frac{T_{i,NY} - T_{i,NY-1}}{(\Delta y)^2}\right] + q''_1\frac{1}{\Delta y} + q''_2\frac{1}{\Delta y} \qquad (3.19)$$

Let $T_J = \frac{3}{4}T_{NY} + \frac{1}{4}T_{NY-1}$

or in general

$$T_J = C_1 T_{NY} + C_2 T_{NY-1}$$

where

$$C_1 = 3/4$$

$$C_2 = 1/4$$

The nodes along the boundary $y = a$ fall into three categories depending on the heat flux at that point.

(1) For those boundary nodes which fall in the region $X^+ < 0$, $(1 \le i \le MX-1)$, $q_1'' = q_2'' = 0$.

(2) For those in the region $X^+ > 0$ $(MX < i \le NX)$, $q_1'' = q_2'' = q''$.

(3) For the boundary node located at the discontinuity in heat flux at $X^+ = 0$, $q_1'' = q''$ and $q_2'' = 0$.

Expressing Equation (3.19) in the dimensionless ADI form we have, for the X-Direction

$$[\alpha_x + \Delta x\ u_j \delta_i - \frac{1}{Pe^2}\delta_i^2]T_{i,J}^{n+1} = \alpha_x T_{i,J}^* + [\Delta x\ u_J \delta_i - \frac{1}{Pe^2}\delta_i^2]T_{i,J}^n \quad (3.20)$$

In terms of C_1 and C_2,

$$C_1[\alpha_x + \Delta x\ u_{NY}\delta_i - \frac{1}{Pe^2}\delta_i^2]T_{i,NY}^{n+1} = -C_2[\alpha_x + \Delta x\ u_{NY-1}\delta_i - \frac{1}{Pe^2}\delta_i^2]T_{i,NY-1}^{n+1}$$

$$+ C_1\{\alpha_x T_{i,NY}^* + [\Delta x\ u_{NY}\delta_i - \frac{1}{Pe^2}\delta_i^2]T_{i,NY}^n\}$$

$$+ C_2\{\alpha_x T_{i,NY-1}^* + [\Delta x\ u_{NY-1}\delta_i - \frac{1}{Pe^2}\delta_i^2]T_{i,NY-1}^n\} \quad (3.21a)$$

$$i = 1,2,\ldots,NX-1$$

Note the ease with which this boundary condition can be implemented using the ADI numerical method. The right hand side of (3.21a) is known since the $T_{i,NY-1}^{n+1}$ $i = 1,\ldots,NX$ row of temperatures are calculated before the NY row.

For $i = NX$, $\delta_i^2 = 0$ and $\delta_{i=NX}(T)$ becomes $\frac{1}{2}(T_{NX,J} - T_{NX-1,J})$ in (3.21a).

If $\delta^2_{j=NY}(T) = 2(T_{i,NY-1} - T_{i,NY}) + \Delta y \; \dfrac{q_1''}{q''} + \dfrac{q_2''}{q''}$ then, using (3.18c) and (3.18d) we have for the

Y-Direction

$$\alpha_y T^*_{i,J} - \delta^2_{j=NY} T^*_{i,NY} = [\alpha_y - \Delta x\beta\, \delta_i + E\, \delta_i^2](C_1 T^n_{i,NY} + C_2 T^n_{i,NY-1}) + \delta^2_{j=NY} T^n_{i,NY} \tag{3.21b}$$

For $i = NX$, $\delta_i^2 = 0$ and $\delta_{i=NX}(T) = \frac{1}{2}(T_{NX,J} - T_{NX-1,J})$ in (3.21b).

For this case, the downstream x-boundary condition, $\partial^2 T^+(L-\ell, y^+, t^+)/\partial X^{+2} = 0$ can be applied before the development length, X^+_{Dev}, is reached without effecting the results in the region near $X^+ = 0$. Therefore, when a smaller mesh size for greater accuracy at $X^+ = 0$ is required, $(L-\ell)$ may be less than X^+_{Dev}. The development length, defined as being that length from the entrance at which the local steady state Nu number is within 5% of its final value, is shown verses Pe number in Figure 3.5. This shows that the Pe number dependence, other than in $X^+ = \frac{x}{aPe}$, is important for $Pe < 20$. The fully developed value of $X^+_{Dev} = 0.186$ agrees with Cess and Schaffer (46).

CASE II: Uniform Tempreature

The boundary conditions for this case are the same as for Case I except for the constant wall temperature, $T^n_{i,NY} = 1 \quad i = MX,\ldots,NX$, and the downstream x-boundary condition.

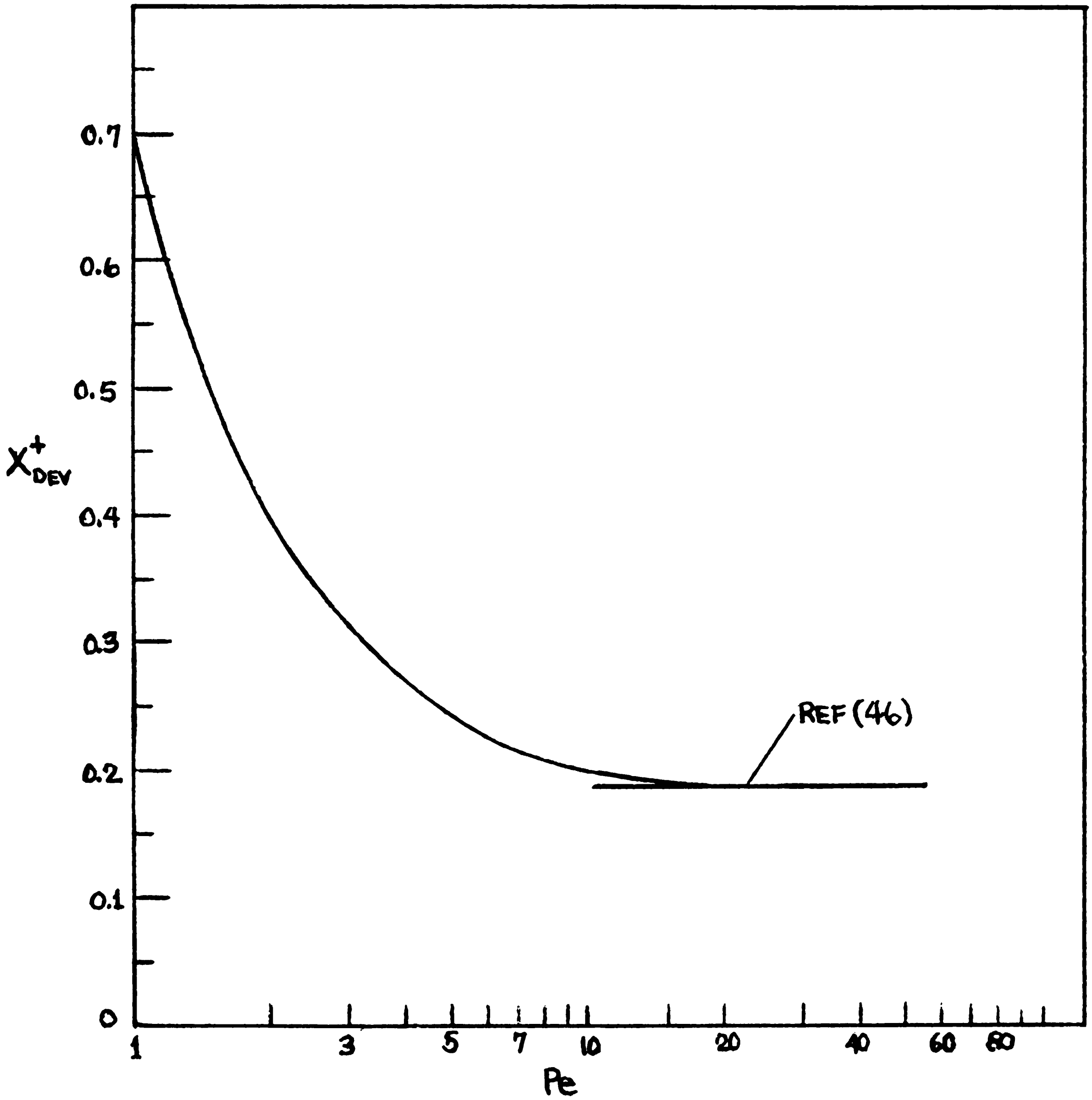

FIGURE 3.5 DEVELOPMENT LENGTH - CASE I

Applying the boundary condition (2.10c) at a location upstream of X^+_{Dev} is more critical to the results in the entrance region than in Case I. However, with the following treatment of this boundary, the region about $X^+ = 0$ appears to be relatively insensitive to the placement of the downstream condition.

Let $\delta_{i=NX} = \delta^2_{i=NX} = 0$

and

$$T^n_{NX,j} = T^n_{NX-1,j}$$

This treatment of the downstream boundary on x eliminates the back-propagation of boundary anomalies into the entrance region resulting from not applying the condition far enough downstream.

IV. DISCUSSION OF RESULTS FOR CASES I AND II

In this chapter we shall investigate the effects of allowing axial conduction upstream of the heated region. Of particular interest are the results at the entrance $X^+ = 0$, since it is here that considerable deviation from previous studies exists.

4.1 Case I

If axial conduction is neglected, the steady state bulk temperature increases linearly with X^+ from zero. As can be seen from Figure 4.1, axial conduction has the effect of increasing the bulk temperatures. Since the region $X^+ < 0$ is insulated, the heat conducted upstream is convected downstream, raising the fully developed, dimensionless bulk temperature, T_b^+, by $1/Pe^2$ as compared to the case with no axial conduction. The steady state, fully developed temperature profile, T^+, and T_b^+ are derived in Appendix B from an energy balance on a control volume which includes the entrance and upstream regions. For $X^+ > X^+_{Dev.}$ the dimensionless steady state temperature T^+ is,

$$T^+ = X^+ + \frac{1}{Pe^2} + \frac{3}{4} y^{+^2} - \frac{1}{8} y^{+^4} - \frac{39}{280} \tag{4.2}$$

and the bulk temperature is,

$$T_b^+ = X^+ + \frac{1}{Pe^2} \tag{4.3}$$

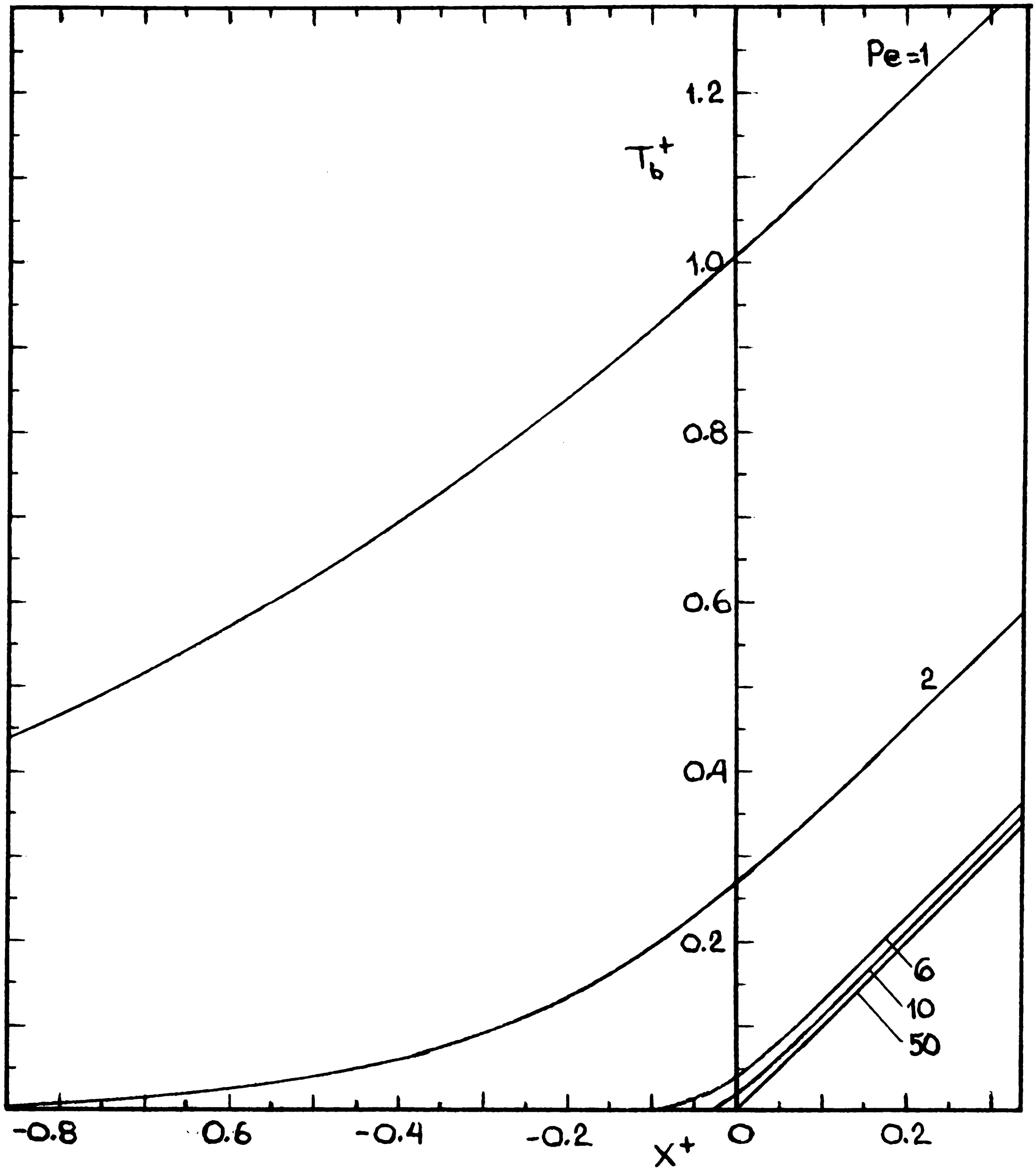

FIGURE 4.1 STEADY STATE BULK TEMPERATURE IN THE ENTRANCE REGION - CASE I

At $X^+ = 0$ and the region immediately downstream, the bulk temperatures are slightly greater than their extrapolated asymptotic or fully developed values and decay exponentially for $X^+ < 0$. Note that the development length for T_b^+ is much shorter than that used to define the entrance region, (i.e. $X^+_{Dev.}$).

The temperature profiles at $X^+ = 0$ for various Pe numbers are given in Figure 4.2. Notice how axial conduction from the heated region alters the temperature profile of the incoming fluid. This clearly shows the error in those papers which make a point of including axial conduction and then, through the boundary condition, force a uniform temperature profile at the entrance. This forces the temperature here to be the same as for the case where axial conduction effects are neglected. However, it is at $X^+ = 0$, more then anywhere else in the entrance region, that these effects are greatest. Also, note that since T_s^+ and T_b^+ at $X^+ = 0$ are both zero only as $Pe \to \infty$, the $Nu_{X^+=0}$ as defined by Equation (2.14) is finite for finite Pe.

The Nu number in the entrance region for Pe = 1,2,6,10, 20,50, and ∞ is given in Figure 4.3. For $X^+ < 0.02$, the Nu number decreases with decreasing Pe, while the opposite is true for $X^+ > 0.02$. This can also be seen from Figure 4.4 which gives the Nu number as a function of Pe for $X^+ = 0$ and several positions downstream of the entrance. The fully developed value of 8.225, as shown in Figure 4.3 is in agreement with Kays (45).

It is apparent from these figures that axial conduction can have a considerable effect on the Nu number. The greater the Pe number the smaller the region about $X^+ = 0$ where the Nu number

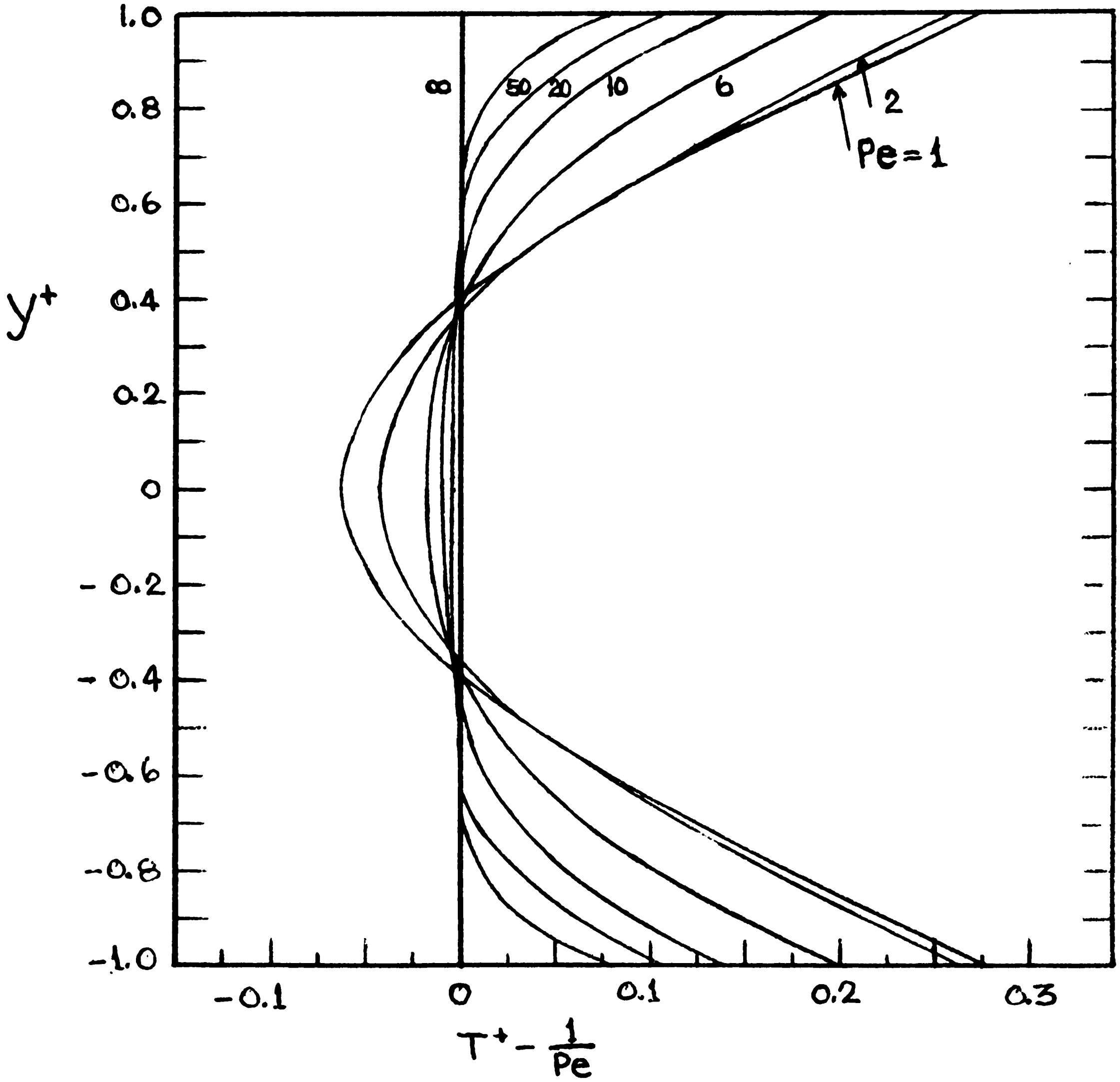

FIGURE 4.2 STEADY STATE TEMPERATURE PROFILES AT X=0 - CASE I

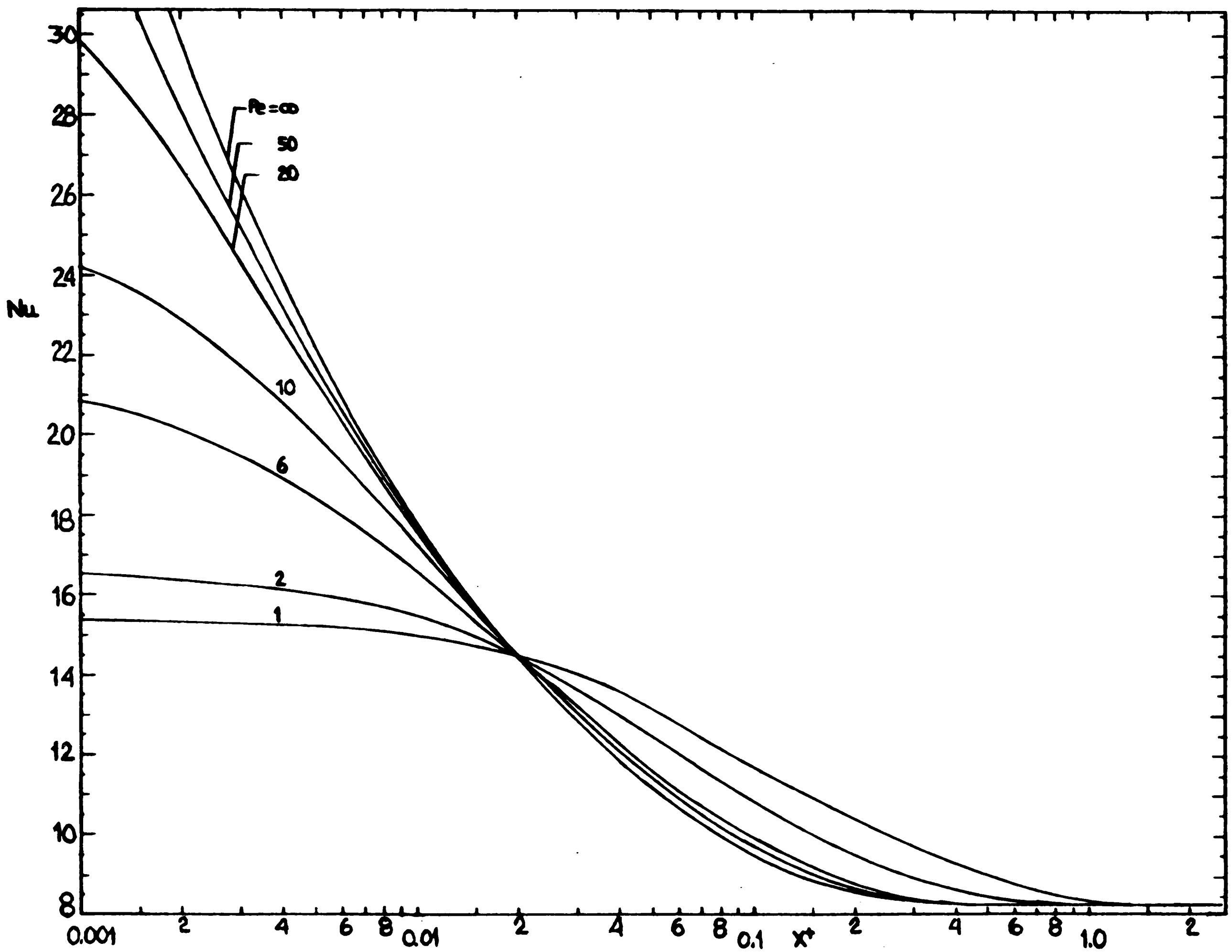

FIGURE 4.3 STEADY STATE NUSSELT NUMBER IN THE ENTRANCE REGION - CASE I

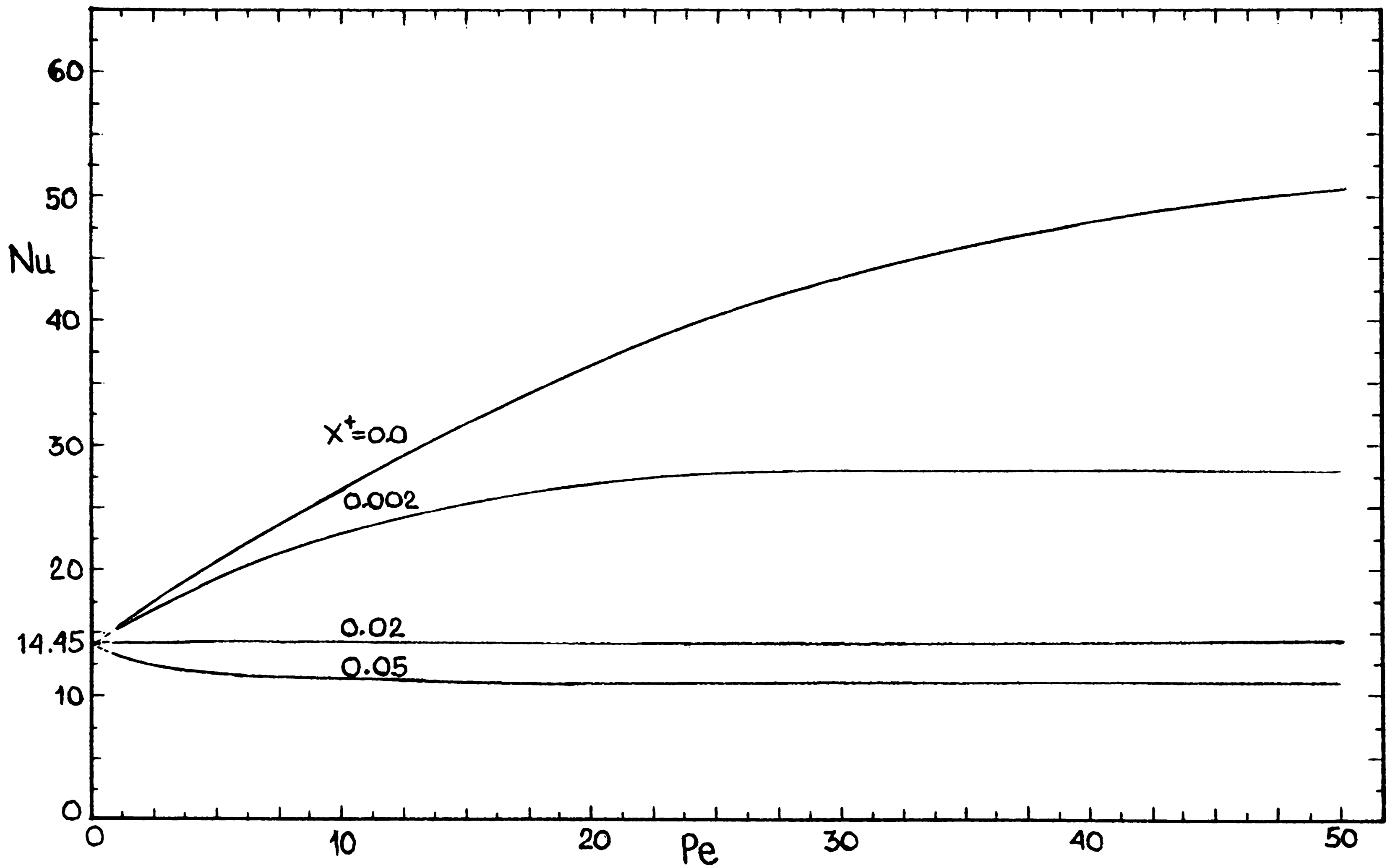

FIGURE 4.4 FUNCTIONAL DEPENDENCE OF NUSSELT NUMBER ON PECLET NUMBER - CASE I

deviates from the case of no axial conduction. However, even for $Pe > 50$ this deviation could be significant when dealing with a wall heat flux varying with X^+.

Since the energy equation is linear, superposition of the basic kernel for a step change in q'' can be used to generate the response to any variable heat flux $q''(X^+)$. In this way, the results in a neighborhood of, and including $X^+ = 0$ would be distributed throughout the region of interest. If the axial conduction is not included the resulting surface temperature and Nu number for such a case could be in substantial error even for large Pe number. For a further discussion on the superposition of solutions, see Chapter 6.

The temperature profiles for $Pe = 6$ in the entrance region are shown in Figure 4.5. The profiles should converge to the fully developed profile envelope as given by Equation (4.2). As can be seen, when $X^+ = 0.45$, the numerical results lie on this envelope.

The transient heat conduction solution for an infinite slab of thickness $2a$ in the y- direction with a constant wall heat flux, q'' is (54),

$$T = \frac{q''t}{\rho C_p a} + \frac{q''a}{k}\left(\frac{3y^2-a^2}{6a^2} - \frac{2}{\pi^2}\sum_{n=1}^{\infty}\frac{(-1)^n}{n^2}e^{-n^2\pi^2\frac{\alpha t}{a^2}}\cos\frac{n\pi y}{a}\right) \tag{4.4}$$

or in terms of the dimensionless variables of the entrance region problem as given in (2.7),

$$T^+(y^+,t^+) = t^+ + \frac{3y^{+2}-1}{6} - \frac{2}{\pi^2}\sum_{n=1}^{\infty}\frac{(-1)^n}{n^2}e^{-n^2\pi^2t^+}\cos n\pi y^+ \tag{4.5}$$

$$T_s^+ = T^+(1,t^+) = t^+ + \frac{1}{3} - \frac{2}{\pi^2}\sum_{n=1}^{\infty}\frac{1}{n^2}e^{-n^2\pi^2t^+} \tag{4.6}$$

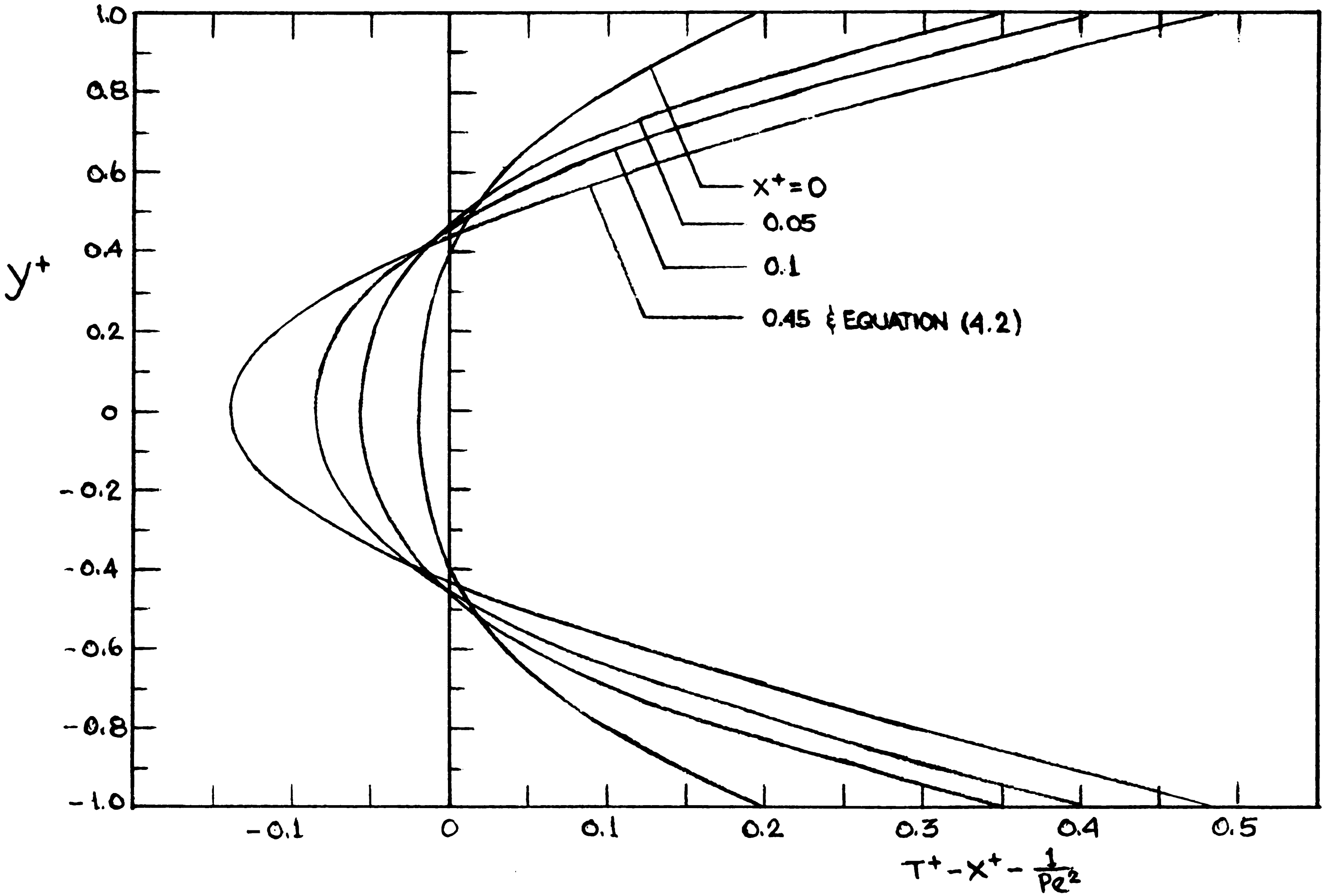

FIGURE 4.5 STEADY STATE TEMPERATURE PROFILES IN THE ENTRANCE REGION - CASE I

For flow in the entrance region downstream of the heat flux discontinuity at $X^+ = 0$, convection has no influence on the temperature response during early times since $\partial T^+/\partial X^+$ is zero then and Equation (2.8) reduces to the heat conduction equation. Therefore, if one were to use the temperatures given by Equations (4.5) and (4.6) in the usual expressions for the bulk temperature (Equation (2.17)) and Nu number (Equation (2.14)), the slab transient heat conduction problem should predict the early transient behavior some distance (dependent on the time considered) downstream of $X^+ = 0$. This is indeed the case as can be seen from Figure 4.6, which gives the transient results before steady state is reached.

Recall the expression for the bulk temperature,

$$T_b^+ = \int_0^1 u^+ T^+ dy^+ = \frac{3}{2}\int_0^1 (1 - y^{+^2}) T^+ dy^+ \tag{4.7}$$

Substituting Equation (4.5) into (4.7) and integrating gives,

$$T_b^+ = t^+ - \frac{1}{15} + \frac{6}{\pi^4} \sum_{n=1}^{\infty} \frac{1}{n^4} e^{-n^2 \pi^2 t^+} \tag{4.8}$$

Equations (2.14), (4.6), and (4.8) are combined to give an effective slab Nu number of,

$$Nu = \frac{2}{\frac{1}{5} - \frac{1}{\pi^2} \sum_{n=1}^{\infty} \left(\frac{1}{n^2} + \frac{3}{\pi^2}\frac{1}{n^4}\right) e^{-n^2\pi^2 t^+}} \tag{4.9}$$

For steady state, Equation (4.9) becomes

$$Nu = 10 \tag{4.10}$$

Notice that the velocity profile enters into the slab Nu number only as the weighting function in the bulk temperature

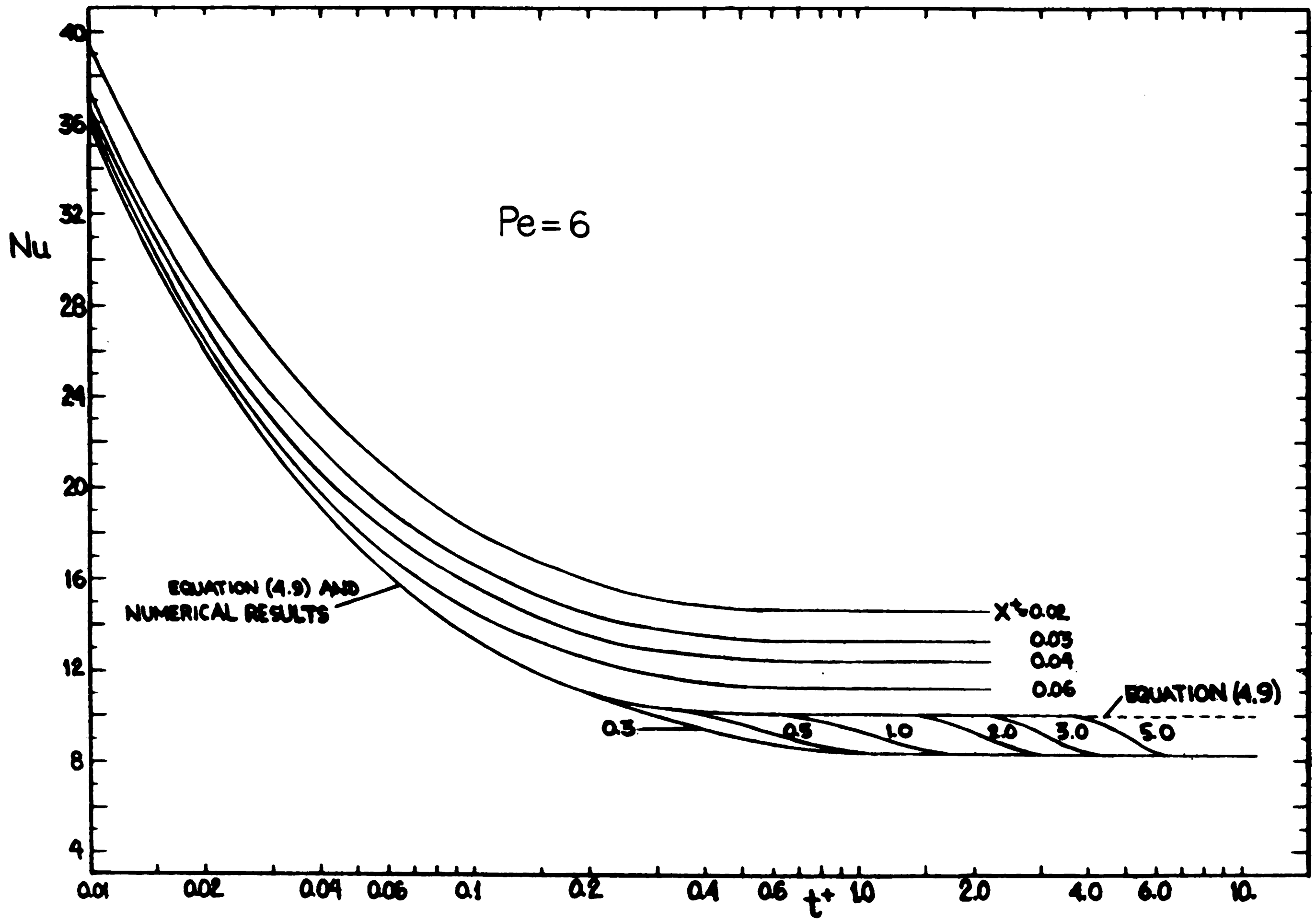

FIGURE 4.6 TRANSIENT NUSSELT NUMBER IN THE ENTRANCE REGION - CASE I

calculation. Hence, we would expect different transient and steady state results to the slab problem depending on the velocity profile assumed.

For the example of $Pe = 6.0$, Figure 4.6 shows the transient Nu numbers for various X^+ positions as well as Equation (4.9) for conduction only, while Figure 4.7 gives the Nu number versus X^+ for various times. The Nu number is infinite at the instant the heat flux is applied and in the entrance region $(X^+ < X^+_{Dev.})$ reduces to a given steady state value depending on the location X^+.

Now, consider the region $X^+ > X^+_{Dev.}$. We have seen that the steady state, fully developed Nu number is 8.225. However, if the distance downstream is sufficiently large $(X^+ > 0.3$ for $Pe = 6)$ the Nu number reaches a secondary steady state dwell at a value of 10 predicted by the transient heat conduction problem, Equation (4.10). Under these conditions, the length of time for the heat conduction response (Equation (4.9)) to reach steady state is shorter than the time required for a slug of fluid experiencing the entrance effects to be convected downstream to this location. Hence, the Nu number remains at this platau of 10 until the convection effects act to reduce its value to the final or primary steady state value of 8.225.

Figure 4.6 shows the numerical results following exactly the curve of Equation (4.9) until convection effects are felt. For the region in the immediate downstream vicinity of $X^+ = 0$, (e.g. the curves shown for $X^+ < 0.06$) convection is significant even for very early times, resulting in transient Nu number curves which differ widely from Equation (4.9).

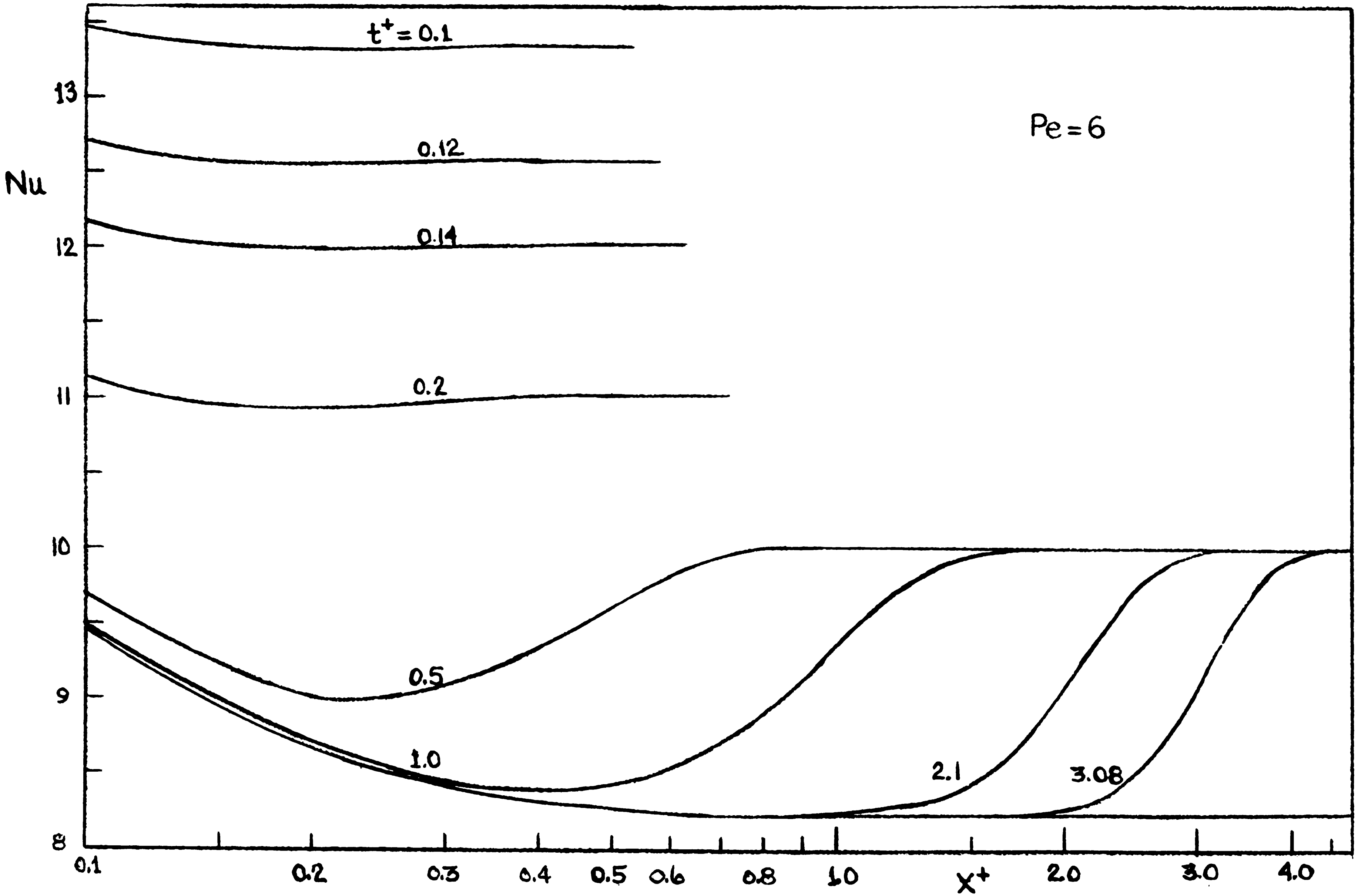

FIGURE 4.7 NUSSELT NUMBER IN THE ENTRANCE REGION AT VARIOUS TIMES - CASE I

Notice the $t^+ = 3.08$ curve in Figure 4.7 reaches, near $X^+ = 1.0$, the final steady state value of 8.225 while at large values of X^+, convection effects are not yet felt and $Nu = 10$. This minimum also exists to a lesser extent for very early times indicating the region of influence of convection.

It is evident from these results that the time constant to reach steady state can be deceptive unless some information is given concerning the X^+ position under consideration.

4.2 Case II

Results for the insulated surface upstream of the constant temperature surface are given in Figures 4.8 - 4.13. Though this case is not required for the inverse problem of Chapter 5, the results are included here for completeness.

Consideration of this mixed boundary condition is motivated by the fact that it could be used in conjunction with the velocity profiles of (40 or (41) in treating the combined hydrodynamic and thermal entry region. If the plates are maintained at the same temperature, the thermal boundary condition at the plane of symmetry in the upstream region ($y = a$, $x < 0$ in Figure 4.14) is zero heat flux in the y-direction analogous to the momentum boundary condition of zero shear used in refs. (40) or (41). The wall temperature could be a function of x and t providing the temperature of the plates at a given position and time is the same.

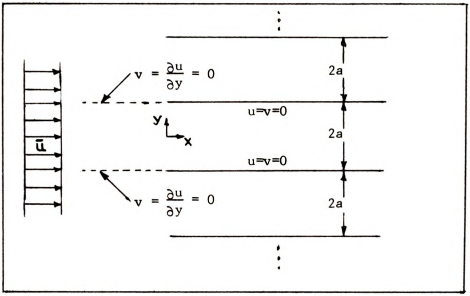

FIGURE 4.14: HYDRODYNAMIC ENTRANCE REGION FOR A SERIES OF PARALLEL PLATES-REFERENCE (40, 41)

This case is not treated in the present work, although no difficult is seen in using velocity profiles from (40) or (41) in Equation (2.1) with the given ADI numerical method. The author strongly recommends investigating this problem.

Figure 4.8 indicates the effect of axial conduction upstream on the bulk temperatures. As discussed in regards to Case I, when axial conduction upstream is significant, the resulting bulk temperatures in the entrance region are larger than for the case of no axial conduction.

Figure 4.9 illustrates the effect of axial conduction upstream on the temperature profiles at $X^{+} = 0$. As in Case I, there is considerable distortion of the uniform profile by the time the fluid reaches the heated region for the smaller Pe numbers.

Figures 4.10 and 4.11 give the temperature profiles at various positions in the entrance region for $Pe = 6$ and 50 respectively.

The Nu number in the entrance region for several Pe numbers is shown in Figure 4.12 while the fully developed transient Nu number is given in Figure 4.13.

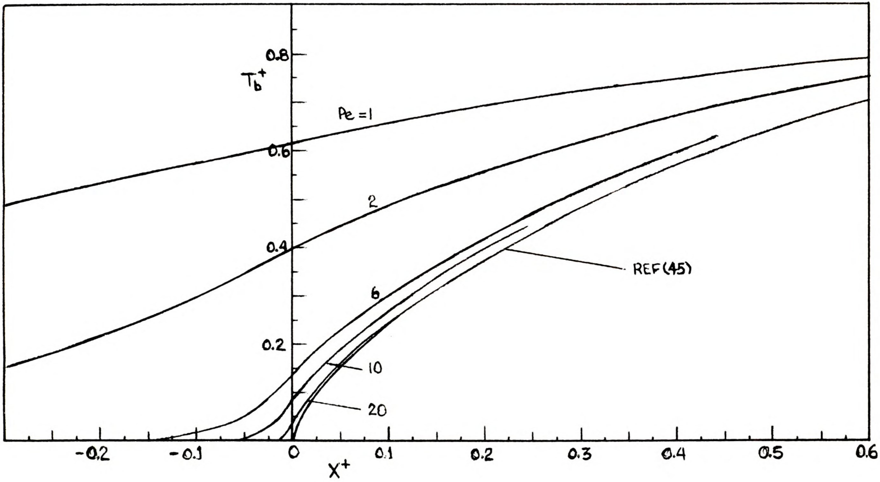

FIGURE 4.8 STEADY STATE BULK TEMPERATURE IN THE ENTRANCE REGION - CASE II

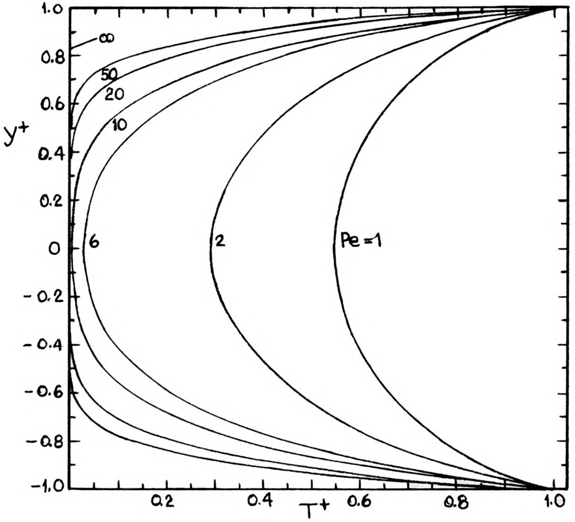

FIGURE 4.9 STEADY STATE TEMPERATURE PROFILES AT X=0 - CASE II

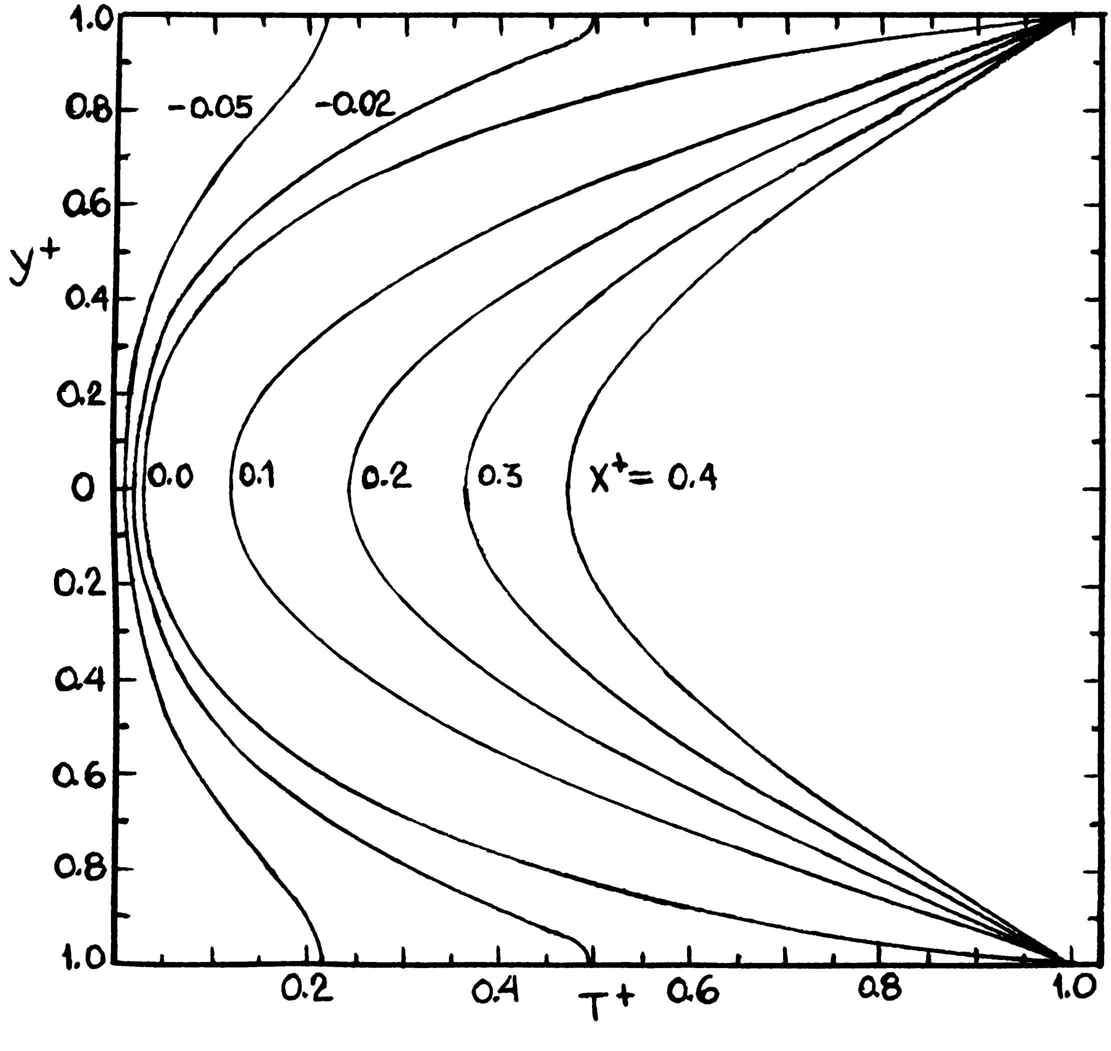

FIGURE 4.10 STEADY STATE TEMPERATURE PROFILES IN THE ENTRANCE REGION FOR Pe = 6

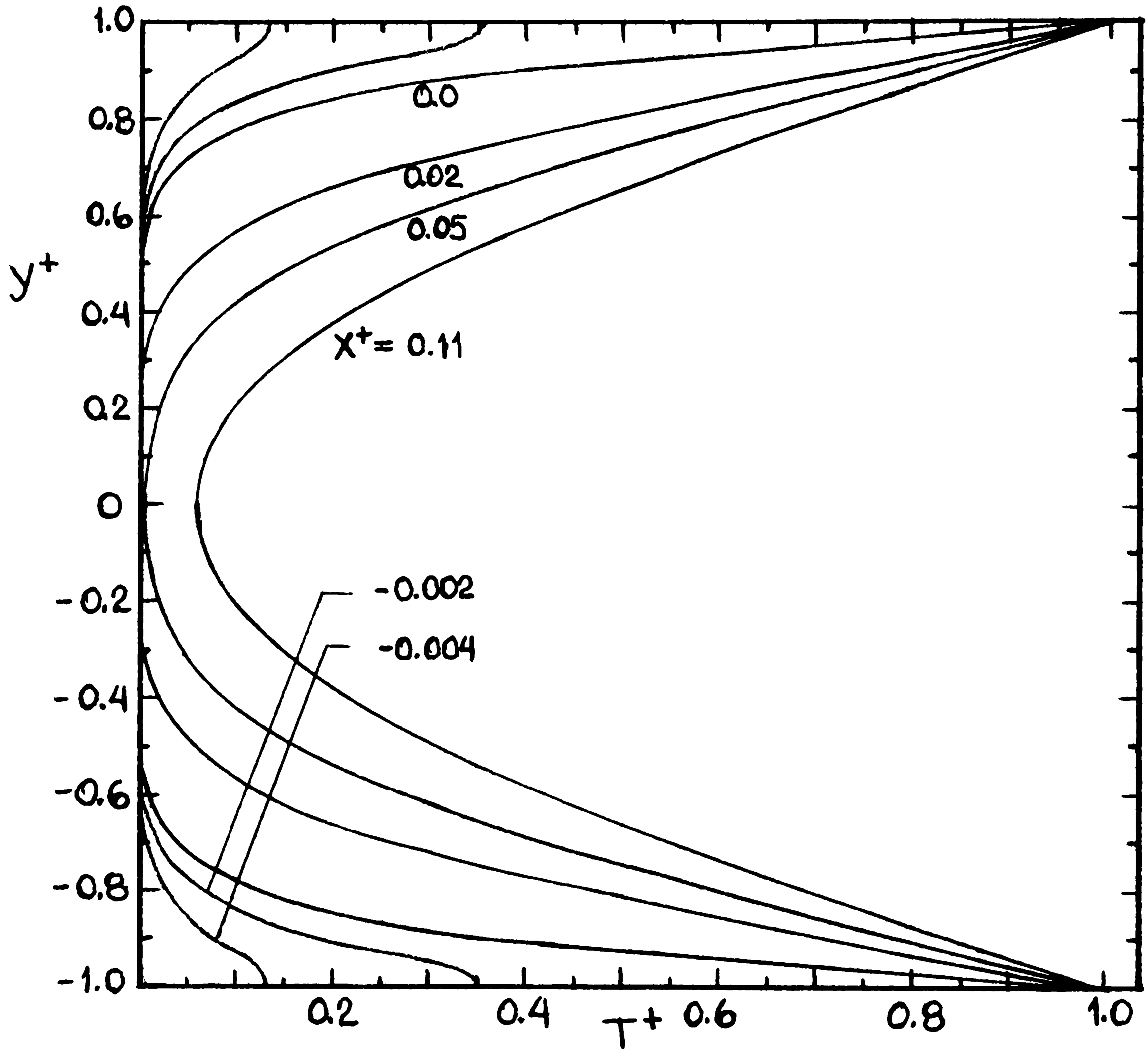

FIGURE 4.11 STEADY STATE TEMPERATURE PROFILES IN THE ENTRANCE REGION FOR Pe = 50

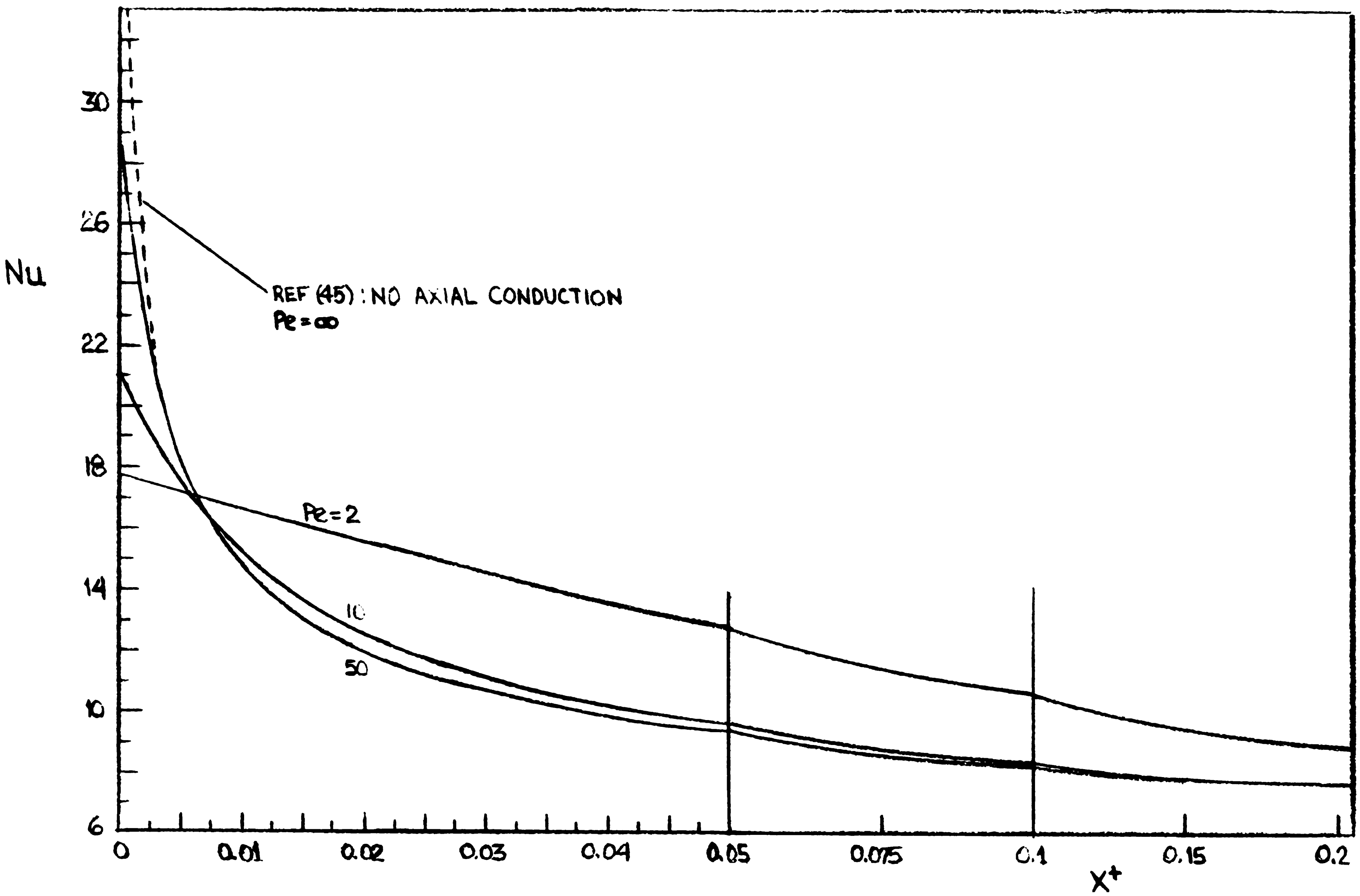

FIGURE 4.12 STEADY STATE NUSSELT NUMBER IN THE ENTRANCE REGION - CASE II

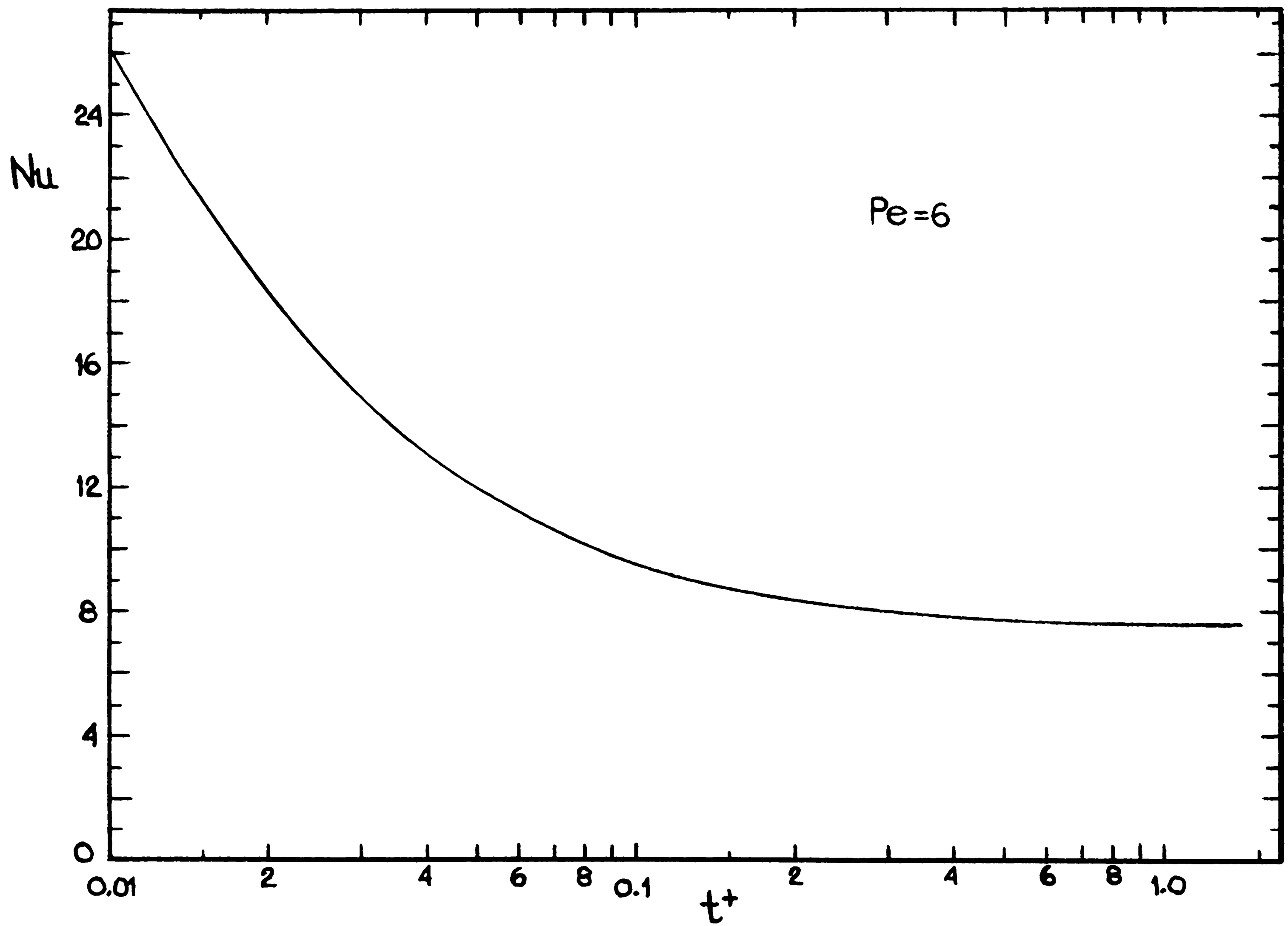

FIGURE 4.13 FULLY DEVELOPED TRANSIENT NUSSELT NUMBER - CASE II

V. OPTIMUM EXPERIMENT FOR DETERMINING THE MEAN VELOCITY FROM THERMAL MEASUREMENTS

In this chapter the solution of Case I is used as a basic building block in the superposition integral (see Chapter VI). As a result, the optimum wall heat flux, $q''(X^+,t^+)$ and optimum placement of thermocouples for a given duration of the experiment are determined so as to yield a maximum sensitivity of wall temperature to a change in some parameter of the velocity profile (in this case the mean velocity) under the constraint of a maximum surface temperature rise. In this sense, the solution of the energy equation, with overspecified wall boundary conditions of given heat flux and temperature measurements, is treated as an inverse problem where the velocity is an unknown coefficient.

5.1 Nonlinear Estimation Procedure

The procedure for calculating unknown parameters appearing in a differential equation which describes a physical process is called nonlinear estimation. A least squares procedure, it utilizes experimental data obtained from the process and the numerical solution of the given equation in calculating the parameters.

Referring to Equations (2.1), (2.2), and (2.3), u is an unknown coefficient. Any parameter of the velocity profile can be determined, but since a parabolic profile is assumed the obvious one is the mean velocity, $\bar{u}$. It is also possible to simultaneously

determine more than one parameter (51-53).

In dimensionless form, Equation (2.8) describes the physical process of interest.

$$\frac{\partial T^+}{\partial t^+} + u^+ \frac{\partial T^+}{\partial X^+} = \frac{1}{Pe^2} \frac{\partial^2 T^+}{\partial X^{+2}} + \frac{\partial^2 T^+}{\partial y^{+2}} \tag{2.8}$$

Since u^+ remains the same for any value of the mean velocity, $\bar{u}$ is determined through evaluation of the Pe number, $Pe = \frac{\bar{u}\, a}{\alpha}$. In terms of Equation (2.8) then, the objective is to determine the Pe number from thermal measurements taken at the boundary during an experiment run under optimum conditions.

For continuous transient temperature measurements from n thermocouples placed on the plate boundary, the sum of squares function F

$$F(Pe) = \sum_{i=1}^{n} \int_0^{\tau} A_i(t)[T_s(t) - \theta(t)]_i^2 dt \tag{5.1}$$

is to be minimized with respect to Pe. The temperature $T_s(t)|_i$ a function of Pe, is the calculated numerical solution to Equation (2.8) at position X_i^+, $y^+ = 1$, and time t, for a specified heat flux, q"(x,t), (derived from the Case I solution by superposition). The corresponding experimental temperature is given by $\theta_i(t)$. The quantity A_i, subsequently taken to be unity, is a weighting factor included here for generality. If the statistics of the errors in the temperature measurements are known, A_i is often taken to be the inverse matrix of the variance-covariance matrix of the errors.

A number of procedures have been suggested for minimizing F, some of which are the method of steepest descent and modifications to the Taylor series approach (47, 48). Under optimum conditions

the Taylor series approach yields very rapid convergence (see the example in Section 6.4) and will be used in this work.

Though the calculated temperature is a nonlinear function of the Pe number, the Taylor series method is an iterative procedure which assumes that at each step the temperature is a linear function of Pe. If Pe_o is an initial estimate of the Pe number, then

$$T_s(Pe) \cong T_s(Pe_o) + \Delta Pe \frac{\partial T_s(Pe_o)}{\partial Pe} \tag{5.2}$$

where $\Delta Pe = Pe - Pe_o$ is the first correction in the Pe number. Noting that at the point Pe^* at which F is a minimum, $\frac{\partial F^*}{\partial Pe}$ is zero, Equations (5.1) and (5.2) can be solved to give the first correction in Pe.

$$\frac{\partial F}{\partial Pe} = 2 \sum_{i=1}^{n} \int_o^\tau [T_s(Pe_o) + \Delta Pe \frac{\partial T_s(Pe_o)}{\partial Pe} - \theta]_i \frac{\partial T_{s,i}(Pe_o)}{\partial Pe} \, dt$$

At the minimum value of F (i.e. F^*) we have,

$$0 = \sum_{i=1}^{n} \int_o^\tau [T_s(Pe_o) - \theta]_i \frac{\partial T_{s,i}(Pe_o)}{\partial Pe} \, dt + \sum_{i=1}^{n} \int_o^\tau [\frac{\partial T_s(Pe_o)}{\partial Pe}]_i^2 \, \Delta Pe \, dt$$

Solving for ΔPe,

$$\Delta Pe = \frac{\sum_{i=1}^{n} \int_o^\tau [\theta - T_s(Pe_o)]_i \frac{\partial T_{s,i}(Pe_o)}{\partial Pe} \, dt}{\sum_{i=1}^{n} \int_o^\tau [\frac{\partial T_s(Pe_o)}{\partial Pe}]_i^2 \, dt} \tag{5.3}$$

For one thermocouple making NT discrete measurements in time τ, Equation (5.3) becomes,

$$\Delta Pe = \frac{\sum_{k=1}^{NT} [\theta - T_s(Pe_o)]_k \frac{\partial T_{s,k}(Pe_o)}{\partial Pe}}{\sum_{k=1}^{NT} [\frac{\partial T(Pe_o)}{\partial Pe}]_k^2} \tag{5.4}$$

$$\tau = NT(\Delta t)$$

An improved value of Pe is given by

$$Pe_1 = Pe_o + \Delta Pe \quad .$$

and the iteration procedure is continued until some convergence criterion is met, say

$$\frac{\Delta Pe}{Pe} < 0.0001$$

5.2 Objective Function for Determining Optimum Experiment

In order to determine an optimum experiment it is necessary to find some basic criterion which when extremized yields the optimum experiment. The criterion is frequently called an objective function. An experiment can be an optimum one in various aspects and thus there may be different optimums depending upon the desired objectives and constraints. For this problem, the best heat flux boundary condition is determined to insure that, for a random distribution of errors in the wall temperature measurement, the resulting error in the mean velocity is a minimum. In maximizing this objective function the following conditions are satisfied.

1. The maximum surface temperature rise is to be ΔT_{max}. This can be chosen small enough to make the assumption of k, ρ, C_p,

and $\bar{u}$ independnet of temperature realistic.

2. The number of thermocouples, n, along the plate is fixed. Specifically, optimum conditions for one thermocouple are found.

3. There is a fixed duration of the experiment, τ. For NT discrete measurements in time, $\tau = NT(\Delta t)$.

Assume that the value of the Pe number at the minimum of F(Pe) is known and is designated Pe^*. The minimum value of the sum of squares function, F^*, need not be zero but it is assumed that the errors in the temperature measurements are small.

Let us examine F(Pe) in the local region near $F^* = F(Pe^*)$. The sum of squares function is,

$$F(Pe) = \sum_{i=1}^{n} \int_{o}^{\tau} [T_s(t) - \theta(t)]_i^2 dt \tag{5.1}$$

$$F(Pe^* + \Delta Pe) \cong \Delta Pe \frac{dF^*}{dPe} + \frac{(\Delta Pe)^2}{2} \frac{d^2F^*}{dPe^2} \tag{5.4}$$

$$\frac{dF^*}{dPe} = 0 = 2 \sum_{i=1}^{n} \int_{o}^{\tau} (T_s^* - \theta)_i \frac{\partial T_s^*}{\partial Pe} dt \tag{5.5}$$

$$\frac{d^2F^*}{dPe^2} = 2 \sum_{i=1}^{n} \int_{o}^{\tau} (T_s^* - \theta)_i \frac{\partial^2 T_s^*}{\partial Pe^2} dt$$

$$+ 2 \sum_{i=1}^{n} \int_{o}^{\tau} (\frac{\partial T_s^*}{\partial Pe})_i^2 dt \tag{5.6}$$

If the error in the temperature measurements is small, then the first term on the right hand side of Equation (5.6) is negligible compared to the second term. Substituting Equations (5.5) and (5.6) into (5.4) we have,

$$F(Pe^* + \Delta Pe) = F^* + (\Delta Pe)^2 \sum_{i=1}^{n} \int_0^\tau \left(\frac{\partial T_s^*}{\partial Pe}\right)_i^2 dt$$

$$= F^* + \left(\frac{\Delta Pe}{Pe^*}\right)^2 \sum_{i=1}^{n} \int_0^\tau \left(Pe^* \frac{\partial T_s^*}{\partial Pe}\right)_i^2 dt$$

Let $$\phi = \sum_{i=1}^{n} \int_0^\tau \left(Pe^* \frac{\partial T_s^*}{\partial Pe}\right)_i^2 dt \tag{5.7}$$

Then $$F(Pe^* + \Delta Pe) - F^* = \left(\frac{\Delta Pe}{Pe^*}\right)^2 \phi \tag{5.8}$$

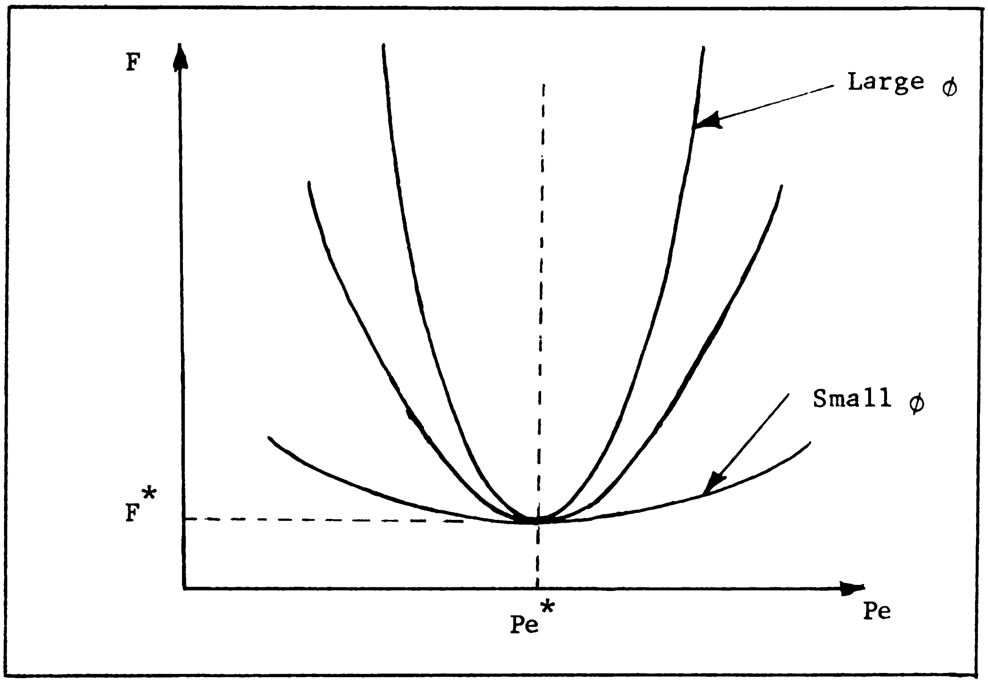

FIGURE 5.1: ILLUSTRATION OF SUM OF SQUARES FUNCTION

Referring to Figure 5.1, we see that for a well defined minimum in $F(Pe)$, ϕ should be a maximum.

Considerable information can be gained from the sensitivity coefficient defined as $Pe \frac{\partial T}{\partial Pe}$ (51). It is the principle quantity of interest in the objective function since it gives in a relative way a measure of how sensitive the temperature is to a change in Pe number. Obviously, if we are to calculate the Pe number from temperature measurements we would like this sensitivity coefficient as large as possible. Also, it can be especially instructive when considering two or more parameters since it establishes to which parameter the temperature is most sensitive.

The objective function, ϕ, must be modified to include the constraints of maximum temperature rise, $\Delta T_{max} = T_{max} - T_o$, and given duration of experiment, τ. This can be accomplished by dividing the right hand side of Equation (5.7) by $\tau \, \Delta T_{max}^2$. The resulting objective function Φ, given by Equation (5.9), is a dimensionless criterion which is to be maximized with respect to the boundary heat flux, $q''(X^+,t^+)$, and thermocouple location.

$$\Phi = \frac{1}{\tau \, \Delta T_{max}^2} \sum_{i=1}^{n} \int_o^{\tau} \left(Pe \frac{\partial T_s}{\partial Pe}\right)_i^2 dt \qquad (5.9)$$

For one thermocouple and NT discrete measurements over time τ, Equation (5.9) is,

$$\Phi = \frac{1}{\tau \, \Delta T_{max}^2} \sum_{k=1}^{NT} \left(Pe \frac{\partial T_s}{\partial Pe}\right)_k^2 dt \qquad (5.10)$$

Before investigating the optimum heat flux, $q''(X^+,t^+)$, which makes Φ a maximum, consider a simple but useful $q''(X^+,t^+)$ profile. Suppose that at any instant the heat flux is uniform over a heating length x_L and that the plates are insulated elsewhere. Also, over a given duration of the experiment, let the heat flux have a constant value such that the maximum temperature rise is less than or equal to ΔT_{max}. The following question is then answered: for a given experiment duration, τ, what is the length of heating, x_L, and placement of one thermocouple, x_θ, which will make Φ a maximum for this constant q''? Once x_L is determined, then the magnitude of q'' which satisfies the ΔT_{max} constraint for a given τ can be determined. This can be done for each experiment duration, giving a full time spectrum of optimum transient experiments for a constant q". These results are given in Table 1. Both x_L and x_θ increase continuously as τ increases, but due to the nature of a finite difference method, the smallest increment detected is Δx. (For Table 1, $\Delta X^+ = 0.015$ and Pe = 6, hence $\Delta x/a = \text{Pe}\ \Delta X^+ = 0.09$) This explains why x_L and x_θ in the table appear to be constant for some time and increase in increments of 0.09.

For example, a particular entry in Table 1 is illustrated in more detail in Figure 5.2. This figure shows that if the duration of the experiment is $\tau^+ = 0.12$, the optimum heating length is $x_L/a = 0.54$ and the optimum placement of the thermocouple is $x_\theta/a = 0.09$.

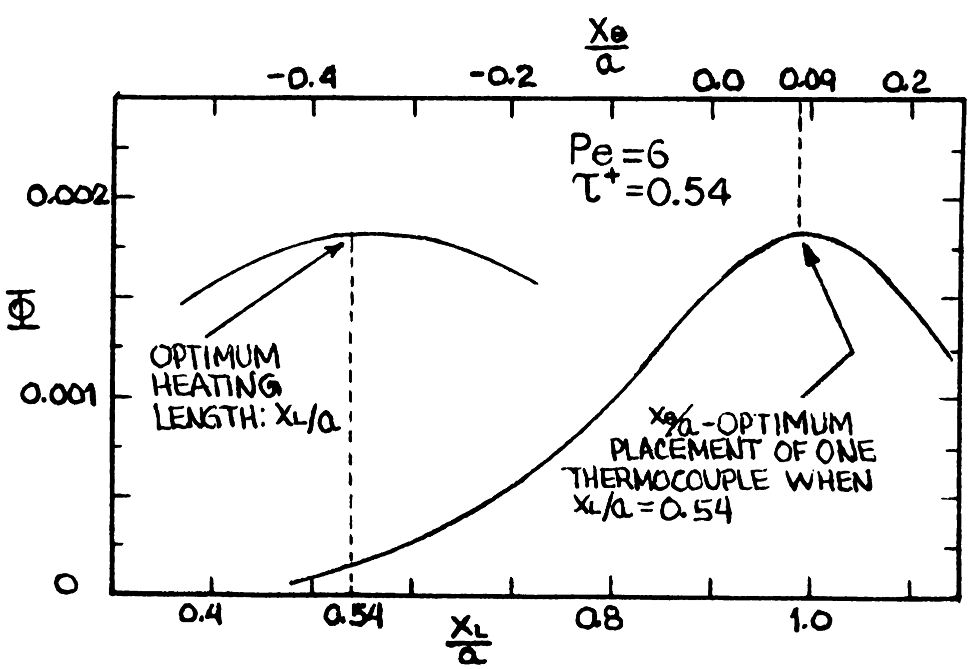

FIGURE 5.2 RELATION OF THE OBJECTIVE FUNCTION TO HEATING LENGTH AND THERMOCOUPLE LOCATION

TABLE 1 OPTIMUM QUANTITIES FOR $q''(X^+, t^+)$ = CONSTANT

DURATION OF EXPERIMENT $\tau^+ = \frac{\tau\alpha}{a^2}$	OPTIMUM HEATING LENGTH $\frac{X_L}{a} = Pe\, X_L^+$	OPTIMUM LOCATION OF ONE THERMOCOUPLE $\frac{X_\theta}{a} = Pe\, X_\theta^+$	Φ
0.02	0.45	0.09	0.000020
.04	.45	.09	.000150
.06	.54	.09	.000399
.08	.54	.09	.000765
.10	.54	.09	.001236
.12	.54	.09	.001802
.14	.54	.09	.002452
.16	.63	.09	.003192
.18	.81	.18	.004117
.20	.90	.18	.005078
.22	.90	.18	.006119
.24	.90	.18	.007214
.26	.90	.18	.008348
.28	.90	.18	.009523
.30	1.08	.27	.010829
.32	1.08	.27	.012167
.34	1.08	.27	.013529
.36	1.08	.27	.014910
.38	1.08	.27	.016301
.40	1.08	.27	.017696
.42	1.17	.36	.019092
.44	1.17	.36	.020578
.46	1.17	.36	.022056
.48	1.17	.36	.023523
.50	1.17	.36	.024974
.52	1.17	.36	.026381
.55	1.26	.45	.028582
.58	1.26	.45	.030787
.61	1.26	.45	.032927
.64	1.35	.54	.035046
.67	1.35	.54	.037196
.70	1.35	.54	.039275
.73	1.44	.63	.041359
.76	1.44	.63	.043424
.79	1.44	.63	.045441
.82	1.53	.72	.047494
.85	1.62	.81	.049505
.88	1.62	.81	.051518
.91	1.71	.90	.053546
.94	1.80	.99	.055572
.97	1.89	1.08	.057620
1.00	1.98	1.17	.059706
1.04	2.07	1.26	.062558
1.08	2.25	1.44	.065528
1.12	2.43	1.62	.068617
1.16	2.61	1.80	.071829
1.20	2.70	1.89	.075172
1.24	2.88	2.07	.078605
1.28	2.97	2.16	.082122
1.32	3.15	2.34	.085703
1.36	3.24	2.43	.089348
1.40	3.24	2.52	.093046
1.44	3.42	2.70	.096802
1.48	3.51	2.79	.100598
1.52	3.60	2.88	.104406
1.56	3.69	2.97	.108221
1.60	3.78	3.06	.112038
∞	∞	∞	1

As discussed in Chapter VI, the solution to a step change in surface heat flux (Case I) is used to calculate the results for the heat flux under discussion,

$$q'' = \begin{cases} \text{constant} & 0 \le X^+ \le X_L^+ \\ 0 & X^+ < 0 \quad \text{and} \quad X^+ > X_L^+ \end{cases}$$

by superposition. The surface temperature does not reach a maximum at the end of the heating length as would be the case if axial conduction upstream were not allowed. As can be seen from Figure 5.3, $\Delta T_{max} = T_{max} - T_o$, occurs some distance upstream of X_L^+. The smaller the Pe number, the greater this distance. Notice that the position of maximum temperature shifts downstream with increasing time. Also, recall from Section 4.1 that the further one goes downstream, the longer is the time required to reach a steady state condition. As a consequence of these two facts, the optimum heating length becomes larger as the duration of the experiment increases, (see Table 5.1).

In terms of the dimensionless variables of Equation (2.7) for Case I, Equation (5.10) becomes,

$$\Phi = \frac{1}{\tau^+ \Delta T_{max}^2} \left(\frac{q''a}{k}\right)^2 \sum_{k=1}^{NT} \left(Pe \frac{\partial T_s^+}{\partial Pe}\right)_k^2 \Delta t^+$$

$$NT = 2,3,\ldots$$

Since $\Delta T_{max}^+ = \dfrac{T_{max} - T_o}{q''a/k}$, we have

$$\Phi = \frac{1}{\tau^+ \Delta T_{max}^{+2}} \sum_{k=1}^{NT} \left(Pe \frac{\partial T_s^+}{\partial Pe}\right)_k^2 \Delta t^+ \tag{5.11}$$

$$NT = 2,3,\ldots$$

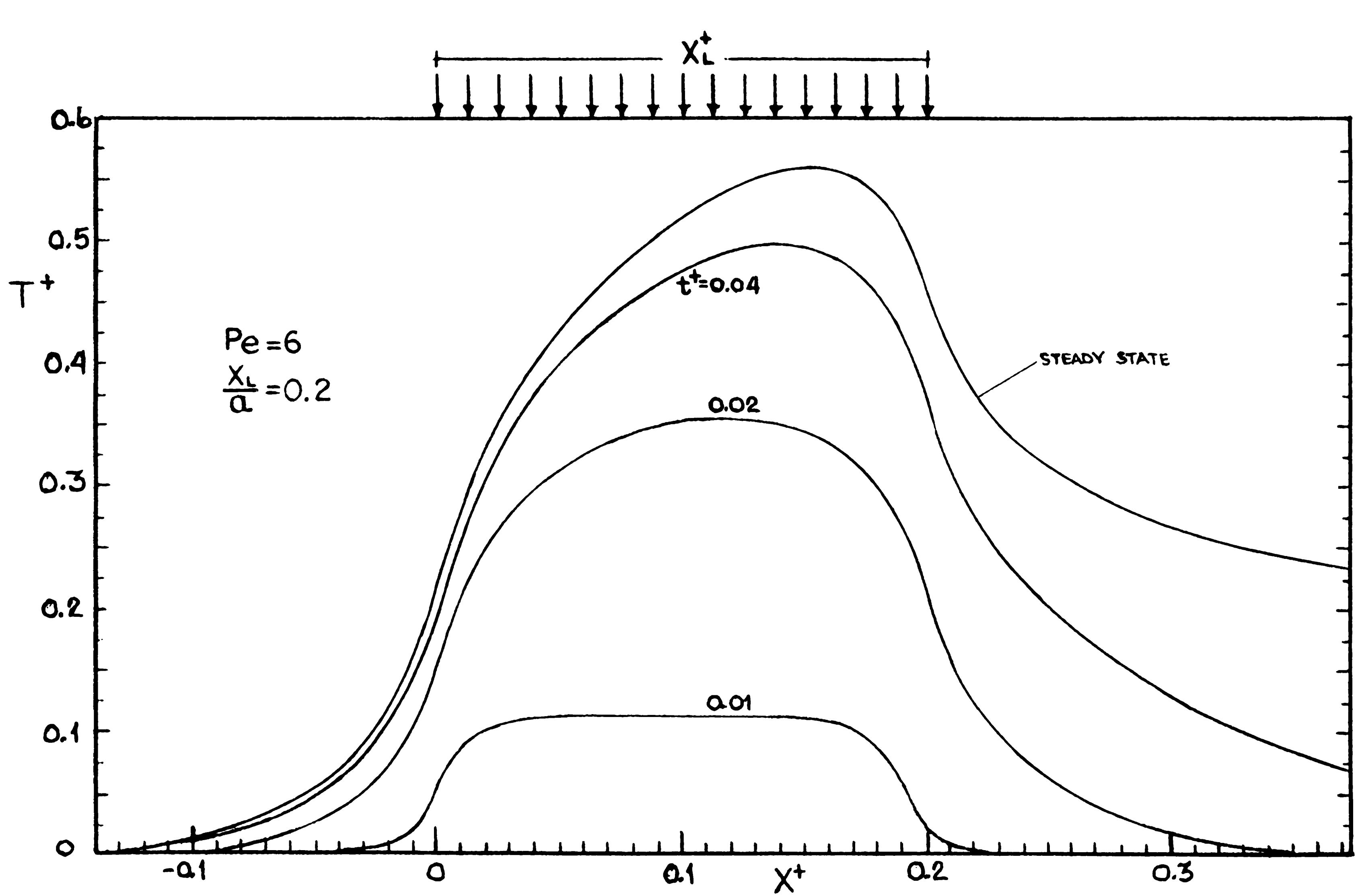

FIGURE 5.3 SURFACE TEMPERATURE FOR A FINITE HEATING LENGTH

The sensitivity coefficient, $Pe \frac{\partial T_s}{\partial Pe}$, is evaluated by solving Case I for two different Pe numbers differing by a small value, such as $\Delta Pe = 0.005$. Then,

$$Pe \frac{\partial T_s}{\partial Pe}\bigg|_i^n \simeq Pe \frac{T^n_{s,i}(Pe + \Delta Pe) - T^n_{s,i}(Pe)}{\Delta Pe}$$

$$i = 0,1,\ldots,NX$$

The coefficient with respect to $\bar{u}$ is actually the quantity of interest. However,

$$\bar{u} \frac{\partial T(x,a,t)}{\partial \bar{u}}\bigg|_x = Pe \frac{\partial T(X^+,1,t^+)}{\partial Pe}\bigg|_{\alpha,a,x}$$

if the dimensionless $\Delta X^+ = \frac{\Delta x}{aPe}$ in Case I is changed proportionately when the Pe number is changed so that $T(Pe + \Delta Pe)$ and $T(Pe)$ are evaluated at the same physical location.

The steady state sensitivity coefficient for a step change in surface temperature is given in Figure 5.4. The entrance results converge to the fully developed value of $-(X^+ + \frac{2}{Pe^2})$ derived in Appendix C.

The transient results for the same boundary condition are given in Figure 5.5. Note that for early times a maximum occurs near $X^+ = 0$, and shifts downstream with increasing time. This causes the optimum placement of the thermocouple to move from the vicinity of $X^+ = 0$ for early times, downstream as the duration of the experiment increases.

The sensitivity coefficient for an arbitrary variation in $q''(X^+,t^+)$ is obtained by superposition of the step change case in the same way as with the temperature, since $Pe \frac{\partial T^+}{\partial Pe}$ is linear in

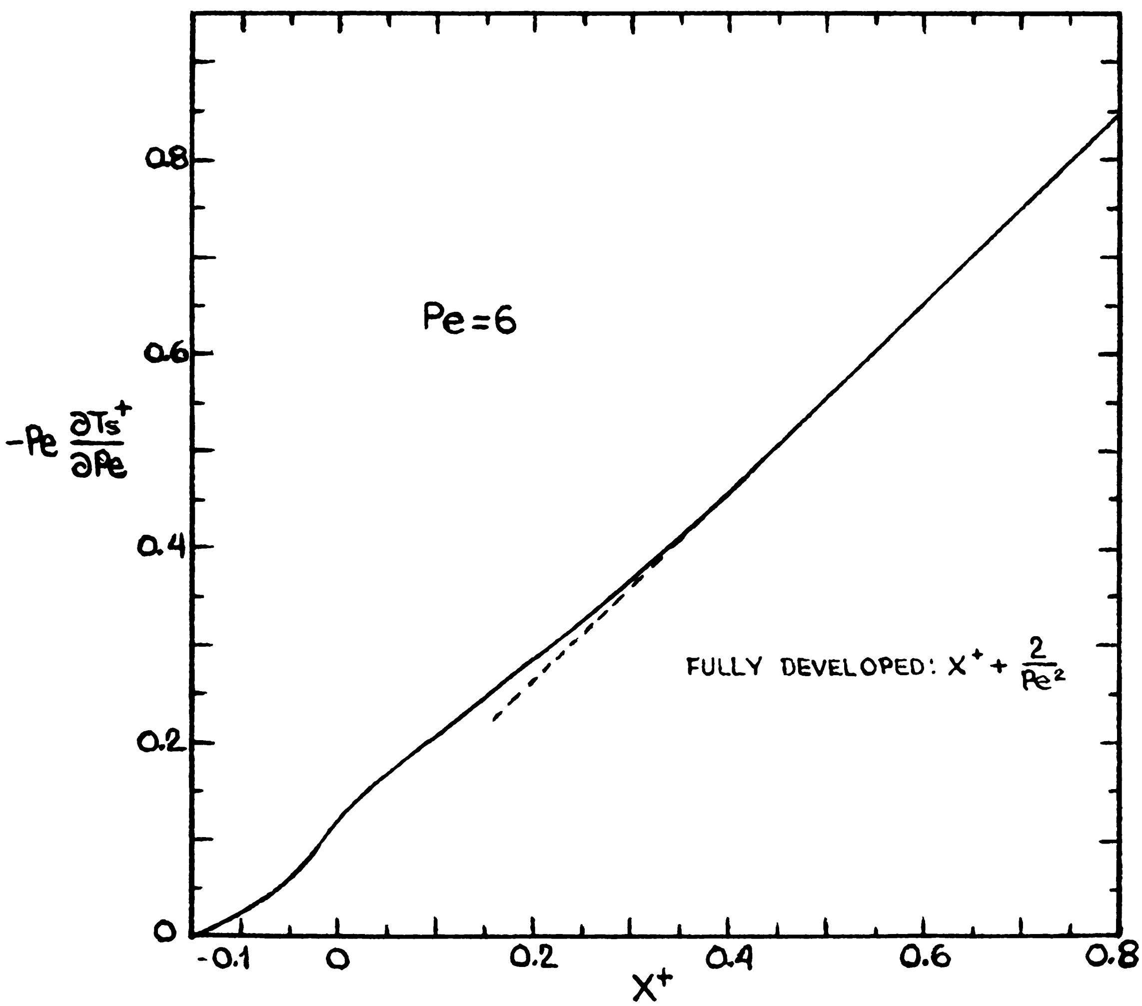

FIGURE 5.4 STEADY STATE SENSITIVITY COEFFICIENT FOR CASE I BOUNDARY CONDITION

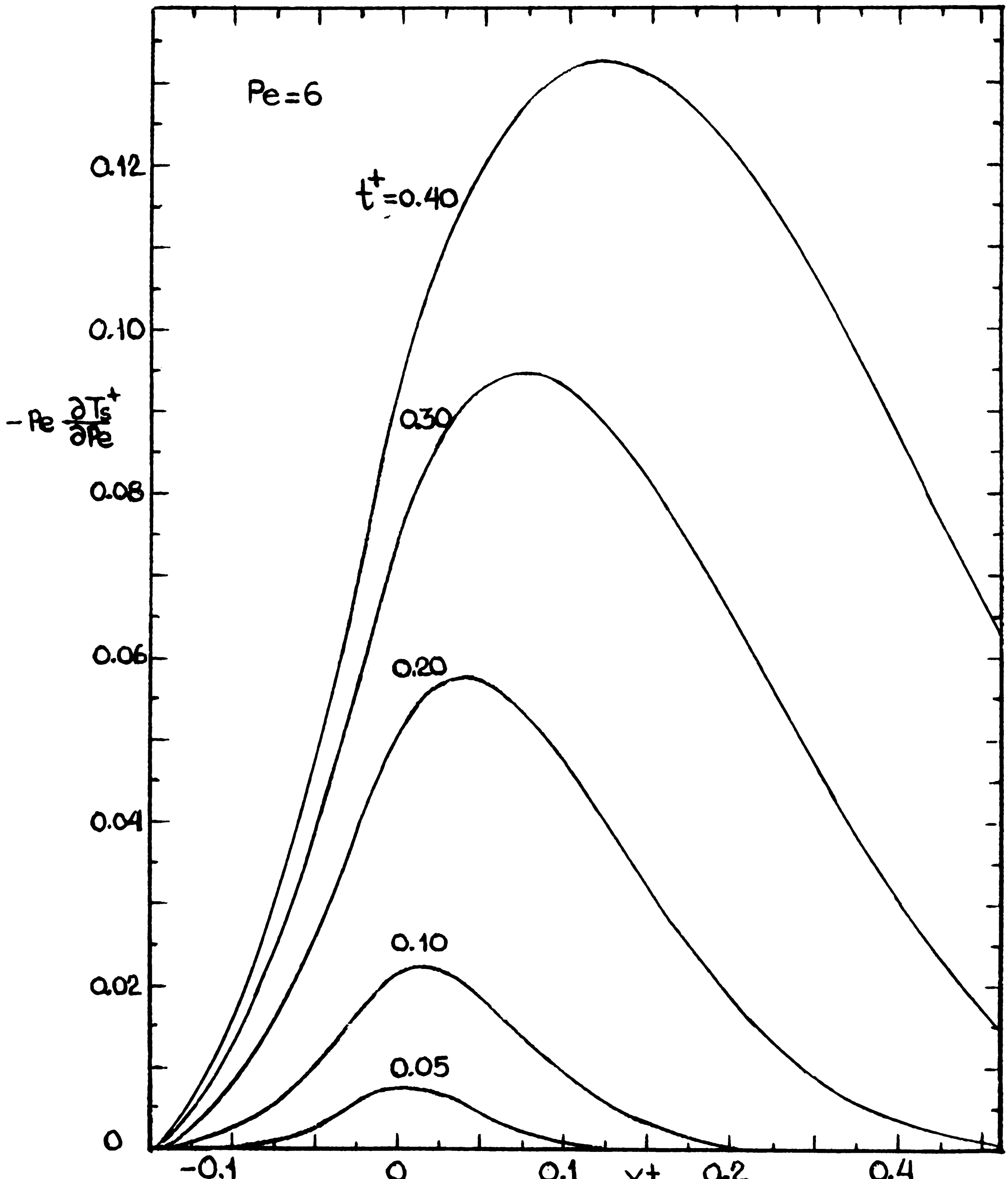

FIGURE 5.5 TRANSIENT SENSITIVITY COEFFICIENT FOR CASE I BOUNDARY CONDITION

X^+ and t^+ for a given Pe number.

Let us investigate what happens to the objective function as the duration of the experiment increases. Since Φ is a time average of the square of the sensitivity coefficient, it takes much longer to approach its final value of

$$\left[\frac{Pe\left.\frac{\partial T_s^+}{\partial Pe}\right|_{X_\theta^+}}{\Delta T_{max}^+}\right]^2$$

than for the temperature response to reach its steady state value. In fact, $\Phi \to 1$ as $\tau^+ \to \infty$. To gain some insight into what happens as $\tau^+ \to \infty$, suppose there is no axial conduction upstream; the optimum location of the thermocouple, X_θ^+, and position of maximum temperature occur at the end of the heating length, X_L^+. The above expression of the summand in Equation (5.11) can be expressed in terms of the fully developed values of $Pe\frac{\partial T_s^+}{\partial Pe}$ and T_s^+ given in Appendix C, since X_L^+ is large for large τ^+. Namely,

$$\frac{Pe\left.\frac{\partial T_s^+}{\partial Pe}\right|_{X_\theta^+}}{\Delta T_{max}^+} \to -\frac{X_L^+ + \frac{2}{Pe^2}}{X_L^+ + \frac{1}{Pe^2} + \frac{17}{35}}$$

The optimum heating length maximizing this quantity as τ^+ increases is $X_L^+ \to \infty$. Allowing axial conduction upstream will not alter these limiting results. Obviously, an infinite heating length is not tolerable, physically.

Since no optimum time duration exists for this case as formulated, the duration of the experiment is left to the choice of the investigator. Once it is chosen, however, x_L, x_θ, and

$q'' =$ constant which make Φ a maximum can be found using Table 1. We would like τ to be small in order that $\bar{u}$ may be estimated even though it is time varying. Also, from a physical consideration, it would be desirable to have the heating length short, and since the optimum x_L increases with the duration of the experiment this means that τ should be made as small as possible. Incidently, the nonlinear estimation procedure requires repeated transient calculations of the Case I solution over the duration of the experiment. Hence, a smaller choice of τ requires less computer time.

We now wish to extend the optimum conditions to include a transient heat flux profile. At a particular instant, let the heat flux be constant over the heating length, X_L^+. However, in addition to maximizing Φ with respect to the heating length and placement of one thermocouple, allow q'' to vary with time in such a way as to make Φ a maximum for a given experiment duration while satisfying the ΔT_{max} constraint.

Consider Equation (5.10). The quantity, $Pe \frac{\partial T_s}{\partial Pe}$, for a given heat flux variation in time can be calculated, using as a basic building block in superposition, the sensitivity coefficient resulting from a unit pulse in the heat flux from $t^+ = 0$ to $t^+ = \Delta t$. Let W_k be this basic building block. Then if $Pe \frac{\partial T_s^+}{\partial Pe}$ is the sensitivity coefficient due to a unit step change in q'' at $t^+ = 0$ $(T_s^+ = T^+(X^+,1,t^+)$ is the solution to Case I at $y^+ = 1)$,

$$W_k = \left(Pe \frac{\partial T_s^+}{\partial Pe}\right)_k - \left(Pe \frac{\partial T_s^+}{\partial Pe}\right)_{k-1}$$

represents the sensitivity coefficient evaluated at $t^+ = k\,\Delta t^+$

due to a unit pulse in q'' for the duration Δt^+ beginning at $t^+ = 0$. The coefficient resulting from a similar pulse in heat flux of magnitude q'' is then $q''_1 W_k$.

The superposition principle gives the following expression for $Pe \frac{\partial T_s}{\partial Pe}$ at time $k\,\Delta t^+$ due to a heat flux varying with time as illustrated in Figure 5.6.

$$(Pe \frac{\partial T_s}{\partial Pe})_k = q''_1 W_k + q''_2 W_{k-1} + \ldots + q''_k W_1 \tag{5.13}$$

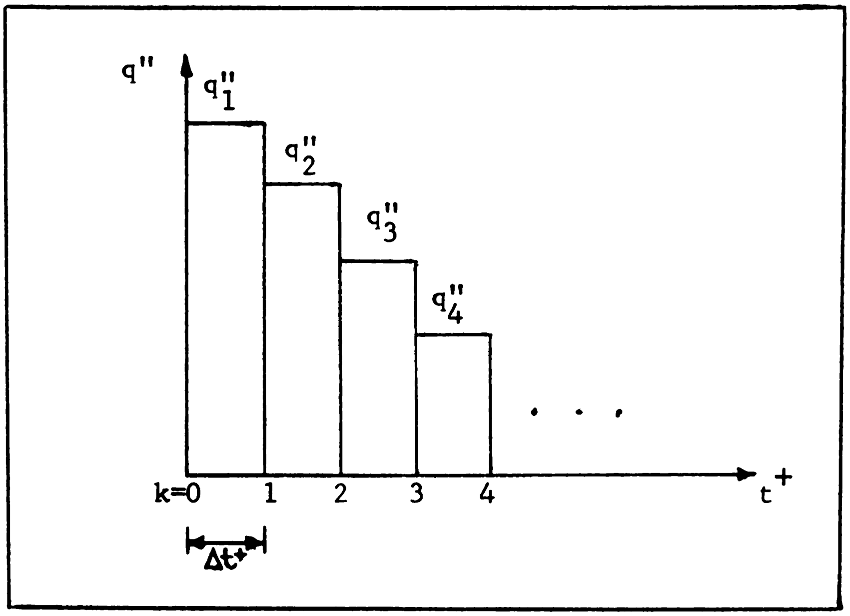

FIGURE 5.6: ILLUSTRATION OF DISCRETE OPTIMUM HEAT FLUX PROFILE

$$(Pe \frac{\partial T_s}{\partial Pe})^2_k = \sum_{j=1}^{k} \sum_{p=1}^{k} q''_j\, q''_p\, W_{k-j+1}\, W_{k-p+1} \tag{5.14}$$

Hence,

$$\Phi = \frac{1}{\tau\, \Delta T^2_{max}} \sum_{k=1}^{NT} \sum_{j=1}^{k} \sum_{p=1}^{k} q''_j\, q''_p\, W_{k-j+1}\, W_{k-p+1} \tag{5.15}$$

If W_k has the same sign for all k, the objective function, Φ, will be a maximum when each term in the sum over k is a

maximum, (i.e. when $(\mathrm{Pe}\ \partial T_s/\partial \mathrm{Pe})_k^2$ in Equation (5.14) is a maximum for any k). The coefficient W_k is always negative since $\partial T_s^+/\partial \mathrm{Pe}$ monotonically decreases in time from its zero initial value. The optimum transient heat flux is one which varies with time in such a way that the surface is maintained throughout the experiment at its maximum permissible value. This insures that the heat flux is as large as possible at every instant. If the q'' illustrated conceptually in Figure 5.6 is this heat flux then its value at any time, q_k'', can not be increased or the ΔT_{max} constraint will be violated. If q_k'' for some k were smaller than the maximum permissible, then noting that W is independent of q'', the terms in the sum in Equation (5.14) would not be maximized.

For example, the optimum transient heat flux for a heating length of $x_L = 1.02\ a$, ($X_L^+ = 0.17$; $\mathrm{Pe} = 6$) is given in Figure 5.7 per degree ΔT_{max}. The position of the maximum temperature varies as before, moving downstream with increasing time until a steady state position of $x = 0.72\ a$ is reached. (Keep in mind that the heat flux at any given instant is constant over the region: $0 \le X^+ \le X_L^+$).

The heating length of $X_L^+ = 0.17$ is an optimum for a choice in experiment duration of $\tau^+ = 0.8$. From Figure 5.8, with Φ given by Equation (5.15), we see that the optimum location of one thermocouple for this example is $X_\theta^+ = 0.06$ or since $\mathrm{Pe} = 6$, $x_\theta = 0.36\ a$.

The choice of the experiment duration is somewhat arbitrary as mentioned before. It can be seen from Figure 5.9, which gives the transient behavior of the objective function, that once the

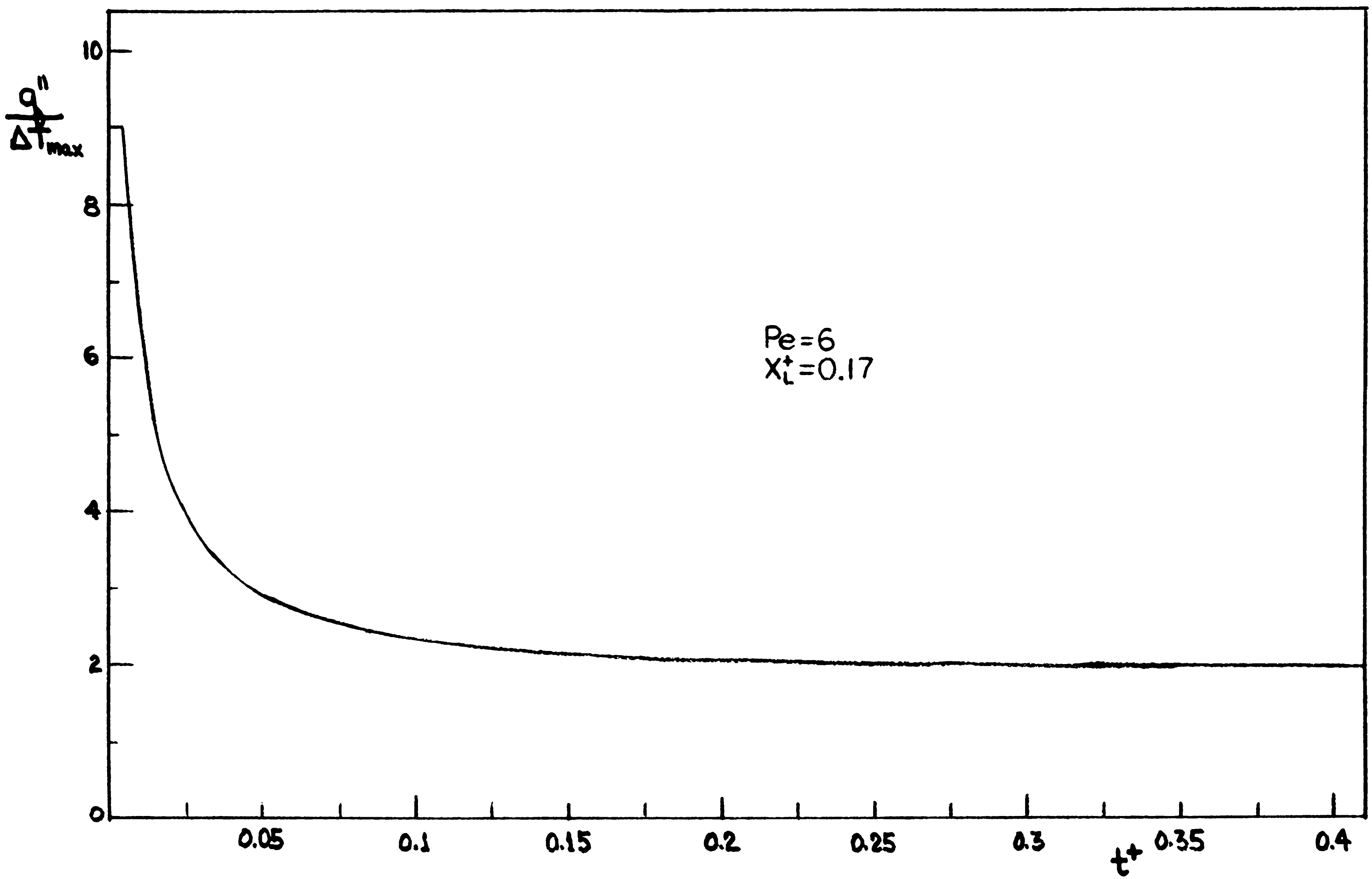

FIGURE 5.7 TRANSIENT WALL HEAT FLUX WHICH MAINTAINS A MAXIMUM SURFACE TEMPERATURE RISE OF ΔT_{MAX}

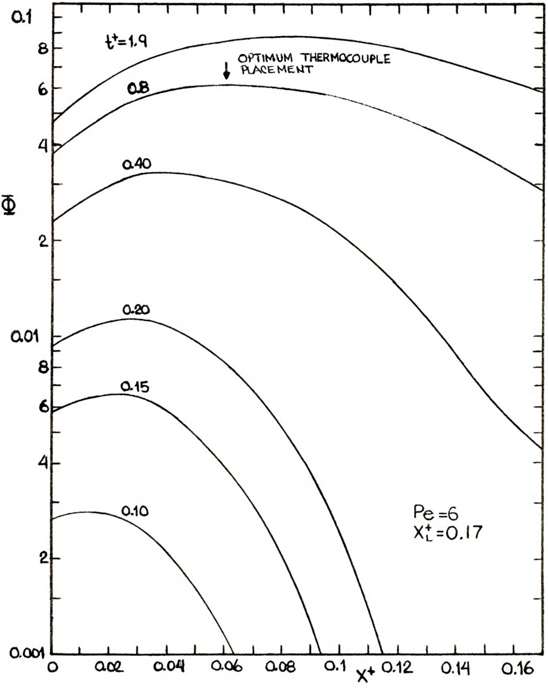

FIGURE 5.8 OBJECTIVE FUNCTION IN THE ENTRANCE REGION FOR OPTIMUM TRANSIENT HEAT FLUX

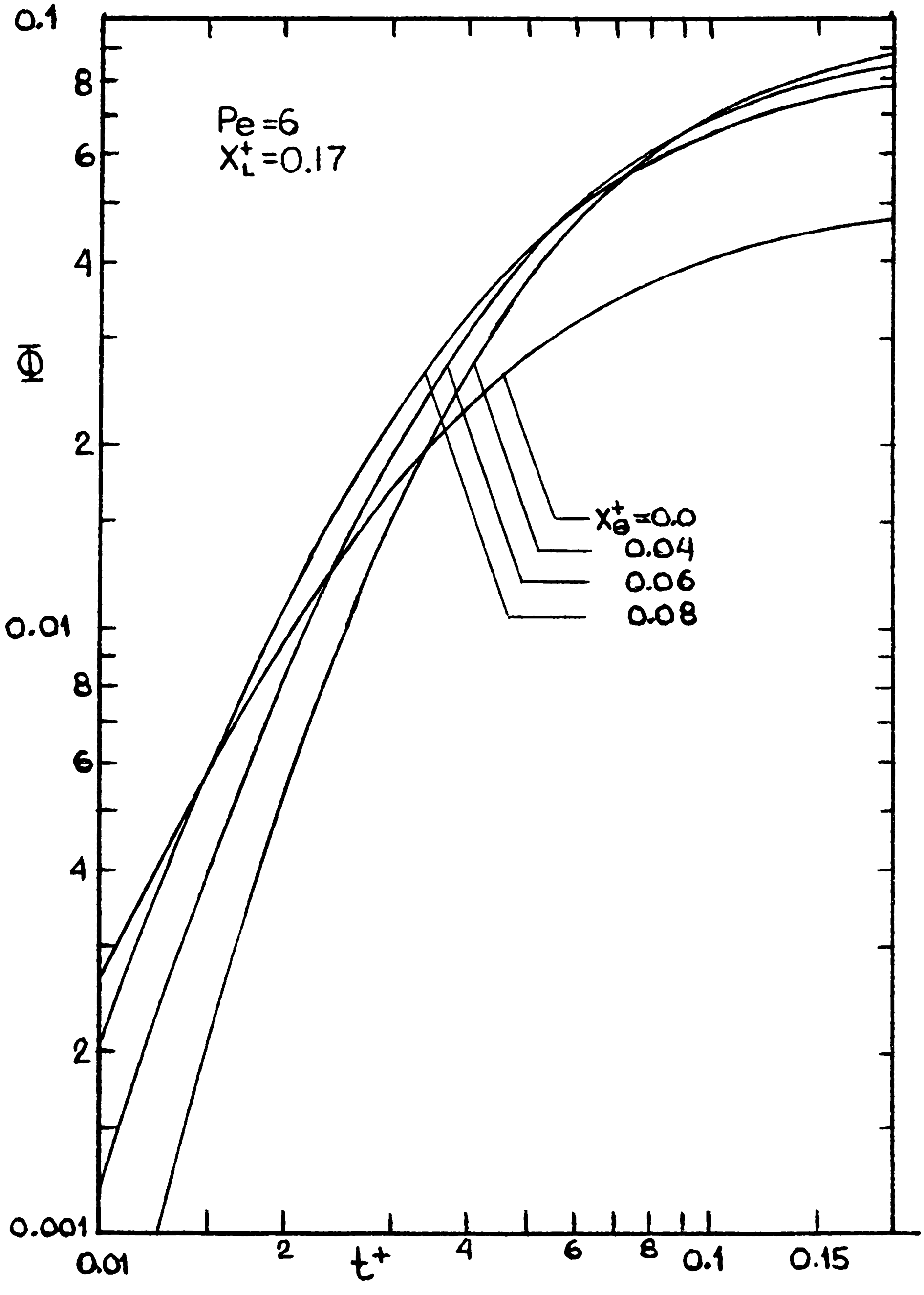

FIGURE 5.9 TRANSIENT OBJECTIVE FUNCTION FOR OPTIMUM TRANSIENT HEAT FLUX

slope $d\Phi/dt^+$ begins to decrease rapidly near $t^+ = 1.0$, the added gain in the magnitude of Φ is offset by the rising rate of increase in the length of time over which the data must be taken. The Φ-curve for $X_\theta^+ = 0.08$ in Figure 5.9 asymptotically approaches a steady state value of 0.107. For some physical dimensions pertaining to this example, see Section 5.4.

5.3 Error Analysis

Let us investigate the errors in calculating Pe (or $\bar{u}$) due to a biased error $\delta(t)$ in the measurements,

$$\delta(t) = \theta(t^+) - \theta^*(t^+) \tag{5.16}$$

where $\theta(t^+)$ is the temperature measured experimentally at t^+ and $\theta^*(t^+)$ is the corresponding true temperature.

Substituting Equation (5.16) into the sum of squares function,

$$F(Pe) = \int_o^\tau [T_s(t^+) - \theta^*(t^+) - \delta(t^+)]^2 dt^+ \tag{5.17}$$

If $\Delta Pe_\epsilon = Pe - Pe^*$ is the error introduced by δ, then for a small δ,

$$T_s = T_s^* + \Delta Pe_\epsilon \frac{\partial T_s^*}{\partial Pe} \tag{5.18}$$

where T^* is the calculated temperature based on $\delta = 0$.

Substituting Equation (5.18) into (5.17) and setting $\frac{\partial F}{\partial Pe} = 0$,

$$0 = \int_o^\tau [(T_s^* - \theta^*) + (\Delta Pe_\epsilon \frac{\partial T_s^*}{\partial Pe} - \delta)](\frac{\partial T_s^*}{\partial Pe} + \Delta Pe_\epsilon \frac{\partial^2 T_s^*}{\partial Pe^2})dt^+ \tag{5.19}$$

Also, since for $\delta = 0$, $F^* = F(Pe^*)$ and $\frac{\partial F^*}{\partial Pe} \equiv 0$, Equation (5.17) gives,

$$0 = \frac{\partial F^*}{\partial Pe} = 2\int_o^\tau (T^* - \theta^*)\frac{\partial T_s^*}{\partial Pe}\, dt^+$$

Using this relation in Equation (5.19) and neglecting second order terms leads to,

$$\int_o^\tau (\Delta Pe_\varepsilon \frac{\partial T_s^*}{\partial Pe} - \delta)\frac{\partial T_s^*}{\partial Pe}\, dt^+ = 0$$

Solving for ΔPe_ε and dividing by Pe^*

$$\frac{\Delta Pe_\varepsilon}{Pe} = \frac{\frac{1}{\tau\, \Delta T_{max}^2}\int_o^\tau \delta(t^+)(Pe^* \frac{\partial T_s^*}{\partial Pe})dt^+}{\frac{1}{\tau\, \Delta T_{max}^2}\int_o^\tau (Pe^* \frac{\partial T_s^*}{\partial Pe})^2 dt^+} = \frac{\frac{1}{\tau\, \Delta T_{max}^2}\int_o^\tau \delta(t^+) Pe^* \frac{\partial T_s^*}{\partial Pe}\, dt^+}{\Phi} \tag{5.20}$$

Hence, to minimize a biased error of $\delta(t^+)$, the objective function Φ should, in general, be a maximum - a result consistent with the basic criterion for an optimum experiment.

For discrete temperature measurements, the integral in Equation (5.20) is replaced by a summation over time.

The effect of one sided biased temperature errors on the calculated Pe numbers in Equation (5.20) is more severe than for random errors which are both positive and negative.

5.4 Example Utilizing the Nonlinear Estimation Procedure

In this section, an example based on the optimum experimental conditions discussed in section 5.2, utilizing the nonlinear estimation procedure outlined in section 5.1, is considered. Let the temperatures, calculated for the Case I set of boundary conditions with Pe = 6, be rounded to three significant figures and used as data. As discussed, the superposition principle is used to build the temperature response to a variable heat flux from the unit step

change in q'' - Case I. Using the heat flux given in Figure 5.7, the maximum surface temperature remains constant and equal to its maximum permissible value throughout the duration of the experiment. The other optimum conditions are as stated in section 5.2: placement of one thermocouple, $x_\theta = 0.36$ a, and heating length $x_L = 1.02$ a. The duration of the experiment is $\tau^+ = 0.8$.

To get an idea of what these dimensions are physically, suppose the fluid between the plates is liquid potassium. From (56), the properties of K at 500°F are,

$$Pr = 0.004$$

$$\alpha = 2.7 \ ft^2/hr$$

$$v = 0.012 \ ft^2/hr$$

$$k = 25 \ Btu/hr \ ft^\circ F$$

For $Pe = PrRe = 6$, $Re = 1500$. Let $a = 0.5$ inches. Then a τ^+ of 0.8 corresponds to,

$$\tau = 0.8 \frac{a^2}{\alpha} = 1.85 \text{ sec.}$$

The measurements are taken at intervals of $\Delta t^+ = 0.01$, which in physical dimensions is $\Delta t = 0.023$ sec. The steady state heat flux magnitude (Figure 5.7) for a ΔT_{max} of 10°F would then be,

$$\frac{q''a}{k} = 1.95 \ \Delta T_{max} \quad \text{or} \quad q'' = 11700 \ Btu/hr \ ft^2$$

In this example, it is known a priori that the data corresponds to $Pe = 6$. However, an initial guess of $Pe_o = 10$ is made.

Introducing the Pe number into Equation (5.4) to form the sensitivity coefficient, the correction in the initial guess is,

$$\frac{\Delta Pe_1}{P_{e_o}} = \frac{\sum_{k=1}^{NT} [\theta - T_s(Pe_o)]_k (Pe_o \frac{\partial T_s(Pe_o)}{\partial Pe})_k}{\sum_{k=1}^{NT} [Pe_o \frac{\partial T_s(Pe_o)}{\partial Pe}]_k^2} \qquad (5.21)$$

Case I is first solved for $Pe_o = 10$. Only the transient response through $\tau^+ = \tau\alpha/a^2 = 0.8$ need be calculated. With $T(Pe_o)$ now known, the Pe number is increased to 10.005 and the transient solution is calculated again. The sensitivity coefficient is obtained according to Equation (5.22),

$$Pe_o \frac{\partial T_s(Pe_o)}{\partial Pe} = Pe_o \frac{T_s(Pe_o + \varepsilon) - T_s(Pe_o)}{\varepsilon}$$

where $\varepsilon = 0.005$.

Using the new value of the Pe number,

$$Pe_1 = Pe_o + \Delta Pe_1$$

the iteration procedure is continued until some convergence criterion is met.

For this example, only three iterations were needed to converge to within 0.0067% of $Pe = 6$ when the initial guess was 66.6% in error.

The results of the iteration are given below.

$Pe_o = 10$	$\Delta Pe_1 = -5.218092$
$Pe_1 = 4.781908$	$\Delta Pe_2 = 1.090112$
$Pe_2 = 5.872019$	$\Delta Pe_3 = 0.127578$
$Pe_3 = 5.999597$	

For the fourth iteration, ΔPe was 0.001373.

Note that if the initial guess is in considerable error a significant over shoot can occur. This can be effectively dealt with by not allowing the correction for any one iteration to exceed a given maximum.

VI. SOME INTEGRAL INVERSE PROBLEMS

Since the energy equation with constant properties is linear, existing solutions may be added to give other solutions. In particular, Case I, a unit step change in heat flux at $X^+ = 0$ and $t^+ = 0$ and insulated upstream, serves as a basic building block in generating solutions with any prescribed time and axially variable heat flux. In the following sections, a number of problems related to the parallel plate geometry are formulated using as a basic kernel in Duhamel's superposition integral (54), the solution of Case I. Included also are a number of inverse problems formulated in terms of a standard integral equation of the first or second kind.

6.1 Heat Flux Varying with Time and Position

By superposition we can use the basic solution already obtained for a constant heat flux in solving the case where the heat flux varies in an arbitrary manner with time and position. Consider the following general heat flux, $q''(X^+,t^+)$ for the parallel plate goemetry,

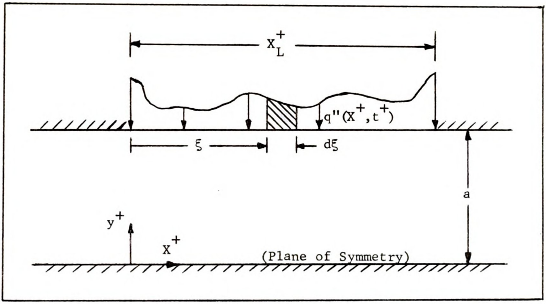

FIGURE 6.1: FLOW BETWEEN HEATED PARALLEL PLATES

with step changes in the heat flux as follows,

$$\text{At } X^+ = 0: \quad q'' = q''(0,t^+)$$
$$X^+ = X_L^+: \quad q'' = q''(X_L^+,t^+)$$
$$t^+ = 0: \quad q'' = q''(X^+,0)$$

Dimensionless variables X^+, y^+, and t^+ are defined by Equation (2.7)

Let $T^+(X^+,y^+,t^+)$ be the temperature resulting from a unit step change in surface heat flux at $X^+ = 0$ and $t^+ = 0$, with uniform initial temperature, T_o, and zero heat flux for $X^+ < 0$ (Solution to Case I). Then Duhamel's theorem states that if the heat flux, $q''(X^+,t^+)$, varies with position and time, the resulting temperature between the plates is given by (58),

$$T(X^+,y^+,t^+) - T_o = \frac{a}{k}\{T^+(X^+,y^+,t^+)q''(0,0) - T^+(X^+-X_L^+,y^+,t^+)q''(X_L^+,0)$$

$$+ \int_o^{t^+} T^+(X^+,y^+,t^+-\tau)\ \frac{dq''(0,\tau)}{d\tau}\ d\tau$$

$$+ \int_o^{X_L^+} T^+(X^+-\xi,y^+,t^+)\ \frac{dq''(\xi,0)}{d\xi}\ d\xi$$

$$- \int_o^{t^+} T^+(X^+-X_L^+,y^+,t^+-\tau)\ \frac{dq''(X_L^+,\tau)}{d\tau}\ d\tau\}$$

$$+ \frac{a}{k}\int_o^{X_L^+}\int_o^{t^+} T^+(X^+-\xi,y^+,t^+-\tau)\ \frac{\partial^2 q''(\xi,\tau)}{\partial\xi\partial\tau}\ d\xi d\tau \qquad (6.1)$$

$$\text{for} \quad -\infty < X^+ < \infty$$

$$t^+ > 0$$

The terms in brackets in the above equation account for the non-zero initial value in q'' as well as its non-zero value at $X^+ = 0$ and the end of the heating length, X_L^+. If no discontinuities in q'' exist, (i.e. if $q''(X^+,0) = q''(0,t^+) = q''(X_L^+,t^+) = 0)$ then Equation (6.1) reduces to

$$T(X^+,y^+,t^+)-T_o = \frac{a}{k}\int_o^{X_L^+}\int_o^{t^+} T^+(X^+-\xi,y^+,t^+-\tau)\ \frac{\partial^2 q''(\xi,\tau)}{\partial\xi\partial\tau}\ d\xi d\tau \qquad (6.2)$$

Integrating by parts of Equation (6.1) leads to the following alternative expression for the integral, noting that

$$\frac{\partial^2 T^+(X^+-\xi,y^+,t^+-\tau)}{\partial X^+\partial t^+} = \frac{\partial^2 T^+(X^+-\xi,y^+,t^+-\tau)}{\partial\xi\partial\tau} = K_1(X^+-\xi,y^+,t^+-\tau) \qquad (6.3)$$

where $K_1(X^+-\xi,y^+,t^+-\tau)$ is defined as the kernel of the integral equation and is known from Case I,

$$T(X^+,y^+,t^+)-T_o = \frac{a}{k}\int_o^{X_L^+}\int_o^{t^+} q''(\xi,\tau)K_1(X^+-\xi,y^+,t^+-\tau)d\xi d\tau \qquad (6.4)$$

Equations (6.1) and (6.4) differ from the result for no axial conduction in that the limit of integration on ξ is over the entire length of heating rather than from 0 to X^+. This is due to the fact that results upstream are effected by downstream conditions. To the author's knowledge, Equation (6.4) does not appear anywhere in the open literature.

As indicated in chapter 4, the temperature resulting from a space variable heat flux could be in significant error unless axial conduction is taken into account. The results at $X^+ = 0$, where the greatest error exists in neglecting axial conduction, are distributed throughout the X^+-domain.

Equation (6.4) becomes an inverse problem if the surface temperature is a known function of position and time and the heat flux is to be determined. The resulting integral equation, with q'' in the integrand unknown, is of the first kind; a Fredholm type on X^+ and a Volterra type on t^+ (60). Parenthetically, it is noted that with this formulation, the constant heat flux results (Case I) can be used to determine the response to a unit step change in surface temperature for $X^+ \geq 0$ (Case II),

$$1 = \frac{a/k}{T_s - T_o} \int_o^{X_L^+} \int_o^{t^+} q''(\xi,\tau) K_1(X^+ - \xi, 1, t^+ - \tau) d\xi d\tau \tag{6.5}$$

There are a number of ways to solve integral equations of this type, some of which are mentioned in references (57, 60). To obtain a solution numerically, suppose the heat flux in Equation (6.5) has been determined for the first $(n-1)$ time steps. At the n^{th} time step an algebraic difference equation can be written for each node in the x direction over the heated region (say m

nodes), then summed over the first n time steps. Each such equation in turn contains a sum over the m nodes in the heated region leaving $(m+1)$ equations and $(m+1)$ unknowns. Once $q''(X^+,t^+)$ is determined from Equation (6.5), it can be used in Equation (6.4) to calculate the temperature response throughout the region between the plates. No reported work has been done on this inverse problem. When using experimental data, severe problems with stability might arise (59).

6.2 Conducting Parallel Plates

Case I assumes that the heat flux applied to the outer surface is conducted through the plate to the fluid without axial conduction losses. It is of considerable practical interest to investigate the case where the plates themselves conduct heat in the axial direction.

Let k_s be the thermal conductivity of the plates and let q''_o be the heat applied to the outer plate surface over a length X^+_L.

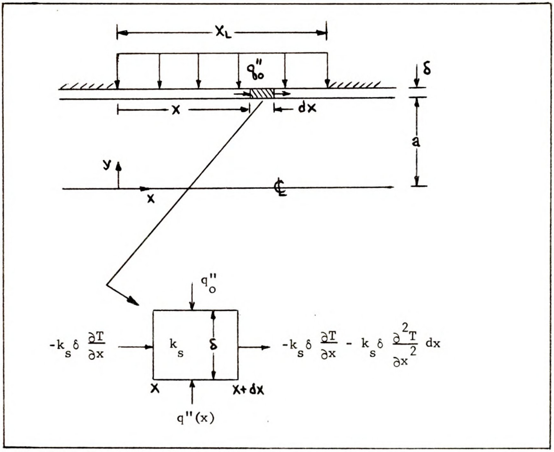

FIGURE 6.2: DIFFERENTIAL ELEMENT IN A CONDUCTING PLATE

The following assumptions are made,

1. Steady state

2. k_s = constant

3. The Biot number, $h\delta/k_s$, is small, say less than 0.1.

Assumption (1) is made in order to direct attention to the conducting plates. The results of section 6.1 could be used to consider transient effects.

An energy balance on the element shown in Figure 6.2 gives,

$$q''_o dx - q'' dx + k_s \delta \frac{\partial^2 T}{\partial x^2} dx = 0$$

By assumption (3),

$$q_o'' + k_s \delta \frac{\partial^2 T_s}{\partial x^2} = q'' \tag{6.6}$$

where T_s is the fluid-plate interface temperature. Note that if the transient case is considered the heat capacity of the plate must be included. This adds an additional term to the left hand side of Equation (6.6), namely, $-(\rho C_p)_s\ \partial T_s/\partial t$.

In dimensionless X^+ and y^+ form, Equation (6.6) is,

$$q_o'' + \frac{k_s\delta}{a^2} \frac{1}{Pe^2} \frac{\partial^2 T_s}{\partial X^{+2}} = q''(X^+) \tag{6.7}$$

$$T_s = T(X^+,1)$$

Note that T_s has the dimension of temperature.

Equation (6.4) for steady state conditions reduces to,

$$T(X^+,y^+) - T_o = \frac{a}{k} \int_{-\infty}^{\infty} q''(\xi) K_2(X^+-\xi, y^+) d\xi \tag{6.8}$$

where now the kernel is $K_2(X^+-\xi,y^+) = \partial T^+(X^+-\xi,y^+)/\partial X^+$ with $T^+(X^+,y^+)$ being the known steady state solution to Case I. The function $q''(X^+)$ is the variable heat flux applied to the fluid (not the plate). Note that the limits of integration on ξ must be over the entire X^+ domain from $-\infty$ to ∞, since $q''(X^+)$ has a non-zero contribution over this range.

Introducing Equation (6.7) into (6.8) gives,

$$T(X^+,y^+) - T_o = \frac{a}{k} \int_0^{X_L^+} q_o''\ K_2(X^+-\xi,y^+) d\xi$$
$$+ \frac{k_s\delta}{k\ a} \frac{1}{Pe^2} \int_{-\infty}^{\infty} \frac{\partial^2 T(\xi,1)}{\partial \xi^2} K_2(X^+-\xi,y^+) d\xi$$

Let q_o'' = constant and note that

$$\frac{\partial T^+(X^+-\xi,y^+)}{\partial X^+} = -\frac{\partial T^+(X^+-\xi,y^+)}{\partial \xi} = K_2(X^+-\xi,y^+).$$

Then we have the following integral equation of the second kind.

$$T(X^+,y^+)-T_o = \frac{q''_o a}{k}\left[T^+(X^+,y^+) - T^+(X^+-X_L^+,y^+)\right]$$

$$+ \frac{k_s \delta}{k\ a}\frac{1}{Pe^2}\int_{-\infty}^{\infty}\frac{\partial^2 T(\xi,1)}{\partial \xi^2} K_2(X^+-\xi,y^+)d\xi \qquad (6.9)$$

The temperature $T^+(X^+,y^+)$, its derivative $K_2(X^+,y^+)$, T_o, and the heat flux, q''_o, are known while $T(X^+,y^+)$, appearing both on the left hand side and in the integrand (for $y^+ = 1$), is to be determined.

One possible method for solving this equation would be to write the finite difference equation for each node at the wall ($y^+ = 1$) over the enitre x domain (say M nodes). The equation for a given node contains all M unknown wall temperatures. One from the left hand side of Equation (6.9) for that node plus the M temperatures resulting from the summation of the second derivative. Hence, there are M equations and M unknowns.

Once the wall temperatures are known, Equation (6.9) reduces to an ordinary integral with the integrand known and the fluid temperature throughout the region between the plates can easily be calculated.

The problem of conducting plates has not been considered in this manner previously to the author's knowledge.

6.3 Combined Convection and Radiation Between Parallel Plates.

Radiation has become of general concern in many applications recently. This section considers the situation where the plates

are of sufficiently high temperature that radiation as well as convection is an important mode of heat transfer. If the fluid is a non-interacting medium, then radiation between the plates is a boundary phenomenon dealing with the entire x-domain from $-\infty$ to $+\infty$. Hence, the solution to Case I serves as a natural basic building block in formulating the integral relation for this situation.

The following assumptions are made:

(1) The plates are gray

(2) The fluid between the plates is non-absorbing and non-emitting

(3) Steady State

(4) Heat flux, q_o'', is applied for $X^+ > 0$

From Love (57), the total heat flux both emitted and reflected leaving the surface is given by,

$$R(X^+) = \epsilon\sigma\, T_s^4(X^+) + \rho \int_a^b R(\eta) F(X^+, \eta)\, d\eta \tag{6.10}$$

where $R(X^+)$ = the radiosity

σ = Stefan-Boltzmann constant

ϵ = emissivity of the gray surface

ρ = reflectivity

T = absolute temperature in ^oR

T_s = steady state plate temperature = $T(X^+, 1)$

η = dummy X^+ variable

The kernel F, a function of the geometry, is related to the shape factor. It is the fraction of radiation leaving an elemental strip at η on one plate which strikes an elemental strip at X^+ on the other plate per unit length (in η direction) of emitting surface. See Figure 6.3.

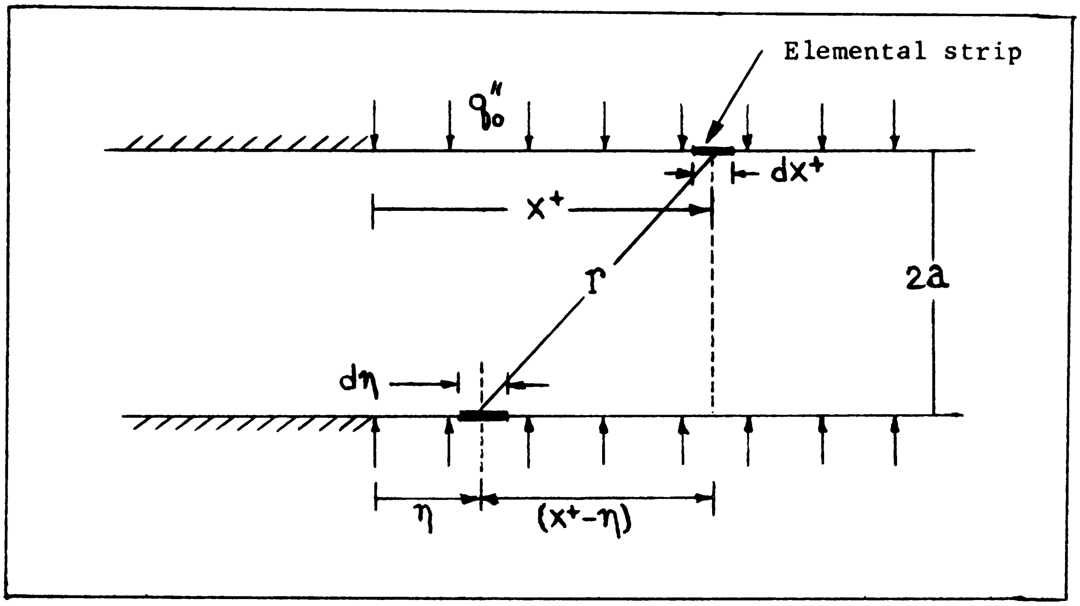

FIGURE 6.3: ILLUSTRATION OF RADIATION BETWEEN PARALLEL PLATES

As given in Ref. (57), the kernel $F(X^+,\eta)$ for this geometry is,

$$F(X^+,\eta) = \frac{1}{2}\left[\frac{(2a^2)}{r^3}\right] = \frac{2a^2}{[(X^+-\eta)^2 + 4a^2]^{3/2}}$$

Hence, from Equation (6.10), the radiosity for either plate is,

$$R(X^+) = \epsilon\sigma T_s^4(X^+) + 2\rho a^2 \int_{-\infty}^{\infty} \frac{R(\eta)d\eta}{[(X^+-\eta)^2 + 4a^2]^{3/2}} \tag{6.11}$$

The total heat flux absorbed by a differential strip dX^+ at X^+ by radiation from the other plate is,

$$q_r''(X^+) = 2\alpha a^2 \int_{-\infty}^{\infty} \frac{R(\eta)d\eta}{[(X^+-\eta)^2 + 4a^2]^{3/2}} - R(X^+) \tag{6.12}$$

where α = absorptivity, ($\alpha = \epsilon$ for a gray surfact). Finally, the total heat flux added to the fluid is,

$$q''(X^+) = q_o''(X^+) + q_r''(X^+) \tag{6.13}$$
$$-\infty < X^+ < \infty$$

The superposition integral for an axially variable heat flux, Equation (6.4), reduces for this case to,

$$T(X^+,y^+)-T_o = \frac{a}{k}\int_{-\infty}^{\infty} q''(\xi)\,\frac{\partial T^+(X^+-\xi,y^+)}{\partial X^+}\,d\xi \tag{6.14}$$

where

$$q''(X^+) = q_o''(X^+) + 2\epsilon a^2 \int_{-\infty}^{\infty} \frac{R(\eta)\,d\eta}{[(X^+-\eta)^2 + 4a^2]^{3/2}} - R(X^+) \tag{6.15}$$

with $R(X^+)$ in turn given by the integral Equation (6.11). Note the limits of integration on Equation (6.14) must run from $-\infty$ to ∞.

Equations (6.11), (6.14), and (6.15) can be solved for R, q'', and T by an iteration procedure. At $y^+ = 1$ these equations are of the inverse type. However, once q'' and R have been determined the temperatures throughout the region between the plates can be calculated by a straightforward integration.

Let the x domain be divided into M nodes. Then for $y^+ = 1$ we have 3M equations and 3M unknowns. If Equation (6.14) is written in finite difference form for each of the M nodes, there results M equations each containing M unknown q'''s and one $T_s = T(X_i^+,1)$. Hence, there are 2M unknowns and M equations. Similarly, Equation (6.11) yields M equations each containing M unknown R's and one T_s^4, or altogether 2M unknowns with M equations. Finally, Equation (6.15) gives M equations each containing M unknown R's and one q'' for a total of 2M unknowns. The three equations simultaneously supply the 3M equations needed to solve for 3M unknowns in q'', R,

and T_s.

One possible iteration procedure would be to pick $T_s(X^+)$ and solve for $R(X^+)$ in Equation (6.11). Then $q''(X^+)$ can be calculated from Equation (6.15) which in turn allows new surface temperatures to be calculated using Equation (6.14).

VII. CONCLUSIONS

In summarizing, the following conclusions can be drawn:

1. Axial conduction has a substantial effect on the temperature distribution and resulting Nusselt number in the entrance region for $Pe < 50$ in both boundary condition cases.

2. In the neighborhood of, and including the location where heating begins, the results are influenced significantly by axial conduction even for Pe numbers much greater than 50. The larger the Pe number, the smaller this region of influence becomes.

3. If axial conduction is important, then the temperature profile in the region upstream of the heated section is significantly altered. Hence, one can not assume a uniform temperature profile at the entrance cross-section in this case.

4. Axial conduction has the effect of increasing the development length. As the Pe number decreases, the development length increases.

5. The early transient response following the application of the wall heat flux can be described by the heat conduction equation if the location of interest is sufficiently far downstream from the entrance cross-section. This location may still be well within the entrance region, however.

6. At axial positions located in the fully developed thermal region, the transient Nusselt number decreases in time until reaching a

"secondary" dwell at a constant value predicted by considering only conduction between the plates. It remains at this intermediate level until the entrance effects are convected downstream to this location. Thereafter, the Nusselt number decreases to its final steady state, fully developed value.

7. An objective function is defined which, when maximized and satisfying given constraints, establishes an optimum experiment to estimate the mean velocity from temperature measurements at the wall.

8. The optimum transient wall heat flux profile is one which decreases with time in such a way as to maintain the maximum wall temperature at its constrained value throughout the duration of the experiment. At any instant the heat flux is constant over a finite heating length in the axial direction.

9. The optimum heating length for a given experiment duration and Pe number is determined. Also, the optimum location of one thermocouple at the wall for this case is found.

10. No optimum experiment duration exists when the objective function is expressed in the given form. This design factor is left to the choice of the investigator. However, there are several important considerations effecting this choice.

11. The optimum heating length and location of one thermocouple are also presented for a simpler wall heat flux which is not only constant over the heating length, but also constant throughout the duration of the experiment. The magnitude of this constant heat flux decreases with increasing experiment duration so as not to exceed the maximum wall temperature constraint.

12. A number of inverse problems are formulated using as a basic building block in the superposition principle, the uniform heat flux case.

BIBLIOGRAPHY

1. Graetz, L., "Über die Wärmeleitfähigkeit von Flüssigkeiten", Ann. Phys., 18, 79, 1883, 25, 337, 1885.

2. Prins, J.A., Mulder, J., and Schenk, J., "Heat Transfer in Laminar Flow Between Parallel Plates", Appl. Sci. Res., A2, 341-348, 1951.

3. Schenk, J. and Beckers, H.L., "Heat Transfer in Laminar Flow Between Parallel Plates", Appl. Sci. Res., A4, 405, 1954.

4. Mercer, A. McD., "The Growth of the Thermal B.L. in Laminar Flow Between Parallel Flat Plates", Appl. Sci. Res., Hague A8, No. 5, 357, 1959.

5. Siegal, R. and Sparrow, E.M., "Transient Heat Transfer for Laminar Forced Convection in the Thermal Entrance Region of Flat Ducts", Trans. ASME, Journal of Heat Transfer, Vol. 81, 29-36, 1959.

6. Siegel, R., "Heat Transfer for Laminar Flow in Ducts with Arbitrary Time Variations in Wall Temperature", Journal of Applied Mechanics, E 27, No. 2, 241, 1960.

7. Kays, W.M., "Numerical Solutions for Laminar-Flow Heat Transfer in Circular Tubes", Trans. ASME, Vol. 77, 1265-1274, 1955.

8. Siegel, R. and Sparrow, E.M., "Simultaneous Development of Velocity and Temperature Distributions in a Flat Duct with uniform Wall Heating", AIChE Journal, Vol. 5, No. 1, 73-75, 1959.

9. Ulrichson, D.L. and Schmitz, R.A., "Laminar-Flow Heat Transfer in the Entrance Region of Circular Tubes", International Journal of Heat and Mass Transfer, Vol. 8, 253, 1965.

10. Tien, Chi and Pawelek, R.A., "Laminar Flow Heat Transfer in the Entrance Region of Circular Tubes", Appl. Sci. Res., A13, 317.

11. Hornbeck, R.W., "An All-Numerical Method for Heat Transfer in the Inlet of A Tube", ASME Publication, 65-WA/HT-36, 1965.

12. Mercer, W.E., Pearce, W.M., and Hitchcock, J.E., "Laminar Forced-Convection in the Entrance Region Between Parallel Flat Plates", Trans. ASME, Journal of Heat Transfer, August 1967.

13. Han, L.S., "Simultaneous Developments of Temperature and Velocity Profiles in Flat Ducts", Interantional Developments in Heat Transfer, International Heat Transfer Conference, Boulder, Colorado, 591-597, 1961.

14. Sparrow, E.M., Lin, S.H., and Lundgren, T.S., "Flow Development in the Hydrodynamic Entrance Region of Tubes and Ducts", Phys. Fluids, Vol. 7, No. 3, 338-347, March 1964.

15. Sparrow, E.M., "Analysis of Laminar Forced-Convection Heat Transfer in Entrance Region of Flat Rectangular Ducts", NACA, TN3331, 1955.

16. Diessler, R.G., "Analytical Investigation of Fully Developed Laminar Flow in Tubes with Heat Transfer with Fluid Properties Variable Along the Radius", NACA TN2410, 1951.

17. Deissler, R.G. and Presler, A.F., "Analysis of Developing Laminar Flow and Heat Transfer in A Tube for A Gas with Variable Properties", NASA TM X-52171.

18. van der Does de Bye, J.A.W. and Schenk, J., "Heat Transfer in Laminar Flow Between Parallel Plates", Appl. Sci. Res., A3, 308-316, 1953.

19. Schenk, J., Dumoré, J.M., "Heat Transfer in Laminar Flow Through Cylindrical Tubes", Appl. Sci. Res., A4, 39-51, 1954.

20. Lundberg, R.E., Reynolds, W.C., and Kays, W.M., NASA TN D-1972, Washington, D.C., 1963.

21. Tyagi, V.P., "Laminar Forced Convection of A Dissipative Fluid in A Channel", Journal of Heat Transfer, 88, No. 2, 161, 1966.

22. Wolf, H., "Heating and Cooling Air and CO_2 in the Thermal Entrance Region of A Circular Duct with Large Gas to Wall Temperature Differences", Journal of Heat Transfer 81, No. 4, 267, 1959.

23. Poppendick, H.F., "Liquid-Metal Heat Transfer", Heat Transfer Symposium, University of Michigan Press, 1953.

24. Sellers, J.R., Tribus, M., and Klein, J.S., "Heat Transfer to Laminar Flow in a Round Tube or Flat Conduit - The Graetz Problem Extended", Trans. ASME, Vol. 78, 441-448, 1956.

25. Schneider, P.J., "Effect of Axial Fluid Conduction on Heat Transfer in the Entrance Regions of Parallel Plates and Tubes", Trans. ASME, Vol. 79, 765, 1957.

26. Hwang, C.L. and Fan, L.T., "Finite Difference Analysis of Forced Convection Heat Transfer in Entrance Region of A Flat Rectangular Duct", Appl. Sci. Res., A13, 401-422, 1964.

27. McMordie, R.K. and Emery, A.F., "A Numerical Solution for Laminar-Flow Heat Transfer in Circular Tubes with Axial Conduction and Developing Thermal and Velocity Fields", ASME Paper No. 66-WA/HT-7.

28. Hsu, C.J., "An Exact Mathematical Solution for Entrance-Region Laminar Heat Transfer with Axial Conduction", Appl. Sci. Res., A17, No. 4-5, 1967.

29. Singh, S.N., "The Determination of Eigenfunctions of a Certain Sturm-Liouville Equation and its Application to Problems of Heat Transfer", Appl. Sci. Res., A7, 237-250, 1957.

30. Singh, S.N., "Heat Transfer by Laminar Flow in a Cylindrical Tube", Appl. Sci. Res., A7, 325-340, 1957.

31. Eraslan, A.H. and Eraslan, N.F., "Heat Transfer in Magnetohydrodynamic Channel Flow", The Physics of Fluids, Vol. 12, No. 1, 120-128, 1969.

32. Harrison, W.B., "Forced Convection Heat Transfer in Thermal Entrance Regions: Part III, Heat Transfer to Liquid Metals", ORNL-915, 1954.

33. Schneider, P.J., "Effect of Axial Fluid Conduction on Heat Transfer in the Entrance Regions of Parallel Plates and Tubes", Trans. ASME 79, 766-773, 1957.

34. Burchill, W.E., Jones, B.G., and Stein, R.P., "Influence of Axial Heat Diffusion in Liquid Metal-Cooled Ducts with Specified Heat Flux", Trans. ASME, Journal of Heat Transfer, 90C, No. 3, 1968.

35. Agrawal, H., "Heat Transfer in Laminar Flow Between Parallel Plates at Small Peclet Numbers", Appl. Sci. Res., A9, 177-196, 1960.

36. Hennecke, D.K., "Heat Transfer by Hagen-Poiseuille Flow in the Thermal Development Region with Axial Conduction", University of Minnesota Heat Transfer Lab., 1968.

37. Hishida, M., "Temperature Distribution in the Entrance Region of Fluid Flow in A Pipe", Trans. Japan Society of Mechanical Engineers 31, 222, 1965.

38. Larkin, B.K., "Some Finite Difference Methods for Problems in Transient Heat Flow", Chem Engrg. Progress Symposium, Series v61, No. 59, 1-11, 1965.

39. Lundburg, D.D. and Miller, J.A., "Laminar Convective Heat Transfer in Entrance Region Between Parallel Flat Plates", U.S. Naval Postgraduate School, Research Paper No. 54, 58, 1965.

40. Wang, Y.L. and Longwell, P.A., "Laminar Flow in the Inlet Section of Parallel Plates", AIChE Journal (10), 323-329, 1964.

41. Pearson, J.D. and Serovy, G.K., "Numerical Solution of the Navier-Stokes Equations for the Entrance Region of Suddenly Accelerated Parallel Plates", Iowa State University Publication, Ames, Iowa.

42. Douglas, J., Jr., "A Survey of Numerical Methods for Parabolic Differential Equations", Advances in Computers 2, 1-54, 1961.

43. Peaceman, D.W. and Rachford, H.H., Jr., "The Numerical Solution of Parabolic and Elliptic Differential Equations", Jour. of the Soc. for Ind. and Appl. Math., 3, 27-41, 1955.

44. Douglas, J., Jr. and Rachford, H.H., "On the Numerical Solution of Heat Conduction Problems in Two and Three Dimensions", Trans. American Mathematical Society 82, 421-439, 1956.

45. Kays, W.M., Convection Heat and Mass Transfer, McGraw-Hill Book Co., Inc., New York, 1966.

46. Cess, R.D. and Shaffer, E.C., "Heat Transfer to Laminar Flow Between Parallel Plates with a Prescribed Wall Heat Flux", Appl. Sci. Res., A8, 339, 1959.

47. Gauss, K.F., "Theoria Motus Corporum Coelestium", Werke, 8, (1809).

48. Box, G.E.P. and Coutie, G.A., "Application of Digital Computers to the Exploration of Functional Relationships", The Inst. of Elec. Eng., Vol. 103, 100, 1956.

49. Box, G.E.P. and Lucas, H.L., "Design of Experiments in Non-linear Situations", Biometrika, Vol. 46, 77-90, 1959.

50. Box, G.E.P., "Fitting Empirical Data", Annals N.Y. Academy of Sciences, Vol. 86, 792, 1960.

51. Beck, J.V., "The Optimum Analytical Design of Transient Experiments for Simultaneous Determinations of Thermal Conductivity and Specific Heat", Ph.D. Thesis, Michigan State University, East Lansing, Mcihigan, 1964.

52. Beck, J.V., "Analytical Determination of Optimum, Transient Experiments for Measurement of Thermal Properties", Proc. of the Third Int. Heat Transfer Conf., Vol. IV, 74-80, 1966.

53. Beck, J.V., "Transient Determination of Thermal Properties", Nuclear Engineering and Design, Vol. 3, 373-381, 1966.

54. Carslaw, H.S. and Jaeger, J.C., Conduction of Heat in Solids, Second Edition, Oxford University Press, London, 1959.

55. Forsythe, G.E. and Wasow, W.R., Finite-Difference Methods for Partial Differential Equations, John Wiley and Sons, New York, 1960.

56. Chapman, A.J., Heat Transfer, Second Edition, The Macmillan Company, New York, 1967.

57. Love, T.J., Radiative Heat Transfer, Merrill Publishing Company, Columbus, Ohio, 1968.

58. Arpaci, V.S., Conduction Heat Transfer, Addison-Wesley Publishing Company, Reading, Mass., 1966.

59. Beck, J.V., "Surface Heat Flux Determination Using an Integral Method", Nuclear Engineering and Design 7, 170-178, 1968.

60. Hildebrand, F.B., Methods of Applied Mathematics, Prentice-Hall, Inc., Englewood Cliffs, N.J., 1956.

61. Hald, A., Statistical Theory with Engineering Applications, John Wiley and Sons, Inc., 1952.

APPENDICES

APPENDIX A

Truncation Error in Approximating Equation (2.8) by the ADI Finite Difference Equation (3.12).

Let the difference, D, between (2.8) evaluated at the point $[i\Delta x, j\Delta y, (n+\frac{1}{2})\Delta t]$ and (3.12) be the truncation error at a typical node. Omitting the superscript "+" from the dimensionless variables for simplicity,

$$\begin{aligned}
&\left[\frac{\partial T}{\partial t} + u\frac{\partial T}{\partial x} - \frac{1}{Pe^2}\frac{\partial^2 T}{\partial x^2} - \frac{\partial^2 T}{\partial y^2}\right]^{n+\frac{1}{2}}_{i,j} - \Bigg[\frac{T^{n+1}_{i,j} - T^{n}_{i,j}}{\Delta t} + \frac{1}{2(\Delta x)} u_j \delta_i (T^{n}_{i,j} + T^{n+1}_{i,j}) \\
&- \frac{1}{2(\Delta x)^2 Pe^2}\delta_i^2 (T^{n}_{i,j} + T^{n+1}_{i,j}) - \frac{1}{2(\Delta y)^2}\delta_j^2 (T^{n} + T^{n+1}) \\
&- \frac{\Delta t}{4(\Delta x)^2(\Delta y)^2 Pe^2}\delta_i^2\delta_j^2 (T^{n}_{i,j} - T^{n+1}_{i,j}) + \frac{\Delta t}{4(\Delta y)^2\Delta x} u_j \delta_j^2 \delta_i (T^{n}_{i,j} - T^{n+1}_{i,j})\Bigg] = D
\end{aligned} \tag{A-1}$$

where $T^{n+\frac{1}{2}} = \frac{1}{2}(T^{n} + T^{n+1})$

Using Equations (3.5) through (3.8)

$$\frac{1}{2(\Delta x)^2}\delta_i^2 (T^{n}_{i,j} + T^{n+1}_{i,j}) \cong \frac{1}{2}(T_{x^2}\big|^{n}_{i,j} + T_{x^2}\big|^{n+1}_{i,j}) + \frac{(\Delta x)^2}{24}(T_{x^4}\big|^{n}_{i,j} + T_{x^4}\big|^{n+1}_{i,j}) \tag{A-2}$$

where the variable subscripts denote differentiation, e.g. $T_{x^4} = \frac{\partial^4 T}{\partial x^4}$.

Similarly,

$$\frac{1}{2(\Delta y)^2}\delta_j^2 (T^{n}_{i,j} + T^{n+1}_{i,j}) \cong \frac{1}{2}(T_{y^2}\big|^{n}_{i,j} + T_{y^2}\big|^{n+1}_{i,j}) + \frac{(\Delta y)^2}{24}(T_{y^4}\big|^{n}_{i,j} + T_{y^4}\big|^{n+1}_{i,j}) \tag{A-3}$$

$$\frac{1}{2(\Delta x)}\delta_i (T^{n}_{i,j} + T^{n+1}_{i,j}) \cong \frac{1}{2}(T_{x}\big|^{n}_{i,j} + T_{x}\big|^{n+1}_{i,j}) + \frac{(\Delta x)^2}{12}(T_{x^3}\big|^{n}_{i,j} + T_{x^3}\big|^{n+1}_{i,j}) \tag{A-4}$$

$$\frac{T^{n+1}_{i,j} - T^{n}_{i,j}}{\Delta t} \cong T_t\Big|^n_{i,j} + \frac{\Delta t}{2} T_{t^2}\Big|^n_{i,j} = \frac{1}{2}(T_t\Big|^n_{i,j} + T_t\Big|^{n+1}_{i,j})$$

$$+ \frac{\Delta t}{4}(T_{t^2}\Big|^n_{i,j} - T_{t^2}\Big|^{n+1}_{i,j}) \qquad \text{(A-5)}$$

$$\frac{1}{(\Delta x)^2(\Delta y)^2} \delta_i^2\delta_j^2(T^n_{i,j} - T^{n+1}_{i,j}) \cong (T_{x^2y^2}\Big|^n_{i,j} - T_{x^2y^2}\Big|^{n+1}_{i,j})$$

$$+ \frac{(\Delta x)^2}{12}(T_{x^4y^2}\Big|^n_{i,j} - T_{x^4y^2}\Big|^{n+1}_{i,j}) + \frac{(\Delta y)^2}{12}(T_{x^2y^4}\Big|^n_{i,j} - T_{x^2y^4}\Big|^{n+1}_{i,j}) \qquad \text{(A-6)}$$

(where the higher order terms have been omitted)

$$\frac{1}{(\Delta y)^2(\Delta x)} \delta_i\delta_j^2(T^n_{i,j} - T^{n+1}_{i,j}) = (T_{xy^2}\Big|^n_{i,j} - T_{xy^2}\Big|^{n+1}_{i,j})$$

$$+ \frac{(\Delta x)^2}{6}(T_{x^3y^2}\Big|^n_{i,j} - T_{x^3y^2}\Big|^{n+1}_{i,j}) + \frac{(\Delta y)^2}{12}(T_{xy^4}\Big|^n_{i,j} - T_{xy^4}\Big|^{n+1}_{i,j}) \qquad \text{(A-7)}$$

Introducing into (A-5) through (A-7) the fact that

$$(T\Big|^n_{i,j} - T\Big|^{n+1}_{i,j}) \cong -\Delta t\, T_t\Big|^n_{i,j} - \frac{(\Delta t)^2}{2} T_{t^2}\Big|^n_{i,j}$$

and neglecting terms higher than second order we have,

$$\frac{T^{n+1}_{i,j} - T^{n}_{i,j}}{\Delta t} \cong \frac{1}{2}(T_t\Big|^n_{i,j} + T_t\Big|^{n+1}_{i,j}) - \frac{(\Delta t)^2}{4} T_{t^3}\Big|^n_{i,j} \qquad \text{(A-5a)}$$

$$\frac{1}{(\Delta x)^2(\Delta y)^2} \delta_i^2\delta_j^2(T^n_{i,j} - T^{n+1}_{i,j}) \cong -\Delta t\, T_{x^2y^2t}\Big|^n_{i,j} - \frac{(\Delta t)^2}{2} T^n_{x^2y^2t^2} \qquad \text{(A-6a)}$$

$$\frac{1}{(\Delta y)^2\Delta x} \delta_i\delta_j^2(T^n_{i,j} - T^{n+1}_{i,j}) = -\Delta t\, T_{xy^2t}\Big|^n_{i,j} - \frac{(\Delta t)^2}{2} T_{xy^2t^2}\Big|^n_{i,j} \qquad \text{(A-7a)}$$

Substituting (A-2), (A-3), (A-4), (A-5a), (A-6a), and (A-7a) into (A-1) the truncation error becomes,

$$D = \frac{(\Delta t)^2}{2}\left[T^n_{t^3} + u\, T^n_{txy^2} - \frac{1}{Pe^2} T^n_{tx^2y^2}\right]_{i,j}$$

$$+ \frac{(\Delta x)^2}{6}\left[\frac{1}{Pe^2} T^{n+\frac{1}{2}}_{x^4} - u\, T^{n+\frac{1}{2}}_{x^3}\right]_{i,j} + \frac{(\Delta y)^2}{6}\left[T^{n+\frac{1}{2}}_{y^4}\right]_{i,j} \qquad \text{(A-8)}$$

APPENDIX B

Stability Analysis for ADI Numerical Method

Let $E(x,y,t)$ be the error in the temperature, T, at a point (x,y) and time t due to the accumulation of round off errors in the numerical calculations.

$$E(x,y,t) = T^*(x,y,t) - T(x,y,t)$$

where T^* is the calculated temperature with a small error and T is the corresponding exact temperature. Changing the usual notation $T^n_{i,j}$ to $T^n_{p,q}$ in order to avoid confusion with the imaginary i, the error expressed in difference notation is,

$$E^n_{p,q} = E(x_p,y_q,t_n) = T^{*n}_{p,q} - T^n_{p,q} \tag{B-1}$$

Using the Fourier series method developed by von Neumann, we assume that the distribution of errors in the x,y plane at $t = 0$ can be expanded in a Fourier series.

$$E(x,y) = \sum_m \sum_n A_{mn} e^{i\beta_m x} e^{i\gamma y}$$

Since the energy equation is linear, and therefore solutions are additive, we need consider only the propagation of the error due to a single term, say $e^{i\beta x}e^{i\gamma y}$ (the coefficient is constant and may be neglected).

To investigate the propagation of this error as t increases, a solution must be found which reduces to $e^{i\beta x}e^{i\gamma y}$ as $t \to 0$. Assume

$$E(x,y,t) = e^{i\beta x} e^{i\gamma y} e^{\eta t}$$

The solution is said to be stable if the initial error does not grow with time. This condition is met if

$$|e^{\eta t}| \leq 1 \qquad \text{(B-2)}$$

Substituting (B-1) into (3.12) we see that the error function satisfies the same difference equation.

$$\frac{E^{n+1}_{p,q} - E^{n}_{p,q}}{\Delta t} + \frac{1}{2(\Delta x)} u_q \delta_p (E^n + E^{n+1}) = \frac{1}{2(\Delta x)^2 Pe^2} \delta_p^2 (E^n + E^{n+1})$$

$$+ \frac{1}{2(\Delta y)^2} \delta_q^2 (E^n + E^{n+1}) + \frac{\Delta t}{4(\Delta x)^2 (\Delta y)^2 Pe^2} \delta_p^2 \delta_q^2 (E^n - E^{n+1})$$

$$- \frac{\Delta t}{4(\Delta y)^2 \Delta x} u_q \delta_q^2 (E^n - E^{n+1})$$

Defining $\alpha_x = \frac{2(\Delta x)^2}{\Delta t}$ and $\alpha_y = \frac{2(\Delta y)^2}{\Delta t}$ as before and substituting $E^n_{p,q} = e^{i\beta x_p} e^{i\gamma y_q} e^{\eta t_n}$ we have after cancelling the exponential factors common to each term,

$$[e^{\eta\Delta t} - 1] = - \frac{\Delta t}{2\Delta x} u \, [e^{\eta\Delta t} + 1][e^{i\beta\Delta x} - e^{-i\beta\Delta x}] +$$

$$\frac{1}{\alpha_x Pe^2}[e^{\eta\Delta t} + 1][e^{i\beta\Delta x} - 2 + e^{-i\beta\Delta x}] + \frac{1}{\alpha_y}[e^{\eta\Delta t} + 1][e^{i\gamma\Delta y} - 2 + e^{-i\gamma\Delta y}]$$

$$- \frac{1}{\alpha_x \alpha_y Pe^2}[e^{\eta\Delta t} - 1][e^{i\beta\Delta x} - 2 + e^{-i\beta\Delta x}][e^{i\gamma\Delta y} -2 + e^{-i\gamma\Delta y}]$$

$$+ \frac{u}{\alpha_y} \frac{\Delta t}{2\Delta x}[e^{\eta\Delta t} - 1][e^{i\beta\Delta x} - e^{-i\beta\Delta x}][e^{i\gamma\Delta y} - 2 + e^{-i\gamma\Delta y}] \qquad \text{(B-3)}$$

Making use of the tigonometric relation,

$$\frac{e^{i\beta\Delta x} - e^{-i\beta\Delta x}}{2i} = \mathrm{Sin}\ \beta\Delta x = 2\ \mathrm{Sin}\ \frac{\beta\Delta x}{2}\ \mathrm{Cos}\ \frac{\beta\Delta x}{2}$$

we have $(e^{i\beta\Delta x} - 2 + e^{-i\beta\Delta x}) = -\ 4\ \mathrm{Sin}^2\ \frac{\beta\Delta x}{2}$

Using these relations in (B-3) and grouping the real and imaginary parts we obtain,

$$e^{\eta\Delta t} = \frac{A + iB}{C + iD} \tag{B-4}$$

with A,B,C, and D given below.

$$\begin{matrix} C \\ A \end{matrix} = 1 \pm \frac{4}{\alpha_x Pe^2}\ \mathrm{Sin}^2\ \frac{\beta\Delta x}{2} \pm \frac{4}{\alpha_y}\ \mathrm{Sin}^2\ \frac{\gamma\Delta y}{2} + \frac{16}{\alpha_y\alpha_x Pe^2}\ \mathrm{Sin}^2\ \frac{\beta\Delta x}{2}\ \mathrm{Sin}^2\ \frac{\gamma\Delta y}{2}$$

$$\begin{matrix} D \\ B \end{matrix} = \frac{2\Delta t}{\Delta x}\ u\ \mathrm{Sin}\ \frac{\beta\Delta x}{2}\ \mathrm{Cos}\ \frac{\beta\Delta x}{2}\ [\frac{4}{\alpha_y}\ \mathrm{Sin}^2\ \frac{\gamma\Delta y}{2} \pm 1]$$

$|C| \geq |A|$

$|D| \geq |B|$

Therefore, $|A + iB| \leq |C + iD|$

and,

$$|e^{\eta\Delta t}| \leq 1$$

Thus, the numerical method is always stable.

APPENDIX C.

Derivation of Fully Developed Temperature Profiles and Sensitivity Coefficients.

For the fully developed region, the steady state energy equation reduces to

$$\frac{u}{\alpha}\frac{\partial T}{\partial x} = \frac{\partial^2 T}{\partial y^2} \tag{C-1}$$

Kays (45) defines the region of fully developed temperature profiles by the criterion,

$$\frac{\partial}{\partial x}\left(\frac{T_s - T}{T_s - T_b}\right) = 0$$

Differentiating,

$$\frac{\partial T}{\partial x} = \frac{dT_s}{dx} - \frac{T_s - T}{T_s - T_b}\frac{dT_s}{dx} + \frac{T_s - T}{T_s - T_b}\frac{dT_b}{dx} \tag{C-2}$$

Also, since $Nu_{x>x_{Dev.}}$ is constant, h is constant and for the constant heat rate, Case I,

$$q'' = h(T_s - T_b) = \text{constant.}$$

$$T_s - T_b = \text{constant}$$

$$\frac{dT_s}{dx} - \frac{dT_b}{dx} = 0 \tag{C-3}$$

Substituting (C-3) into (C-2)

$$\frac{\partial T}{\partial x} = \frac{dT_s}{dx} = \frac{dT_b}{dx} \tag{C-4}$$

Equation (C-1) becomes,

$$\frac{u}{\alpha}\frac{dT_b}{dx} = \frac{\partial^2 T}{\partial y^2}$$

$$u = \frac{3}{2}\,\bar{u}\left(1 - \frac{y^2}{a^2}\right)$$

$$\frac{\partial^2 T}{\partial y^2} = \frac{1}{\alpha}\,\frac{3}{2}\,\bar{u}\left(1 - \frac{y^2}{a^2}\right)\frac{dT_b}{dx}$$

Integrating twice, applying the boundary conditions

$$T = T_s \quad \text{at} \quad y = a$$

$$\frac{\partial T}{\partial y} = 0 \quad \text{at} \quad y = 0$$

we have,

$$T = T_s + \frac{3\bar{u}}{2\alpha}\,\frac{dT_b}{dx}\left(\frac{y^2}{2} - \frac{y^4}{12a^2} - \frac{5a^2}{12}\right)$$

Nondimensionalizing according to Equation (2.7)

$$T^+ = T_s^+ + \frac{3}{2}\,\frac{dT_b^+}{dX^+}\left(\frac{y^{+2}}{2} - \frac{y^{+4}}{12} - \frac{5}{12}\right) \qquad \text{(C-5)}$$

Consider an energy balance on an element in the fully developed region,

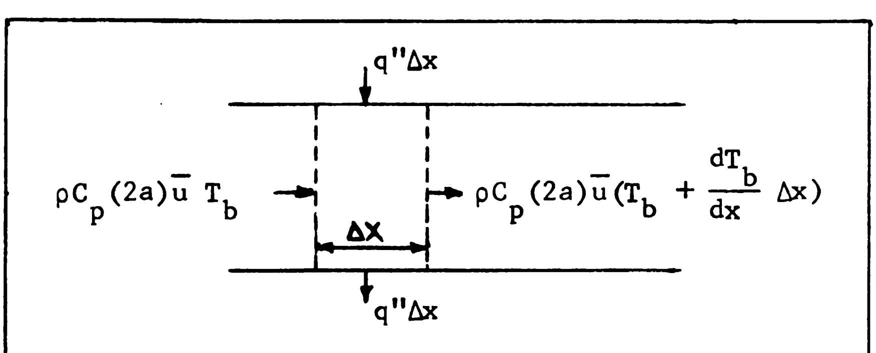

FIGURE C.1: ENERGY BALANCE ON A FLUID ELEMENT

$$\rho C_p \bar{u} a \frac{dT_b}{dx} = q''$$

or
$$a \; Pe \frac{dT_b}{dx} = \frac{q''a}{k}$$

$$\frac{dT_b^+}{dX^+} = 1 \tag{C-6}$$

Hence, (C-5) becomes

$$T^+ = T_s^+ + \frac{1}{8}(6y^{+2} - y^{+4} - 5) \tag{C-7}$$

$$T_b^+ = \int_o^1 u^+ T^+ dy^+$$

Substituting the temperature profile given in (C-6) and the parabolic velocity profile and integrating, the bulk temperature becomes,

$$T_b^+ = T_s^+ - \frac{17}{35} \tag{C-8}$$

To evaluate the unknown T_s^+ consider an energy balance on a control volume which includes the entrance and upstream regions.

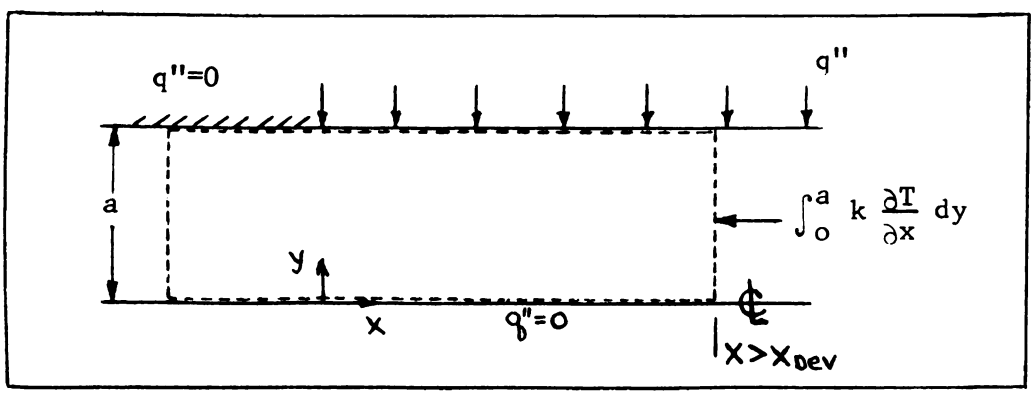

FIGURE C.2: ENTRANCE REGION CONTROL VOLUME

The energy balance gives,

$$q''x + \int_o^a k \frac{\partial T}{\partial x} dy = \int_o^a \rho C_p u(T - T_s) dy$$

In dimensionless form, using (C-4) we have

$$X^+ + \frac{1}{Pe^2}\int_o^1 \frac{dT_b^+}{dX^+}\,dy^+ = \frac{3}{2}\int_o^1 T^+(1 - y^{+2})dy^+$$

where $\dfrac{dT_b^+}{dX^+} = 1$ from (C-6).

Integrating and solving for T_s^+,

$$T_s^+ = X^+ + \frac{1}{Pe^2} + \frac{17}{35} \tag{C-9}$$

Substituting (C-9) into (C-7) and (C-8)

$$T^+ = X^+ + \frac{1}{Pe^2} + \frac{3}{4}y^{+2} - \frac{1}{8}y^{+4} - \frac{39}{280} \tag{C-10}$$

$$T_b^+ = X^+ + \frac{1}{Pe^2} \tag{C-11}$$

From (C-9) we can obtain the expression for the fully developed steady state sensitivity coefficient,

$$\frac{\partial T_s^+}{\partial Pe} = \left(\frac{\partial}{\partial Pe}X^+\right)_{x,a} + \frac{\partial}{\partial Pe}\left(\frac{1}{Pe^2}\right)$$

$$\frac{\partial T_s^+}{\partial Pe} = -\frac{x}{a}\frac{1}{Pe^2} - \frac{2}{Pe^3}$$

or

$$Pe\,\frac{\partial T_s^+}{\partial Pe} = -\left(X^+ + \frac{2}{Pe^2}\right) \tag{C-12}$$